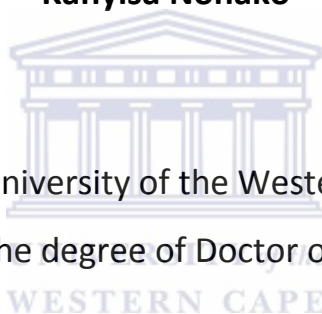


# **IMMUNOSENSORS DEVELOPED ON CLATHRATE PLATFORM COMPOUNDS**

**By**

**Kanyisa Nohako**



A thesis submitted to the University of the Western Cape in fulfilment of the requirements for the degree of Doctor of Philosophiae in the

CHEMISTRY DEPARTMENT, SENSORLAB  
FACULTY OF NATURAL SCIENCES  
UNIVERSITY OF THE WESTERN CAPE

**May 2013**

Supervisor: Professor PGL Baker

Co-Supervisor: Professor E Iwuoha

## Key words

Host-guest

Clathrates

Immunosensors

Organic host compounds

Voltammetry

Antibody-antigen

Immunoassay

Atomic force microscopy

Electrochemical impedance

Powder x-ray diffraction

Parvalbumin



## Abstract

Organic noncyclic compounds were used in the development of immunosensor for rapid fish species detection. Flourene derivatives show unique chemical and physical properties because they contain a rigid planar biphenyl unit, and the facile substitution at C<sub>9</sub> position of the flourene can improve the solubility and processability of materials containing flourene without significantly increasing of steric interactions in the compounds backbone. 9-(4-methoxyphenyl)-9H-xanthen-9-ol is bulky, rigid and has an hydroxyl moiety that may act as a hydrogen – bond donor, as well as a pyranil oxygen which is a potential hydrogen –bond acceptor.

We have successfully synthesised 9,9'-(ethyne1,2-diyl)bis(flouren-9-ol) by reflux method and 9-(4-methoxyphenyl)-9H-xanthen-9-ol through stirring at room temperature. The products were characterised using spectroscopic methods and were found to be both UV/Vis active ( $\lambda_{\text{max}} = 400 \text{ nm}$  flourene derivative and  $\lambda_{\text{max}} = 337 \text{ nm}$  xanthene derivative ) and fluorescent (440nm and 467nm flourene derivative and 344 and 380 xanthene derivative). These compounds were drop coated onto commercial glassy carbon electrode (GCE) to produce thin films. Scan rate dependent cyclic voltammetry (CV) confirmed the electrodynamics of the thin films to be consistent with monolayer diffusion ( $D_e = 1.37 \times 10^{-21} \text{ cm}^2/\text{s}$  flourene derivative and  $D_e = 9.79 \times 10^{-21} \text{ cm}^2/\text{s}$  xanthene derivative). Surface concentration was estimated to be  $1.55 \times 10^{-13} \text{ mol cm}^{-2}$  flourene derivative and  $2.00 \times 10^{-13} \text{ mol cm}^{-2}$ .

These compounds were used for the inclusion of parvalbumin antibodies immobilised onto clathrate platform by incubation and were evaluated as immunosensors for fish species identification. The antibody/antigen binding event was evaluated using UV/Vis spectroscopy, electrochemical impedance spectroscopy (EIS) and atomic force microscopy (AFM). The immunosensor response to parvalbumin in real samples of snoek (an indigenous fish species), tuna, fish paste, eyeshadow, lipstick, omega 3&6 and Scott's emulsion was evaluated. The sensitivity as calculated from EIS for each immunosensor was found to be  $5.36 \times 10^4$  flourene derivative immunosensor and  $4,11 \times 10^4$  xanthene derivative immunosensor and the detection limit of 1.50 pg/ml flourene derivative immunosensor and 2.42 pg/ml xanthene derivative immunosensor. The antibody/antigen binding was

monitored as decrease in charge transfer resistance and increase in capacitance by EIS. The interfacial kinetics of the immunosensors were modelled as equivalent electrical circuit based on EIS data. The UV/Vis spectroscopy was used to confirm the binding of the antibody/antigen in solution by monitoring the intensity of the absorption peak.



## Declaration

I declare that development of 9,9'-(ethyne-1,2-diyl)bis(flouren-9-ol) and 9-(4-methoxyphenyl)-9H-xanthen-9-ol immunosensors for rapid detection of fish species is my own work, that it has not been submitted for any degree or examination in any other university, and that all sources I have used or quoted have been indicated and acknowledged by means of complete references.

Kanyisa L Nohako



May 2013

## Acknowledgements

Firstly, I would like to thank God for allowing this to happen, for giving me strength and hope when I felt like giving up. I would like to thank my supervisor Professor P. Baker for giving me a chance and for believing in me. Also for her guidance, courage, patience, understanding and for assisting me throughout my project and for the opportunity to go to Germany. I would like to thank Neubrandenburg University, Food Technology department for making this project possible and for the support I got when I visited them.

I would like to thank Monwabisi Maqashu for his support, words of wisdom, encouragement, for being there for me and the push to the right direction. Umbulelo ongazenzisiyo kuba uzincamile ezakhe izinto wabeka mna kuqala. Zama Ngqumba for computer skills as I am technologically challenged. My family and friends for their support. I would like to thank my enemies their jealousy inspired me. I would like to thank my aunt Nompumelelo Macingwane for being a mother and a friend to me for praying with me and her support, spiritually and emotionally. SensorLab group for help when I needed it the most to mention a few Xolile Fuku, Gcineka Mbambisa, Euodia Hess, Stephen, Dr F Ajaye and Dr Waryo . Last but not least I would like to thank National Research Foundation for funding.

## Dedication

I would like to dedicate this thesis to my late grandmother Nofundile Gaxela, ndinjenjenje kungenxa yakho Fundie. I am who I am because of you. May your soul rest in peace. To my mother Welekazi Nohako and my father Monwabisi Nohako if it weren't for you I wouldn't be here. Keep up the good work. Lastly to the Almighty God.

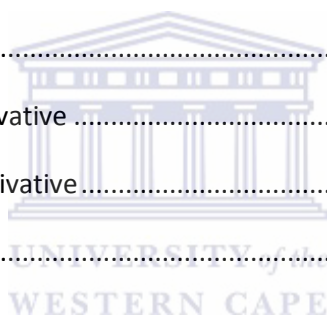


# Table of Contents

|  |       |
|--|-------|
| Title page.....                                    | i     |
| Key words.....                                     | ii    |
| Abstract.....                                      | iii   |
| Declaration.....                                   | v     |
| Acknowledgements.....                              | vi    |
| Dedication.....                                    | vii   |
| List of figures.....                               | xi    |
| List of schemes.....                               | xvi   |
| List of tables.....                                | xvii  |
| List of abbreviations.....                         | xviii |
| Chapter 1.....                                     | 1     |
| 1.1 Introduction.....                              | 1     |
| 1.2 Scope.....                                     | 2     |
| 1.3 Immunosensors.....                             | 5     |
| 1.4 Aptamer – Based Immunosensors.....             | 6     |
| 1.5 Deoxyribonucleic acid (DNA).....               | 7     |
| 1.6 Ribonucleic acid (RNA).....                    | 8     |
| 1.6.1 RNA comparison with DNA.....                 | 9     |
| 1.7 Antibody – Antigen.....                        | 10    |
| 1.7.1 Monoclonal antibody.....                     | 12    |
| 1.7.2 Polyclonal antibody.....                     | 13    |
| 1.8 Aptamers versus Antibodies.....                | 17    |
| 1.9 Enzyme-Linked Immunosorbent Assay (ELISA)..... | 18    |
| 1.9.1 Indirect ELISA.....                          | 19    |
| 1.10 Problem statement.....                        | 23    |



|  |    |
|--|----|
| Chapter 2.....   | 24 |
| 2.1 Methodology.....                                       | 24 |
| 2.1.1 Differential Scanning Calorimeter (DSC).....         | 24 |
| 2.1.2 Fourier transform infrared spectroscopy (FTIR) ..... | 26 |
| 2.1.3 Ultraviolet visible spectroscopy (UV/Vis).....       | 28 |
| 2.1.4 Fluorescence spectroscopy.....                       | 32 |
| 2.1.5 Electrochemical techniques .....                     | 34 |
| 2.1.5.1 Cyclic voltammetry (CV).....                       | 35 |
| 2.1.5.2 Squarewave voltammetry (SWV).....                  | 38 |
| 2.1.5.3 Electrochemical impedance spectroscopy (EIS).....  | 40 |
| 2.1.6 Powder x-ray diffraction (PXRD) .....                | 42 |
| 2.2 Materials .....  | 44 |
| 2.2.1 Synthesis of flourene derivative .....               | 45 |
| 2.2.2 Synthesis of xanthene derivative.....                | 46 |
| 2.2.3 Parvalbumin .....                                    | 46 |
| Chapter 3.....   | 48 |
| 3.1 Immunoassay .....                                      | 48 |
| 3.1.1 Optimisation of Immunoassay .....                    | 48 |
| 3.2 Moulds causing mycotoxins.....                         | 49 |
| 3.2.1 Aspergillus.....                                     | 50 |
| 3.2.2 Penicillium.....                                     | 50 |
| 3.3 Standard sandwich ELISA .....                          | 53 |
| 3.3.1 Results.....   | 57 |
| Chapter 4.....   | 59 |
| 4.1 Characterization of Flourene derivative .....          | 59 |
| 4.2 Xanthene derivative characterization.....              | 64 |
| Chapter 5.....   | 73 |



|  |     |
|--|-----|
| 5.1 Immunosensor development.....                  | 73  |
| 5.2 Immunosensor characterization .....            | 74  |
| 5.2.1Flourene derivative immunosensor .....        | 74  |
| 5.3 Xanthene derivative immunosensor .....         | 77  |
| Chapter 6.....                                     | 82  |
| 6.1 Immunosensor response .....                    | 83  |
| 6.2 Antibody/Antigen binding UV/Vis analysis ..... | 88  |
| Chapter 7.....                                     | 92  |
| 7.1 Applications.....                              | 92  |
| 7.2 Sample preparation .....                       | 94  |
| 7.3 Results and discussion .....                   | 94  |
| Chapter 8.....                                     | 97  |
| <i>Appendix 1</i> .....                            | 99  |
| References .....                                   | 100 |



## List of figures

|  |    |
|--|----|
| Figure 1: Chemical structure of DNA  | 8  |
| Figure 2: Chemical structure of RNA  | 9  |
| Figure 3: Difference between the sugars in DNA and RNA   | 9  |
| Figure 4: Examples of antibody complexes   | 10 |
| Figure 5: Antibody structure   | 10 |
| Figure 6: Monoclonal antibody production   | 13 |
| Figure 7: Polyclonal antibodies production   | 14 |
| Figure 8: ELISA diagram  | 19 |
| Figure 9: Indirect ELISA process   | 20 |
| Figure 10: Sandwich ELISA process  | 20 |
| Figure 11: Differential scanning calorimeter sample and reference holder, furnace block top view cover off | 25 |
| Figure 12: Typical DSC curve   | 25 |
| Figure 13: Optical diagram of an FTIR spectroscopy   | 26 |
| Figure 14: Typical IR spectrum   | 27 |
| Figure 15: Regions of the infrared spectrum in which vibration bands are observed                          | 28 |
| Figure 16: The component colours of the visible portion separated by passing sunlight through a prism      | 29 |
| Figure 17: Visible wavelengths within the electromagnetic spectrum   | 29 |
| Figure 18: Full electromagnetic spectrum   | 30 |

|   |    |
|---|----|
| Figure 19: Electronic transitions   | 31 |
| Figure 20: UV/Vis spectroscopy  | 32 |
| Figure 21: A simplified Jablonski diagram with absorbance, internal conversion, fluorescence, intersystem crossing and phosphorescence  | 33 |
| Figure 22: Fluorescence spectroscopy schematic diagram  | 34 |
| Figure 23: A typical cyclic voltammogram showing reduction and oxidation current peaks. <a href="http://en.wikipedia.org/wiki/Cyclic_voltammetry">en.wikipedia.org/wiki/Cyclic_voltammetry</a>                        | 36 |
| Figure 24: Instrumentation for cyclic voltammetry. Electrode designation<br>   | 37 |
| Figure 25: Dimensionless square wave voltammogram for the reversible oxidation-reduction case. <a href="http://www.hindawi.com/journals/ijelc/2011/538341/fig1/">www.hindawi.com/journals/ijelc/2011/538341/fig1/</a> | 39 |
| Figure 26: Electrochemical impedance spectroscopy instrument. WE-working electrode, RE-reference electrode, AE-auxiliary electrode  | 40 |
| Figure 27: Complex plane impedance spectrum, series resistance, capacitance and parallel resistance capacitance   | 41 |
| Figure 28: An electrified interface in which the electrode is negatively charged  | 42 |
| Figure 29: Diffractometer components and geometry   | 44 |
| Figure 30: Parvalbumin structure  | 47 |
| Figure 31: Aspergillus moulds growing on maize  | 50 |
| Figure 32: Penicillium moulds grown on oranges  | 51 |
| Figure 33: Atlantic cod   | 52 |
| Figure 34: Alaska Pollock   | 53 |
| Figure 35: ELISA – washer, program number four with three washing periods was   | 54 |

chosen

- Figure 36: Fifth step of the sandwich – ELISA, colour change after the addition of the substrate solution indicating positive results 55
- Figure 37: Shows the colour change from blue to yellow after the addition of the stopping solution (4N H<sub>2</sub>SO<sub>4</sub>) 55
- Figure 38: ELISA – reader, wavelength set at 450 nm 56
- Figure 39: Absorbance versus concentration of fish allergens with PBS as the control sample 57
- Figure 40: DSC curve showing melting point of flourene derivative 59
- Figure 41: IR spectrum showing flourene derivative functional groups 60
- Figure 42: UV – Vis Spectra. Absorption maxima of flourene derivative in methanol is 400 nm which is attributed to the  $\pi$ - $\pi^*$  transition with energy gap of 3.1eV. Flourenyl is rigid and bulky 61
- Figure 43: Emission and excitation spectra for flourene derivative 62
- Figure 44: Cyclic voltammograms flourene derivative on GCE in 0.2 M PBS pH 7.12. Scanrate (v<sup>1/2</sup>). Plot of  $i_{pc}/i_{pa}$  versus scanrate<sup>1/2</sup> from voltammograms 63
- Figure 45: SWV data with the formal potential of -134 mV 63
- Figure 46: Powder pattern for 9,9'-(ethyne-1,2-diyl)bis(flouren-9-ol) (red) and 9,9-bis(4-(2-hydroxyethoxy) phenyl) fluorene (black) 64
- Figure 47: DSC curve showing melting point of xanthene derivative 65
- Figure 48: IR spectrum showing functional groups of xanthene derivative and spectra for xanthone starting material 66
- Figure 49: UV – Vis Spectra. Absorption maxima of xanthene derivative in ethanol is 337 nm which is attributed to the  $\pi$ - $\pi^*$  transition with energy gap of 3.6 eV 67

|   |    |
|---|----|
| Figure 50: Emission and excitation spectra for xanthene derivative  | 68 |
| Figure 51: Cyclic voltammograms of xanthene derivative on GCE in 0.2 M PBS pH 7.12. Scanrate ( $v^{1/2}$ ). Plot of $i_{pc}/i_{pa}$ versus scanrate $^{1/2}$ from voltammograms | 69 |
| Figure 52: SWV data with the formal potential of -134 mV  | 69 |
| Figure 53: Xanthene derivative powder pattern (red) and xanthone powder pattern (black)   | 70 |
| Figure 54: Immunosensor development   | 73 |
| Figure 55: AFM. A = Topography of flourene derivative, B = Topography of flourene derivative plus antibody, C = Topography of flourene derivative Ab/Ag                         | 75 |
| Figure 56: Flourene derivative and immunosensor surface roughness   | 75 |
| Figure 57: Nyquist diagram to illustrate clathrate and immunosensor response for flourene derivative  | 76 |
| Figure 58: AFM. A = Topography of xanthene derivative, B = Topography of xanthene derivative plus antibody, C = Topography of xanthene derivative Ab/Ag                         | 78 |
| Figure 59: Xanthene derivative and immunosensor surface roughness   | 78 |
| Figure 60: Nyquist diagram to illustrate clathrate and immunosensor response for xanthene derivative  | 79 |
| Figure 61: A graph showing decrease in $R_{ct}$ and an increase in capacitance in flourene derivative immunosensor response   | 83 |
| Figure 62: A graph showing decrease in $R_{ct}$ and an increase in capacitance in xanthene derivative immunosensor response   | 83 |
| Figure 63: Equivalent circuit used for all impedance analysis   | 84 |
| Figure 64: EIS complex plot for analyte additions and bode plot using flourene derivative immunosensor  | 85 |

|  |    |
|--|----|
| Figure 65: A plot of capacitance vs concentration for flourene derivative immunosensor response        | 85 |
| Figure 66: EIS complex plot for analyte additions and bode plot using xanthene derivative immunosensor | 87 |
| Figure 67: A plot of capacitance vs concentration for xanthene derivative immunosensor response        | 87 |
| Figure 68: UV/Vis antibody/antigen binding confirmation  | 89 |
| Figure 69: UV/Vis antibody/antigen binding confirmation calibration curve                              | 90 |
| Figure 70: Fish and fish products used as sample for immunosensor application                          | 94 |



## List of schemes

|   |    |
|---|----|
| Scheme 1: Project scope   | 4  |
| Scheme 2: Antibody vs aptamer   | 6  |
| Scheme 3 : 9-(4-methoxyphenyl)-9H-xanthen-9-ol                                    | 45 |
| Scheme 4: 9,9'-(ethyne-1,2-diyl)bis(fluoren-9-ol)                                 | 45 |
| Scheme 5: Immunosensor schematic  | 47 |
| Scheme 6: Schematic illustration of the stepwise immunosensor development process | 74 |
| Scheme 7: Immunosensor application  | 82 |



## List of tables

|   |    |
|---|----|
| Table 1: Comparison between monoclonal antibody and polyclonal antibody   | 14 |
| Table 2: Absorption results from the ELISA – reader with calculated mean and standard deviation                       | 58 |
| Table 3: EIS parameters obtained from the circuit fitting of impedance data for GCE/F and GCE/F/Ab                    | 76 |
| Table 4: Calculation results for time constant, exchange current and homogeneous rate constant for GCE/F and GCE/F/Ab | 77 |
| Table 5: EIS parameters obtained from the circuit fitting of impedance data for GCE/X and GCE/X/Ab                    | 79 |
| Table 6: Calculation results for time constant, exchange current and homogeneous rate constant for GCE/X and GCE/X/Ab | 80 |
| Table 7: Concentration and capacitance results obtained for flourene derivative immunosensor                          | 86 |
| Table 8: Concentration and capacitance results obtained for flourene derivative immunosensor                          | 88 |
| Table 9: Summary of results obtained from EIS for samples   | 96 |

## List of abbreviations

|        |   |
|--------|---|
| F      | 9,9'-(ethyne-1,2-diyl)bis(flouren-9-ol) |
| X      | 9-(4-methoxyphenyl)-9H-xanthen-9-ol     |
| Ab     | Antibody                                |
| Ag     | Antigen                                 |
| MAb    | Monoclonal antibody                     |
| PAb    | Polyclonal antibody                     |
| CV     | Cyclic voltammetry                      |
| SWV    | SquareWave voltammetry                  |
| FTIR   | Fourier transform infrared spectroscopy |
| EIS    | Electrochemical impedance spectroscopy  |
| PXRD   | Powder x-ray diffraction                |
| ELISA  | Enzyme-Linked Immunosorbent Assay       |
| DSC    | Differential scanning calorimetry       |
| UV/Vis | Ultraviolet visible spectroscopy        |
| AFM    | Atomic force microscopy                 |
| GCE    | Glassy carbon electrode                 |
| DNA    | Deoxyribonucleic acid                   |
| RNA    | Ribonucleic acid                        |
| HOMO   | Highest occupied molecular orbital      |
| LUMO   | Lowest unoccupied molecular orbital     |

|          |                            |
|----------|----------------------------|
| SAM      | Self-assembly monolayer    |
| $R_{ct}$ | Charge transfer resistance |
| $C_{dl}$ | Double-layer capacitor     |
| $R_s$    | Solution resistance        |
| THF      | Tetrahydrofuran            |



# Chapter 1

*In this chapter we provide an overview of clathrate compounds, immunosensor, platform requirements and antibody/antigen interactions.*

## 1.1 Introduction

Host guest chemistry offers many new possibilities for creating a link between chemistry and biology [1] by forming biosensors and immunosensors with host compounds that form clathrates by entrapment of biomolecules (antibodies, protein, etc). The development and application of biochemical sensors and immunosensors is of great interest. The key step is to develop an immunosensor that is simple, fast and lead to robust materials with stable and highly active immobilized reagent which does not leach from the substrate [2]. Encapsulation of antibodies into different matrices i.e. physical entrapment within a porous matrix becomes increasingly popular [2]. Porous matrices are mechanical rigid with controllable surface area and average pore size, high suitability for optical application and enhanced stability of the encapsulated biomolecule. Dunn et al. described the physical immobilization of anti – cortisol antibody in the pores of the sol – gel silica matrix prepared in both monoliths and thin film forms [3]. Macrocyclic host molecules have electron rich cavity, can form complexes with cations, their exteriors are hydrophobic and the cavity size is proportional to ring size [4]. It is important for the host to have chemical and biochemical inertness, good mechanical stability and uniformity in particle size, should be easily activated to allow antibody attachment, have large pore size because antibodies are large molecules and the immobilization procedure should maintain the specific activity of antibodies [5]. Macrocyclic molecules are capable of recognizing specific analytes or catalyzing reactions.

Biomolecules are desirable reagents because of they are highly efficient at recognizing specific analytes or catalyzing reactions in aqueous biological media. It is important to use an aqueous medium that does not lead to partial or total denaturation and loss of reactivity by the biomolecule [6]. The development of immunosensors that are proficient in detecting low molecular weight (12kDa) are of interest and their response result from interactions between an antibody and its corresponding antigen. The two major approaches towards

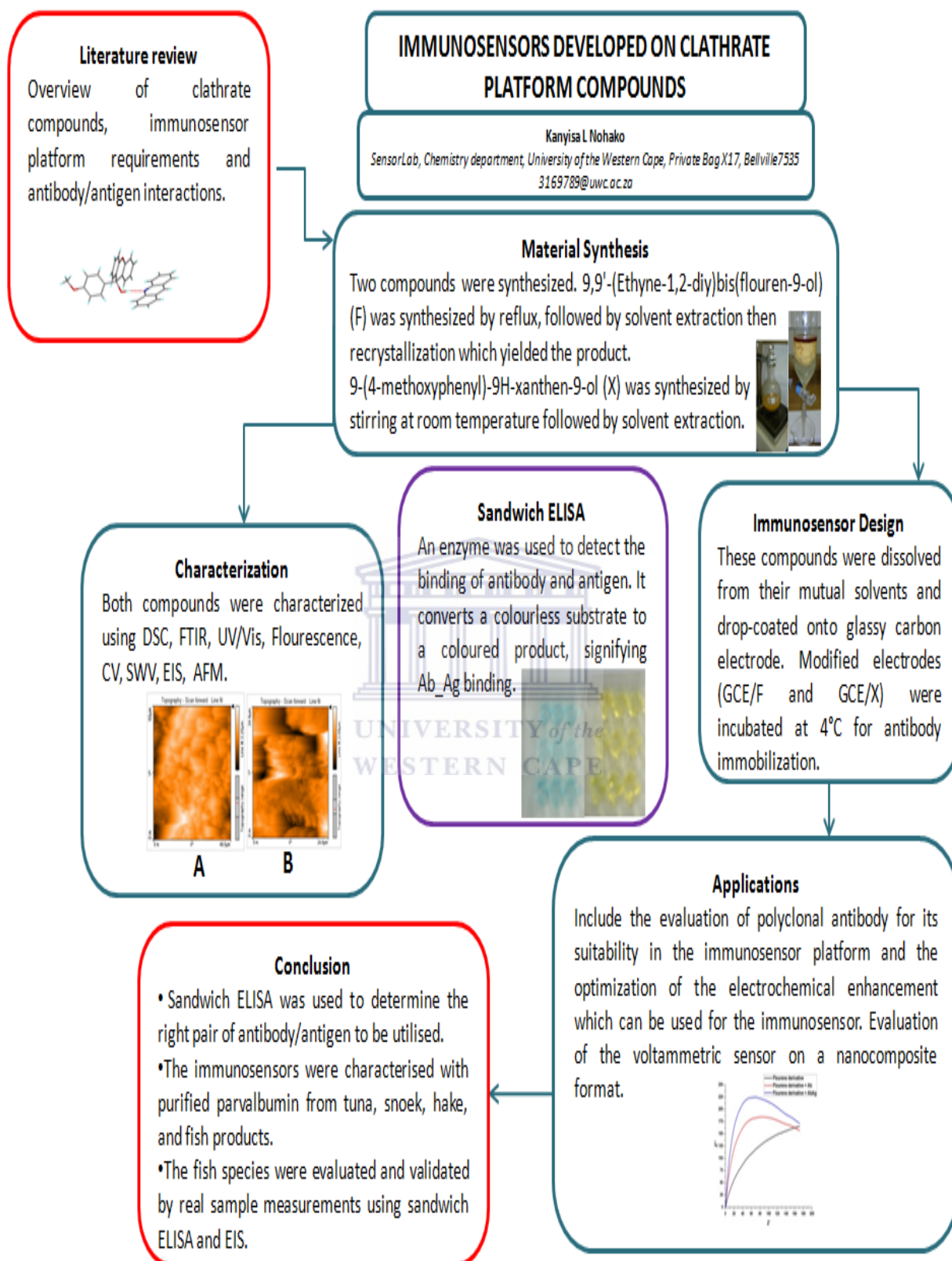
antibody immobilization are physical adsorption and covalent immobilization. The antibody can attach covalently via a nonsite directed or site directed approach. A specific region located away from the antigen binding sites of the antibody is targeted with site directed attachment. Fc region (carbohydrate region) has become increasingly important for immunosensor development and has opened new avenues for antibody surface immobilization strategies. Immunosensor surfaces that are capable of directly detecting antibody – antigen interactions are in demand. Antibodies and antigens have a net electrical charge which depends on the isoelectric points of the species and the ionic composition of the solution in aqueous solution. The surface charge of the electrode will depend on the net charge of the immobilized antibody, when the antibody is immobilized on the electrode. The immunochemical reaction will take place at the interface with a resulting change of the surface charge when antigen is present in the solution. This change can be measured potentiometrically against the reference electrode immersed in the same solution [7].

## 1.2 Scope

The aim of this study was to develop a rapid method for detection of fish allergen parvalbumin ( $\text{Ca}^{2+}$  binding protein).  $\text{Ca}^{2+}$  binding proteins are proteins that partake in calcium cell signaling pathways by binding to  $\text{Ca}^{2+}$ . Our bones consist of 99% calcium and 1% is found in our nervous system in an ionic form and acts as second messengers to control a broad range of physiological effects. In our cells, without calcium we cannot think, feel or move. Even so the right balance must be maintained to prevent calcium overload. Parvalbumin causes food allergies. It affects through inhalation of airborne allergens during outdoor drying, skin contact while filleting and cooking food, ingestion of fish meals. Its level must be monitored for people who are allergic to fish. This was achieved by the development of immunosensors for fish species using organic host compounds. Two platform compounds were synthesized: Fluorene derivative which was synthesized by reflux, followed by solvent extraction then recrystallization which yielded yellow powder. Xanthene derivative which was synthesized by stirring at room temperature followed by solvent extraction whereby the solvent was left to evaporate and yielded off white powder. Glassy carbon electrode was modified with each platform compound solution by drop coating onto the electrode. Rabbit polyclonal anti-parvalbumin was immobilized onto the

modified electrode by incubation at 4 °C for two hours. Antibody/antigen binding was monitored using electrochemical impedance spectroscopy in phosphate buffer solution. The immunosensor was applied in real sample measurements using fish species and fish products.





Scheme 1: Project scope.

### 1.3 Immunosensors

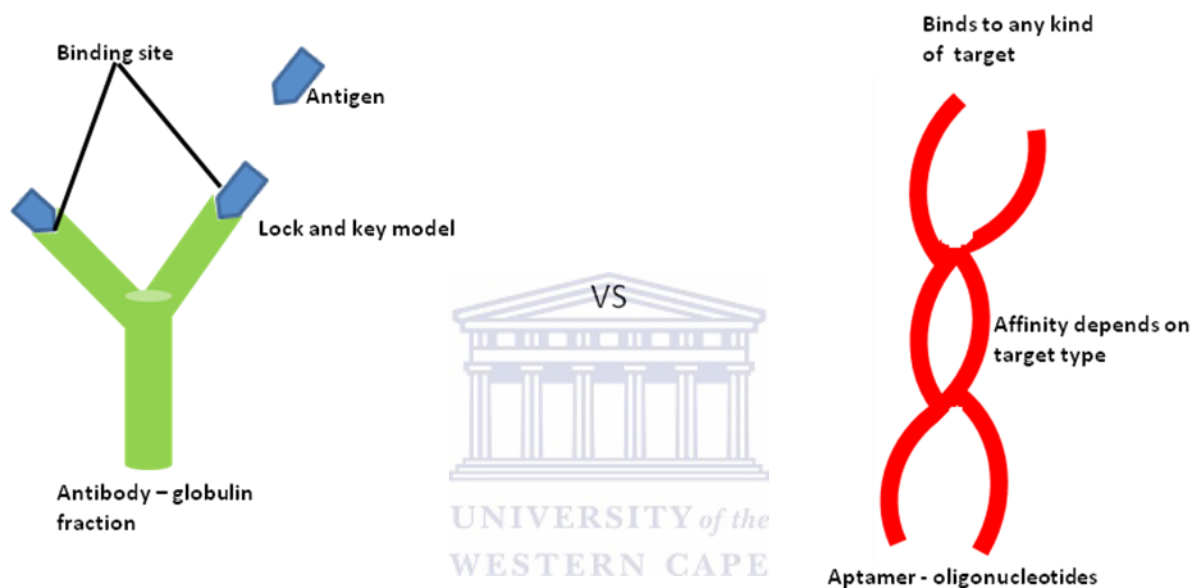
Recent development of various kinds of immunosensors have produced systems that allow possibility of generating a large number of antibodies for the analysis of numerous chemical species in real time for applications in areas such as clinical, environmental and food analysis. Researchers have different views of this concept; therefore there is no strict definition of an immunosensor. They are described as analytical tool that detects the binding of an antigen to its specific antibody by immobilization of the reaction to the surface of a device known as a transducer. The transducer converts physical quantity to be measured into a detectable electrical signal [8; 9; 10].

Despite the transducer of application involved, the most suitable system would have the following specification (i) An ability to detect and quantify the antigen within the required concentration range and a reasonable time. (ii) A capacity to transducer the binding event without externally added reagents. (iii) A capacity to repeat the measurement on the same device. (iv) The ability to detect the specific binding of the antigen in real samples. Very few systems possess all of the above properties [8]. Three techniques are used to classify immunosensors namely: optical, mass – sensitive or electrochemical. As determined by the transducer, the electrochemical immunosensor is categorized as amperometric, potentiometric, impedimetric and conductometric [11; 12]. Immunosensors are being applied for diagnosis of various diseases states and also to improve effective drug administration, therefore it is very important for the results obtained to be reproducible and repeatable [13].

Sandwich, competitive, or indirect format is used to monitor the affinity reaction of an immunosensor by tracer [14]. Immunosensor response characteristics is affected by the following conditions which must be crucially examined: purity of reagents, incubation temperature in different steps of immunoassay, ionic strength and solution composition, working pH range, condition of the electrode surface and the oxygen content of the solution. Immunosensors are basically about the specificity of the molecular recognition of antigens by antibodies to form a stable complex. Modern transducer technology enables the label – free detection and quantification of the immune complex as compared to immunoassay. Commercial applications of immunosensor in clinical diagnostic are few due

to unresolved fundamental questions relating to immobilization, orientation and specific properties of the antibodies or antibody – related reagents on the transducer surface. Immunosensor device must meet the following criteria: low imprecision, small lot – to – lot variations, high analytical sensitivity, optimum analytical specificity and accuracy with long calibration stability and low interferences by drugs or normal and pathological sample components [15].

### 1.4 Aptamer – Based Immunosensors



Scheme 2: Antibody vs aptamer

Aptamers are diminutive artificial oligonucleotides that can explicitly recognize [16] and bind to almost any kind of target, including ions, whole cells, drugs, toxins, low – molecular – weight ligands, peptides and proteins. Though natural aptamers also exist in riboswitches, but they are typically produced by selecting them from a large random sequence pool. An aptamer’s affinity depends on its target type. Aptamers are able to differentiate between targets using slight structural differences such as the presence of a hydroxyl group or methyl group and can also discriminate between enantiomers [17; 18; 19; 20].

They appear to have a higher degree of specificity compared with antibody preparations. As a matter of fact they provided high molecular differentiation between theophylline and caffeine, which differ only in a methyl group [17] with the binding affinity for the

theophylline aptamer being tenfold higher than for the caffeine aptamer. Whereas when antibodies were used as the biorecognition element, caffeine produced significant interference in the detection of theophylline [21]. Aptamers can be classified as:

- a. DNA or RNA aptamers, they consist of strands of oligonucleotides.
- b. Peptide aptamers, they consist of a short variable peptide domain, attached at both ends to a protein scaffold.

Aptamers have been applied in blocking receptors and inhibit protein activity with high affinity and specificity. They were used to validate drug targets and screen drug candidates. Aptamers have been proven to be good candidates for therapeutic [22; 23] applications due to their small size, quick elimination, low – production – cost, biocompatibility, biodegradability and no cross – reactivity with antibody binding receptors. They have been applied successfully in the treatment of age – related macular degeneration, also they have been used in the field of separation chemistry [24]. Aptamers have been also applied as biosensors [25; 26; 27] (environmental, industrial, defence and medical fields) and electrochemically in the detection of thrombin [27].

### **1.5 Deoxyribonucleic acid (DNA)**

DNA is a ladder – like double – stranded nucleic acid containing the genetic instructions used in the development and functioning of all known living organisms except for few viruses that have only RNA. The two long polymers of the DNA molecule are form of chains of nucleotide subunits, with backbones made of deoxyribose sugars, base (adenine with thymine and guanine with cytosine) and phosphate groups joined by ester bonds (fig. 1). It is the main constituent of chromosomes and in organisms other than bacteria it is found only in the cell nucleus.

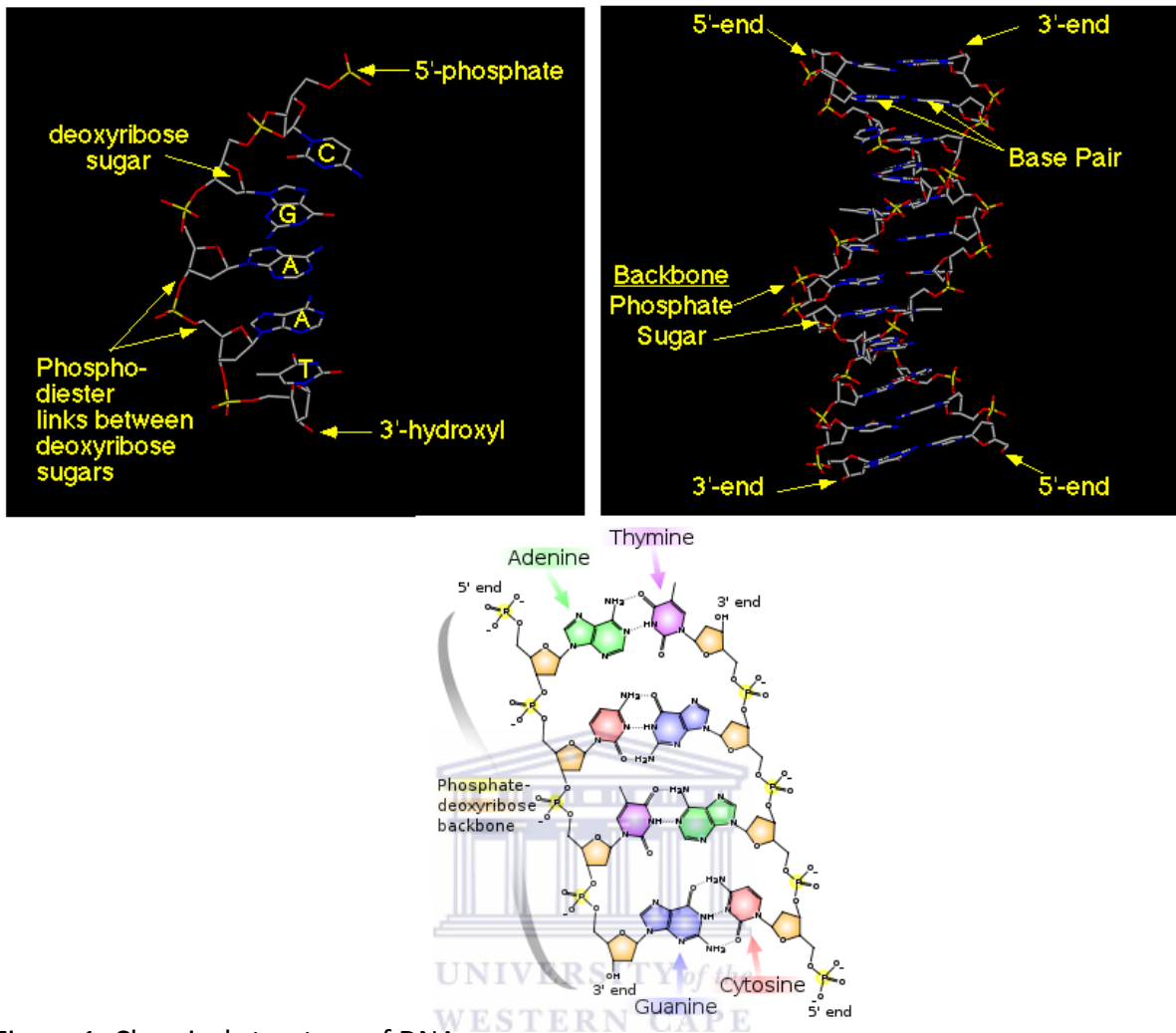


Figure 1: Chemical structure of DNA.

## 1.6 Ribonucleic acid (RNA)

RNA is a single – stranded molecule composed of nucleic acid building blocks present in all living cells. Similar to DNA it consists of long chain nucleotide units, a ribose sugar and a phosphate group. RNA base consists of adenine, cytosine, guanine and uracil (fig. 2).

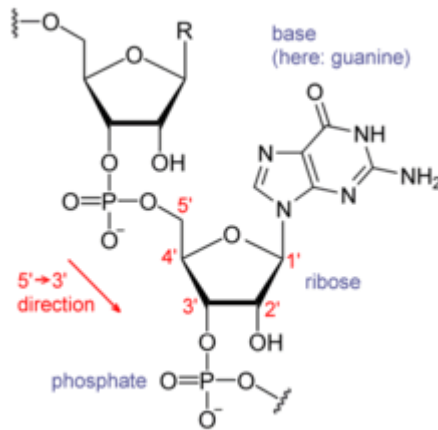


Figure 2: Chemical structure of RNA.

### 1.6.1 RNA comparison with DNA

- DNA is a double – stranded molecule whereas RNA is a single – stranded molecule unlike DNA in many of its biological roles and has a much shorter chain of nucleotides.
- DNA contains deoxyribose sugar while RNA contains ribose sugar (fig. 3). The hydroxyl groups in ribose sugar make RNA less stable than DNA because it is more prone to hydrolysis.
- The pairing base to adenine is not thymine, as it is in DNA but rather uracil which is an unmethylated form of thymine.
- DNA can be harmed by exposure to ultra – violet rays whereas RNA is more resistant to damage.

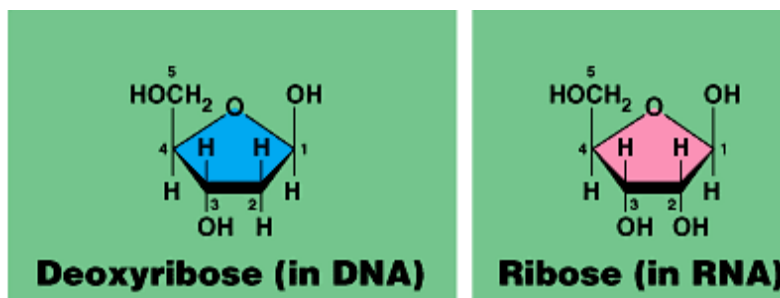


Figure 3: Difference between the sugars in DNA and RNA.

## 1.7 Antibody – Antigen

Antibody is immune system – related protein called immunoglobulin (Ig). They are produced by mammalian immune system to bind and mark foreign substances and fragments of bacteria and viruses. The electrophoretic mobility of the antibodies usually places them in the  $\gamma$  – globulin fraction of serum. Each antibody consists of four polypeptides – two heavy chains and two light chains joined to form a Y shaped [28; 29] and consist of one Fc and two Fab fragments [30; 31; 32]. Antibodies can directly inactivate antigens (any substance that causes the production of antibodies by the body’s immune system) and indirectly lead to their destruction through enhanced phagocytosis and complement activation. There are five classes of antibodies: IgA, IgG, IgD, IgE, IgM and they differ in antigenicity, charge, function and size. These differences explain antibody functions such as (1) versatility in antigen binding, (2) binding specificity and (3) biologic activities.

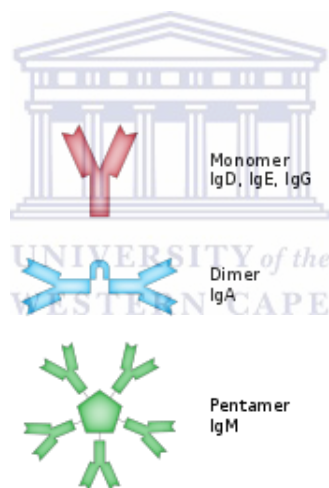


Figure 4: Examples of antibody complexes.

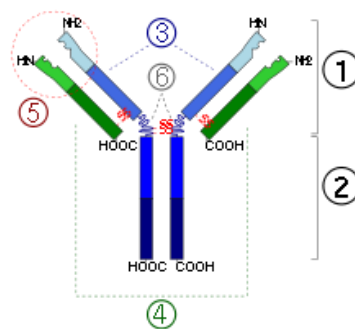


Figure 5: Antibody structure.

1. Fab region
2. Fc region
3. Heavy chain (blue) with one variable ( $V_H$ ) domain followed by a constant domain ( $C_{H1}$ ), a hinge region, and two more constant ( $C_{H2}$ ) and ( $C_{H3}$ ) domains.
4. Light chain (green) with one variable ( $V_L$ ) and one constant ( $C_L$ ) domain.
5. Antigen binding site (paratope).
6. Hinge regions

Fab fragments react with antigens to yield immune complexes. The antibody and the antigen have a lock-and-key model that binds the two molecules together whereby the lock is the antibody and the key is the antigen. Lock and key consist of a strong non-covalent bond and this includes hydrogen bonds, electrostatic bonds, van der Waals forces and hydrophobic bonds. A higher or lower amount of Fab fragments appears to be available for the interaction with the antigen present in the solution depending on the immobilized molecule orientation on the carrier surface. The method of antibody immobilization determines its orientation and as a result its activity in immunoassay can vary. Antibody immobilization occurs in the case of hydrophobic sorption as well as when carriers containing the aldehyde, iminoester, halogenoacetyl or other electrophilic groups are used to react with protein amino groups [31]. In order to analyze substance, immunoassay methods rely on specific interactions between antibodies and antigens. The substances range from complex viruses and microorganisms to simple pesticide molecules and industrial pollutants. Penalva et. al [33]. give the factors that should be considered when extending immunoassay methods to hydrophobic compounds using mainly non – polar organic solvents. These are (1) the sample treatment, extraction, separation and quantification of hydrophobic analytes and (2) the effect of organic solvents on the antigen – antibody interaction and on any enzymatic tracer used. Enzymes in organic solvents can only be denatured in thermodynamic terms, but not due to restriction of water by kinetic terms. The following are important factors that need to be considered when working with enzymes in organic media (i) selection of the solvent (ii) selection of the enzyme, (iii) immobilization procedure for the enzyme, and (iv) heterogeneity (two phases) of the interaction.

There are two types of antibodies: (i) Monoclonal antibody (MAb)

(ii) Polyclonal antibody (PAb)

### **1.7.1 Monoclonal antibody**

Monoclonal antibodies are antibodies that all have affinity for the same antigen because they are made by identical immune cells that are clones of a unique parent cell [34]. They bind to the same epitope because they consist of monovalent affinity. Kohler and Milstein in 1976 [35] made one of the most important contributions to immunology that has a strong impact on biotechnology. Their work has made possible to create pure and uniform antibodies against specific antigens and the technology is called hybridoma technology. The modern approach to produce hybridoma or fused cell is to fuse a myeloma (cancer) cell with a normal antibody producing lymphocyte (spleen cells). Cultivated myeloma cells are fused with spleen cells obtained from an immunized animal (mouse) (fig. 6). The spleen cells are the source of antibodies and they can only produce one type of antibody i.e hybridoma clone will produce one type of specific antibody.

The monoclonal antibody can be applied in the following:

- In selective elimination of undesired cells, such as tumour cells or activated T lymphocytes in transplantation patients.
- Monoclonal antibodies are used in the treatment of drug overdose.
- They are excellent as the primary antibody in an assay or for detecting antigens in tissue and will often give significantly less background staining than polyclonal antibodies due to their specificity.

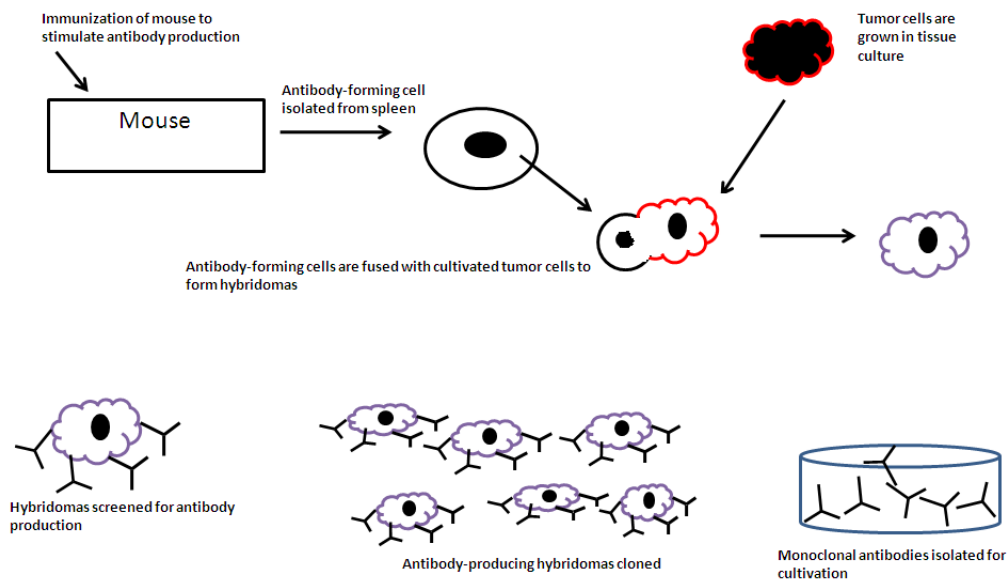


Figure 6: Monoclonal antibody production.

### 1.7.2 Polyclonal antibody

Polyclonal antibodies are antibodies that are found in different B cell resources. They are a combination of immunoglobulin molecules secreted against a specific antigen, each identifying a different epitope. Inoculation of a suitable mammal such as a mouse, rat, rabbit, goat, or horse is done to produce polyclonal antibodies. The amount of serum to be collected can determine which mammal to be used, the larger the mammal the greater the serum. An antigen is introduced into the mammal and this encourages the B – lymphocytes to produce IgG immunoglobulins specific for the antigen (fig. 7). Polyclonal IgG is purified from the mammal's serum.

Polyclonal antibodies are applied in the sandwich ELISA for tumour markers or other antigens can be designed with polyclonal antibodies as the coating antibody, followed by addition of standard antigen/sample and then addition of relevant MAb conjugate to HRPO.

They are useful in histopathological analysis using immunoperoxides staining technique. And they are used in the affinity purification of antigens.

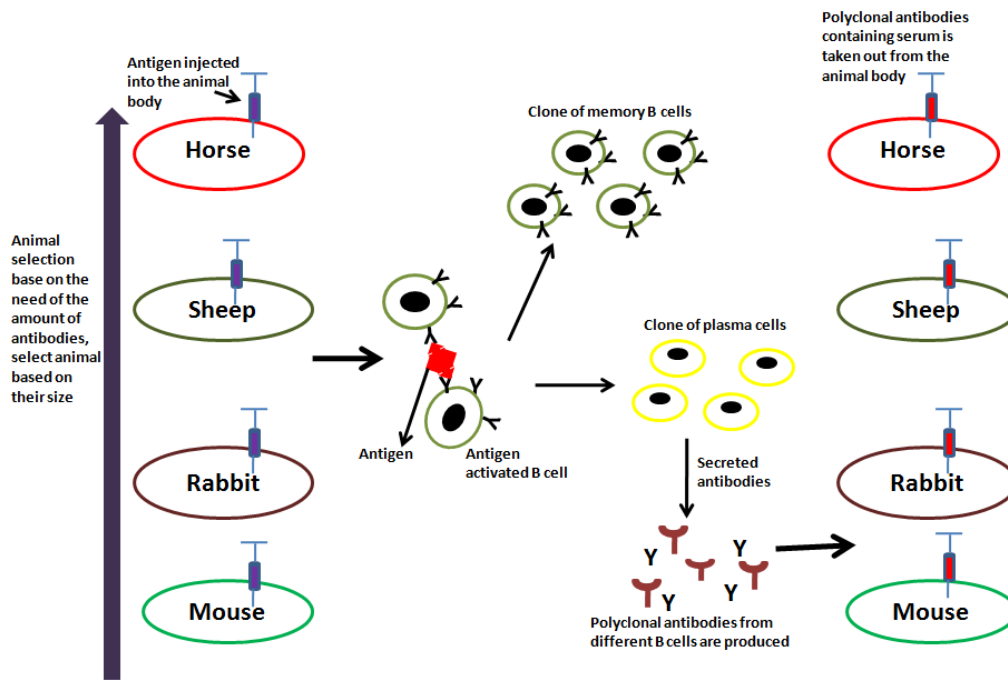


Figure 7: Polyclonal antibodies production.

| Monoclonal  | Polyclonal  |
|---|---|
| 1) Expensive to produce, high technology required.  | Inexpensive to produce, low technology is required.                                 |
| 2) Training is required for the technology use, time scale is long for hybridomas.  | Skills required are low, time scale is short.                                       |
| 3) Can produce large amounts of specific antibodies but may be too specific.  | Produces large amounts of non specific antibodies.                                  |
| 4) Recognizes only one epitope on an antigen. Once a hybridoma is made it is a constant and renewable source and all batches will be identical. | Recognizes multiple epitopes on any one antigen. Can be batch to batch variability. |

Table 1: Comparison between monoclonal antibody and polyclonal antibody.

Although the monoclonal antibody production is more costly, it assures a long – term availability of reproducible antibodies that does not require animals for further large – scale

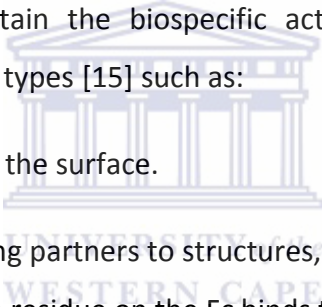
production [5]. Inducing an immune response, compounds of low molecular mass have to be modified by bonding to a larger carrier molecule before immunization and mostly a functional group is introduced into the selected molecule in order to make possible this coupling. The selection of the functional group is often based on trial – and – error assay; the molecule should keep as much as possible the identity of the analyte. The toxicity of the analyte is an important feature when making antibodies designed to recognize organic pollutants or drugs [5]. Maurer and co – workers encountered problems when generating antibodies against the very toxic amanitins for the detection an early diagnosis of an intoxication with amanita mushrooms [36], the conjugation of amanatoxins to proteins made them more poisonous than the native toxins, enhancing their uptake into protein – consuming cells.

In recent years toxins have been targeted. Mycotoxins are toxic secondary metabolites [37; 38] produced by various fungi growing in a wide range of food and animal feedstuffs [5] (nuts, peanuts, corn, cereals, grain, oilseeds, dry figs and raisins, milk, apple juice). They are not destroyed by temperature treatments such as cooking and freezing, nor by decomposition in digestion, they remain in meat and dairy products. Monitoring is very important because about 20% of food products, mainly of plant origin are contaminated. Many applications (such as immunoassays including RIA and ELISA methods, as well as several novel immunochemical screening tests) deal with the determination of mycotoxins in foodstuffs that include aflatoxins [39; 40] (associated with commodities such as cotton, peanuts, spices, pistachios and maize), ochratoxins [41; 42] (commodities including beverages such as beer and wine), fumonisins [43; 44] (cereal such as wheat and maize), patulin [45; 46] (associated with a range of mouldy fruits and vegetables) and zearalenone (not correlated to any fatal toxic effects in animals or humans. These methods are sensitive, specific and simple to operate. Specific antibodies have also been used as immunohistochemical reagent and to arm affinity columns that are used as a cleanup tool for analysis of mycotoxins by other methods.

Aquatic microalgae produce other toxins (microcystins) that are responsible for shellfish and fish contamination. There are two toxins associated with shellfish, paralytic poisoning (should be controlled in shellfish) and diarrhetic poisoning (encountered worldwide).

Alternative methods are required, mouse bioassay is commonly used. Microcystins are cyclic nonribosomal peptides produced by cyanobacteria which represent an increasing environmental hazard. China, Brazil, Australia, the United States and much of Europe are faced with microcystins – containing “blooms” problem. They may cause serious damage to the liver. In Europe the use of synthetic corticosteroids as growth promoters is prohibited, but it still continues for commercial reasons because the meat that is produced is more appealing to consumers [5].

In the development of an immunosensor the solid support also plays a role in the antibody orientation. It should have chemical and biochemical inertness, good mechanical stability and uniformity in particle size, the solid support should be easily activated to allow antibody attachment, have large pore size because antibodies are large molecules, and should be hydrophilic in order to avoid any non – specific interactions. It is important for the immobilization procedure to retain the biospecific activity of antibodies. Coupling of antibodies is oriented in different types [15] such as:

- 
- Binding to Fc receptors on the surface.
  - Binding of the other binding partners to structures, covalently linked to the Fc part of the antibody e.g the biotin residue on the Fc binds to surface – coated streptavidin.
  - Coupling to the solid support via an oxidized carbohydrate moiety on the C<sub>H2</sub> Fc domain.
  - Binding of Fab fragments to the surface of the device via a sulfhydryl group in its C – terminal region.

Optimization of the antibody immobilization through oriented bonding procedures has been attempted. Agarose – based and silica – based supports involve covalent coupling via lysine ε – amino groups, which are encountered throughout antibody molecules, allowing thus several different antibody orientations thus the coupling is considered random immobilization. Utilization of antibody fragments will increase the number of integral binding site without causing steric hindrance [5]. Entrapment of antibodies against PAHs, 1-nitropyrene, s-triazines and TNT, the sol –gel method has been used. In theory leaching of

antibodies can be a problem in sol – gel techniques because of the high porosity of the matrix and the fact that antibodies are not covalently bound to it, however in the aforementioned studies no or negligible leaching was observed. The degree of purification of the antibody solution is also important. Non – purified antisera for bonding has been used, but one can expect a reduced bonding density due to the co – immobilization of the other proteins. Recent developments are to use purified PAbs and MAbs [5].

## 1.8 Aptamers versus Antibodies

- Antibody identification process relies on an animal host and that makes antibody generation difficult with molecules that are not well tolerated by animals such as toxins. It is a challenge to raise antibodies against molecules that are inherently less immunogenic. Aptamers are designed in vitro and they do not depend on animals, cells or even in vivo conditions. Additionally, the properties of aptamers can be changed to obtain an aptamer that interacts with specific target regions or under differing binding conditions.
- Antibody use in therapeutic applications is limited because the generation of hybridomas are restricted to rat and mouse. Although, in aptamer recognition toxins as well as molecules that do not obtain good immune responses can be used to generate high – affinity aptamers because animals or cells are not involved.
- The recital of the same antibody tends to differ from batch – to – batch, due to the challenges encountered during the production of antibodies, requiring immunoassays to be reoptimized with each new batch of antibodies. Whereby there is little or no batch – to – batch variation expected in aptamer production because they are produced by chemical synthesis with extreme accuracy and reproducibility and are purified under denaturing conditions.
- Antibody – target interactions cannot be changed on demand, they are large and complex molecules that are sensitive to nonphysiological pH and temperature, which can limit their use in reusable sensors. However, aptamers can be changed on demand.

- Antibodies have a limited shelf life, are sensitive to temperature and undergo irreversible denaturation. Aptamers undergo denaturation, but the process is reversible, they are stable to long – term storage and can be transported at ambient temperature.

Even though aptamers are more sensitive than antibodies, due to their smaller size the excretion is faster than in antibodies resulting from weaker binding. Aptamers that are unmodified are highly vulnerable to degradation by many nucleases.

### **1.9 Enzyme-Linked Immunosorbent Assay (ELISA)**

For antibody/antigen binding, the standard method used is the ELISA. ELISA is an immunoassay technique used in the optimization of the methodology for detection of the presence of an immobilized active antibody or antigen and to monitor the lifetime and stability of the immobilized biological molecule and is also used to characterize the steps of immunosensor construction. It is a popular format of a wet – lab type analytic biochemistry assay that uses one sub – type of heterogeneous, solid – phase enzyme immunoassay (EIA) to detect the presence of a substance in a liquid sample or wet sample.

Carrying out an ELISA entails at least one antibody with specificity for a particular antigen. Immobilize the sample with an unknown amount of antigen on a solid support either non – specifically or specifically. Add the detection antibody forming a complex with the antigen, it could be covalently linked to an enzyme or can itself be detected by a secondary antibody that is linked to an enzyme through bioconjugation. To remove any proteins or antibodies that are not specifically bound, the plate is typically washed with a mild detergent solution between each step. Enzymatic substrate is added to produce a visible signal, which indicates the quantity of antigen in the sample after the final wash step (fig. 8).

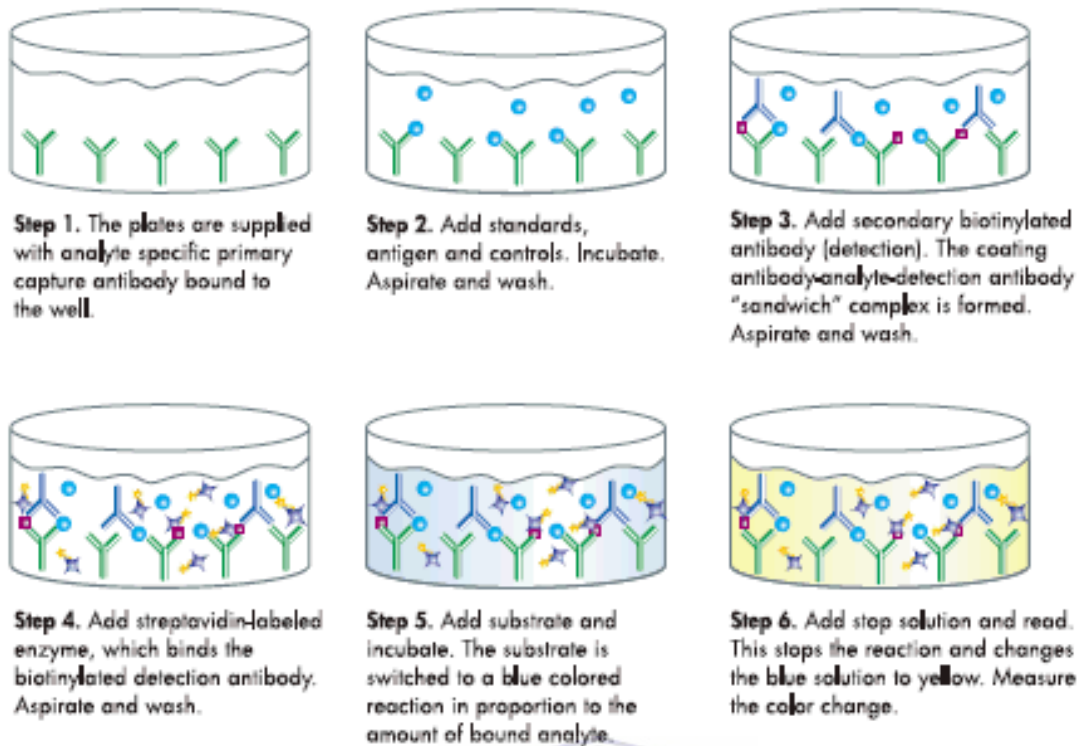


Figure 8: ELISA diagram.

Different types of ELISA may be established on the basis of sensitivity and whether one is trying to detect an analyte or the antibody response to it. The four most widely used types of ELISA may be described as follows:

### 1.9.1 Indirect ELISA

Indirect ELISA is used to detect sample antibody. Steps are as follow:

- A well of a microtiter plate is coated with antigen and left to incubate.
- Blocking agent (Bovine Serum Albumin BSA or Casein) is added to the well to block plastic surface that remains unreacted by the antigen.
- Specific antibody that binds to the antigen is then added.
- Then enzyme – linked antibody is added that binds to specific antibody.
- A substrate is then added and it changes colour upon reaction with the enzyme (fig. 9).

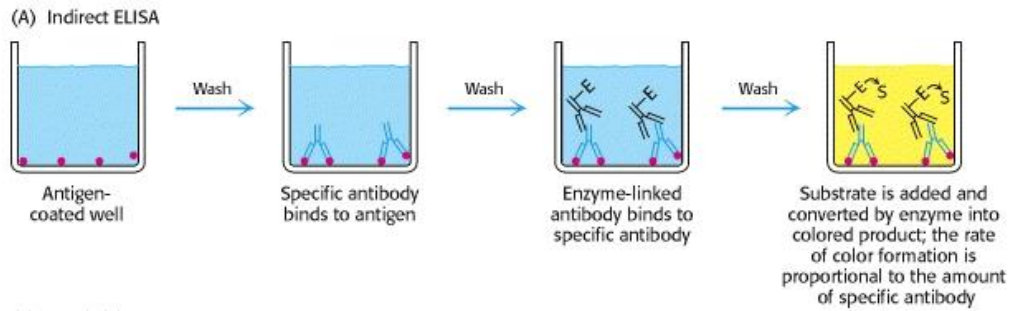


Figure 9: Indirect ELISA process.

Indirect ELISA is mainly used for the detection of HIV antibodies. It is very high in sensitivity.

### 1.9.2 Sandwich ELISA

Sandwich ELISA is used to detect sample antigen. Steps are as follow:

- A primary unlabelled antibody is bound to the wells. Any non – specific binding sites on the surface are blocked by blocking agent.
- Antigen – containing sample is applied to the plate. To remove the unbound antigen the plate is washed.
- Introduced is the second set of labelled antibodies which bind to the antigen bound to the primary antibody hence the “sandwich”.
- Enzyme – linked secondary antibodies are applied as detection antibodies that also bind specifically to the antibody’s Fc region. The plate is then washed to remove any unbound antibody – enzyme conjugates.
- A substrate for the enzyme is then added to produce an optically measurable signal (fig. 10)

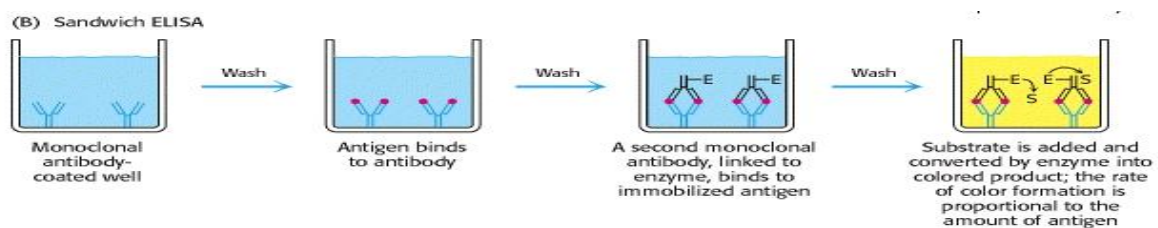


Figure 10: Sandwich ELISA process.

Sandwich ELISA is applied in the home pregnancy test.

### 1.9.3 Competitive ELISA

The steps for this ELISA are a bit different than the indirect and sandwich ELISA. It can be used to establish if a molecule is present in the sample and also how much of that sample is present, example the concentration of certain hormone. The steps are as follow:

- In the presence of the antigen (sample) unlabeled antibody is incubated.
- This complex (bound antibody/antigen) is then added to an antigen – coated well.
- To remove the unbound antibody the plate is washed. The more antigen in the sample the less antibody will be able to bind to the antigen in the well.
- A secondary antibody that is coupled to an enzyme is added. A substrate is then added to produce a chromogenic or fluorescent signal. In order to prevent eventual saturation of the signal the reaction is stopped.

### 1.9.4 Reverse ELISA

Reverse ELISA is a new technique that uses a solid phase made up of an immunosorbent polystyrene rod with ogives. This device is immersed fully in a test tube containing the collected sample and the following steps (washing, incubation in conjugate and incubation in chromogeneous) are performed through dipping the micro – wells with the prepared concentration. Reverse ELISA is more sensitive than the other ELISA; it can detect different reagents permitting simultaneous detection of different antibodies and different antigens for multi-target assays. The test sensitivity in clinical (blood, saliva, urine), food (bulk milk, pooled eggs) and environmental (water) sample can be improved by increasing the sample volume. To measure the non – specific reactions of the sample, the one ogive is left unsensitized. It makes possible the development of ready – to – use lab – kits and on – site kits.

ELISA may be applied as follows:

- It is applied in screening donated blood for evidence of viral contamination.
  - HIV-1 and HIV-2 (presence of anti – HIV antibodies).
  - Hepatitis C (presence of antibodies)
  - Hepatitis B (testing for both antibodies and viral antigen).
- It is used to measure hormone levels such as:
  - HCG (as test for pregnancy)
  - LH (determining the time of ovulation)
  - TSH, T3 and T4 (for thyroid function).
- ELISA is applied in the detection of infections
  - Sexually – transmitted agents like HIV, syphilis and Chlamydia
  - Toxoplasma gondii.
- For the detection of allergens in food and house dust.
- It is used in measuring rheumatoid factors and other autoantibody in autoimmune diseases like lupus erythematosus.
- Applied in measuring of toxins in contaminated food.
- For detecting prohibited drugs such as cocaine and opiates.

In doing the sandwich ELISA we were able to establish the suitability, sensitivity and selectivity of parvalbumin for fish species and the detection levels in  $\mu\text{g/ml}$ . ELISA is time-consuming and a costly affair. It must be optimized to provide consistent results. ELISAs are poorly suited for the detection of extremely low concentrations of antigen. The immunosensors are inexpensive, highly sensitive and have long-term reliability and reproducibility.

## 1.10 Problem statement

Development of rapid detection method for fish allergen parvalbumin with focus on sustainable resource management in fisheries. Sustainable resource management is the management of the use, development and protection of the resources in a way, or at a rate, which enables people and communities, including indigenous peoples, to provide for their present social, economic and cultural well – being while also sustaining the potential of those resources to meet the reasonably foreseeable needs of future generations and safe guarding the life – supporting capacity of air, water and soil ecosystems.

When the body recognizes the proteins in fish as harmful, it sends out an antibody called immunoglobulin E to attack the invading allergen. The body reacts by displaying various allergic symptoms such as sneezing, nasal congestion, runny nose, swelling and tenderness of the mouth, difficulty breathing, flushing or rash, burning and itching of skin, hives, nausea or vomiting, abdominal cramps and diarrhea.

South Africa's industrial fisheries are extensively considered to be among the best managed in the world, through fishing policies, international laws and protocols that ensures the sustainability of its marine resources, while maximising economic opportunities. It is the department's responsibility to protect and prevent illegal marine activity and ensure compliance with legislation. Up to date, fishery control officers monitor landed fish at harbours, slipways and fish – processing establishments on an ongoing basis to ensure that permit holders comply with their permit conditions and declare all their catches.

## Chapter 2

*Spectroscopic, microscopic and electrochemical techniques were used in this study. In chapter two we discuss these methods such as Differential scanning calorimeter, Ultraviolet visible spectroscopy, Fourier transform infrared spectroscopy, Cyclic voltammetry, Squarewave voltammetry, Electrochemical impedance spectroscopy, Powder x-ray diffraction and materials used.*

### 2.1 Methodology

#### 2.1.1 Differential Scanning Calorimeter (DSC)

DSC is the thermoanalytical technique whereby heat is measured into or out of the sample relative to a reference and heats the sample with a linear temperature ramp. It determines the enthalpy of melting and boiling points, glass transitions, crystallization time and temperature, percent crystallinity, heats of fusion and reactions, specific heat, oxidative/thermal stability, rate and degree of curve, reaction kinetics and purity. Quantitative and qualitative information about physical and chemical changes are provided by these measurements that involve endothermic (heat flows into the sample) or exothermic (heat flows out of sample) processes. Both the sample and a reference are maintained at nearly the same temperature; therefore the difference in heat flow to both is recorded as a function of temperature. Empty aluminium pan is normally used as a reference. Heat flow is equivalent to enthalpy changes due to constant pressure in the DSC. The temperature is increased at a constant rate for both the sample and reference.

DSC is composed of a sample holder and a reference holder fig 12. To allow high temperature operation they are both built from platinum. There is a resistance heater and temperature sensor under each holder. The temperature is increased at the selected rate by applying current to the two heaters. Nitrogen gas flow is applied over the sample to form a reproducible and dry atmosphere and it also eliminates air oxidation of the samples at high temperatures. The sample is potted into a small aluminum pan and the pan can hold up to about 10 mg material.

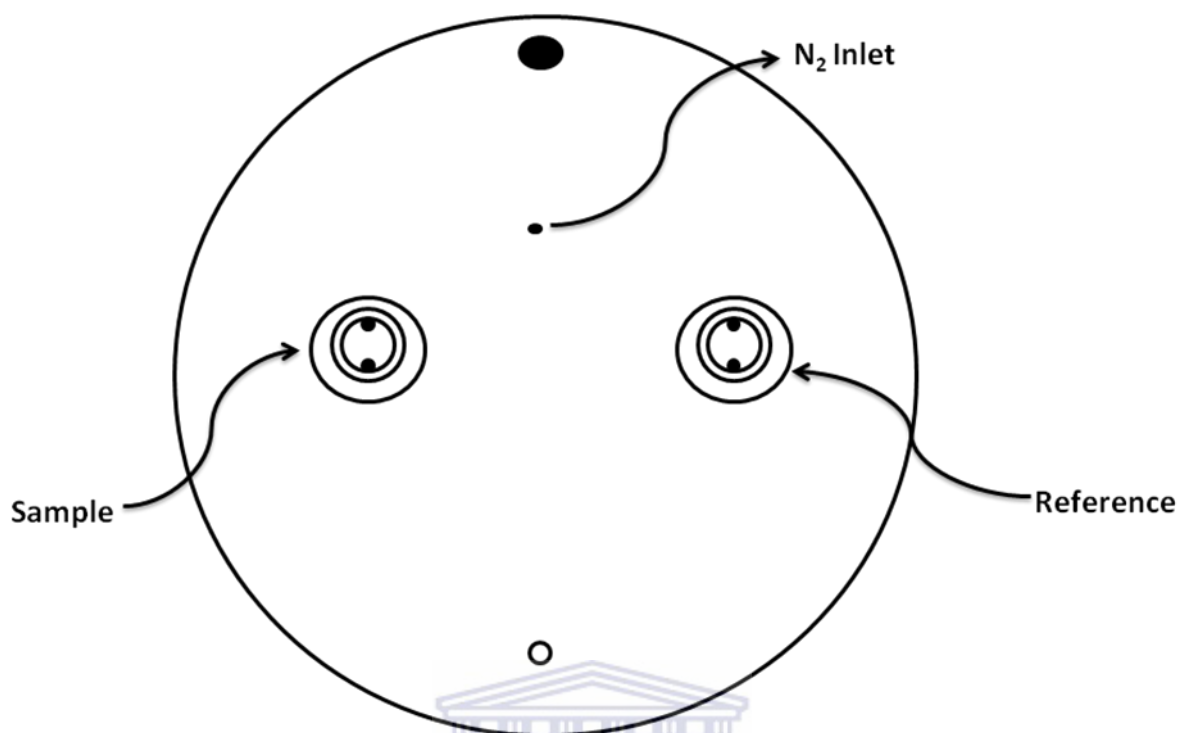


Figure 11: Differential scanning calorimeter sample and reference holder, furnace block top view cover off.

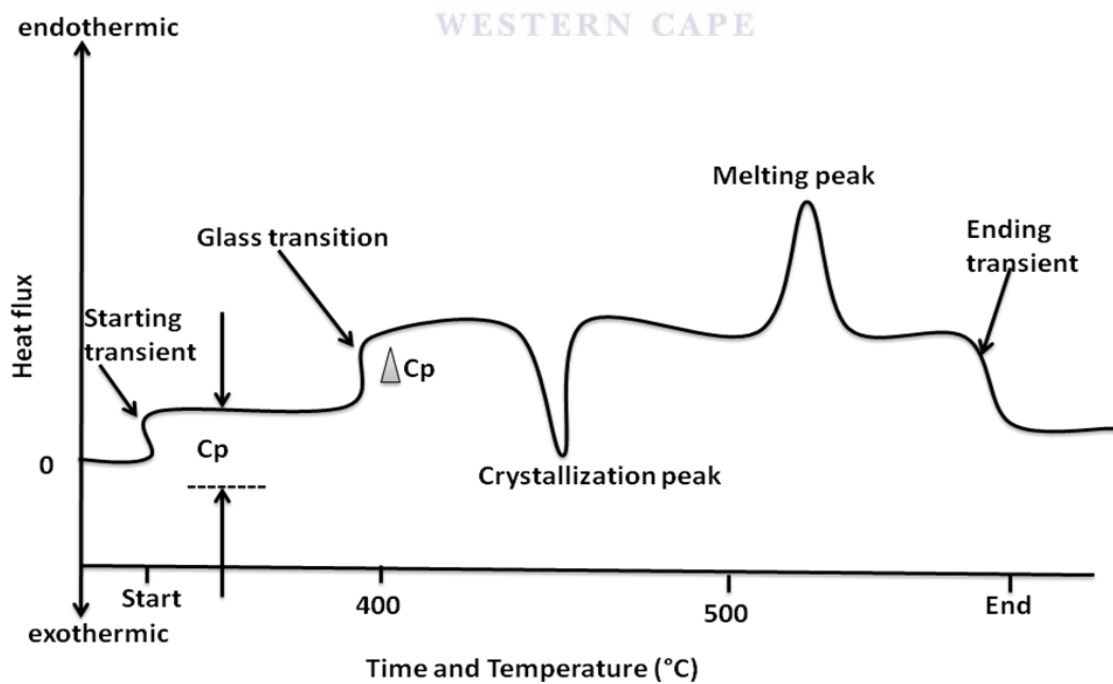


Figure 12: Typical DSC curve.



The normal instrumental process is as follows: from the source infrared is emitted from a glowing black – body source the beam passes through an aperture which controls the amount of energy presented to the sample. The beam enters the interferometer where the “spectral encoding” takes place. The resulting interferogram signal then exits the interferometer. Then the beam enters the sample compartment where it is transmitted through or reflected off of the surface of the sample, depending on the type of analysis being accomplished. This is where specific frequencies of energy, which are uniquely characteristic of the sample, are absorbed. Finally the beam passes to the detector for final measurement. The detectors used are specially designed to measure the special interferogram signal the measured signal is digitized and sent to the computer where the fourier transformation takes place. The final infrared spectrum is then presented to the user for interpretation and any further manipulation. Runs were achieved using PerkinElmer precisely spectrum 100 FT – IR spectrometer. The sample holder and the presser were first cleaned with acetone. The background was measured and the sample was added and pressed onto the sample holder and it was scanned.

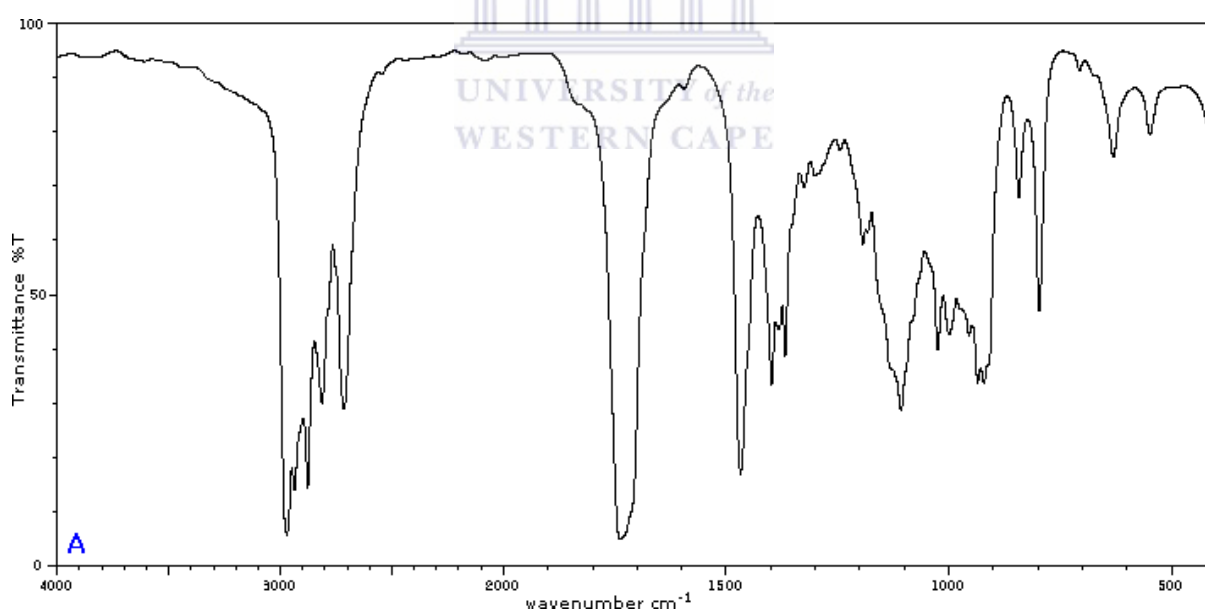


Figure 14: Typical IR spectrum.

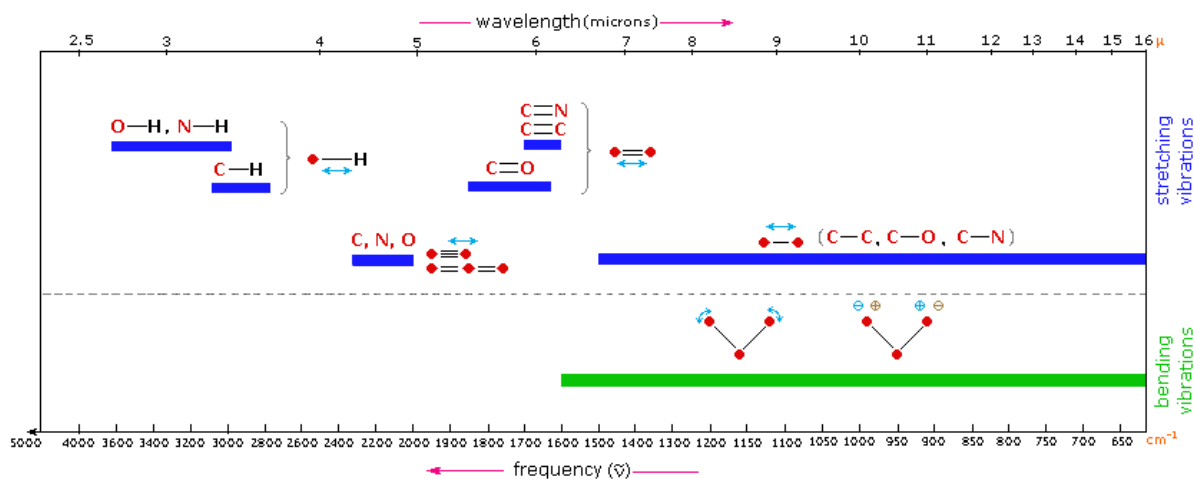


Figure 15: Regions of the infrared spectrum in which vibration bands are observed.

### 2.1.3 Ultraviolet visible spectroscopy (UV/Vis)

Colour is an obvious difference between certain compounds and many of the colours of the objects in the world around us including the green of vegetation, the colours of flowers, the synthetic dyes, and the colours of pigments and minerals, twig from transitions in which an electron makes a transition from one orbital of a molecule or ion into another. The primary energy harvesting step by which our planet captures energy from the Sun and uses it to drive the non – spontaneous reaction of photosynthesis occurs when chlorophyll absorbs red and blue light (leaving green to be reflected) resulting in relocation of an electron. On that note the human eye is functioning as a spectrometer analyzing the light reflected from the surface of a solid or passing through a liquid. Sunlight (white light) is a mixture of light of all different colours and the removal, by absorption of any one of these colours from the white light results in the complementary colour being observed (fig 17). It consists of a broad range of radiation wavelengths in the ultraviolet (UV), visible and infrared (IR) portions of the spectrum, even though we see it as uniform or homogeneous in colour.

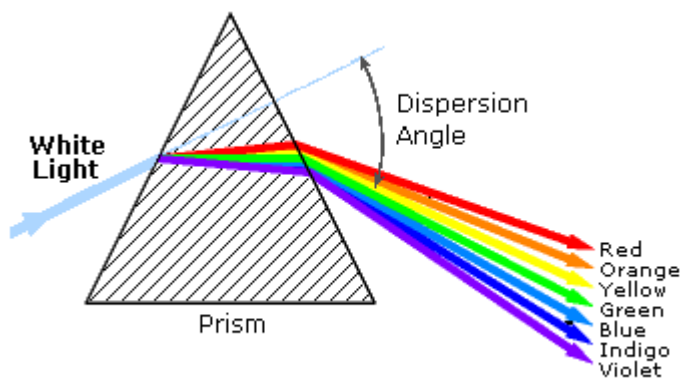


Figure 16: The component colours of the visible portion separated by passing sunlight through a prism.

UV/Vis absorption spectroscopy is the measurement of the decrease in intensity of a beam of light after it passes through a sample or after reflection from a sample surface. Absorption measurements can be at a single wavelength (distance between adjacent peaks or troughs fig 17).

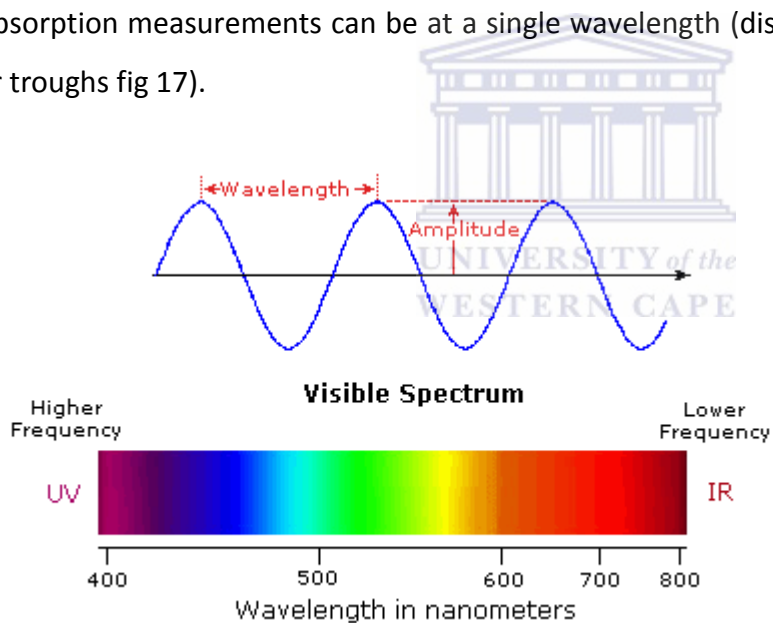


Figure 17: Visible wavelengths within the electromagnetic spectrum.

Various molecules absorb ultraviolet or visible light and the absorbance of a solution increases as attenuation of the beam increases. Absorbance is directly proportional to the path length,  $b$ , and the concentration,  $c$ , of the absorbing species. Beer's law states that:

$$A = \epsilon bc, \text{ where } \epsilon \text{ is a constant of proportionality, called the absorptivity.}$$

Different molecules absorb radiation of different wavelength. The visible spectrum constitutes but a small part of the total radiation spectrum. Dedicated sensing instruments can detect unseen radiation that surrounds us. Electromagnetic spectrum ranges from very short wavelengths (including gamma and x – rays) to very long wavelengths (including microwaves and broadcast radio waves). Fig 19 displays many of the important regions of this spectrum and demonstrates the inverse relationship between wavelength and frequency.

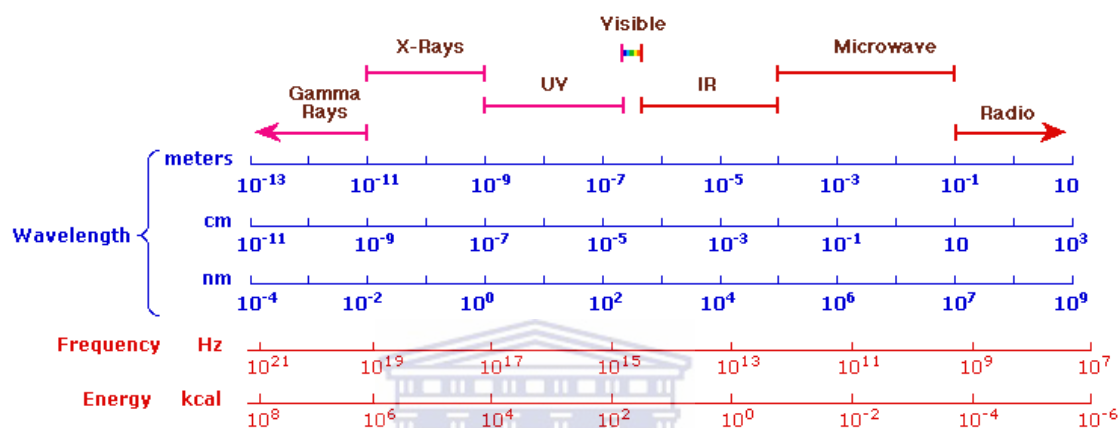


Figure 18: Full electromagnetic spectrum.

Measurements of light absorption at different wavelengths in and near the visible of the spectrum are made to understand why some compounds are coloured and other are not and to determine the relationship of conjugation to colour. The visible region spectrum consists of photon energies of 36 to 72 kcal/mole, and the near ultraviolet region, out to 200nm extend this energy range to 143 kcal/mole. When an atom or molecule absorbs energy, electrons are promoted from their ground state to an excited state. In a molecule, the atoms can rotate and vibrate with respect to each other. These vibrations and rotations also have discrete energy levels, which can be considered as being packed on top of each electronic level. Fig 20 shows the various kinds of electronic excitation that may occur in organic molecules. As a rule, energetically favoured electron promotion will be from the highest occupied molecular orbital (HOMO) to the lowest unoccupied molecular orbital (LUMO), and the resulting species is called an excited state.

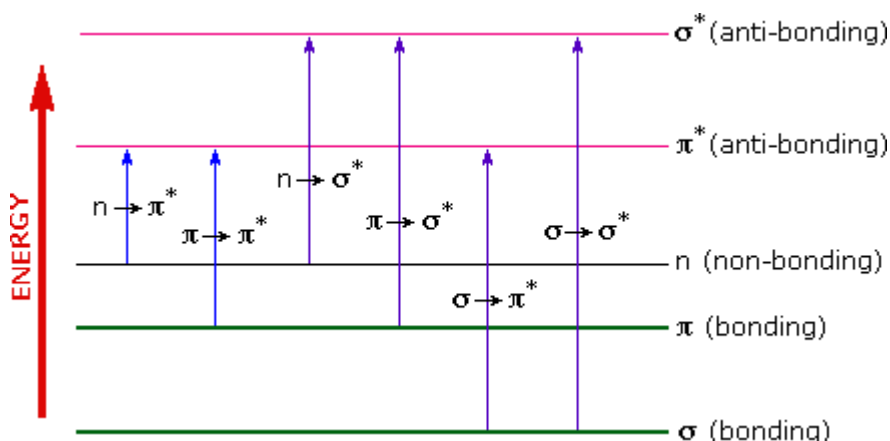


Figure 19: Electronic transitions.

The functioning UV/Vis instrument (fig 21) is relatively straightforward. A beam of light from a visible and/or UV light source is separated into its component wavelengths by a prism or diffraction grating. Each monochromatic (single wavelength) beam in turn is split into two equal intensity beams by a half-mirrored device. One beam, the sample beam, passes through a small transparent container (cuvette) containing a solution of the compound being studied in a transparent solvent. The other beam, the reference, passes through an identical cuvette containing only the solvent. The intensities of these light beams are then measured by electronic detectors and compared. The intensity of the reference beam, which should have suffered little or no light absorption, is defined as  $I_0$ . The intensity of the sample beam is defined as  $I$ . Over a short period of time, the spectrometer automatically scans all the component wavelengths in the manner described. The ultraviolet (UV) region scanned is normally from 200 to 400 nm, and the visible portion is from 400 to 800 nm.

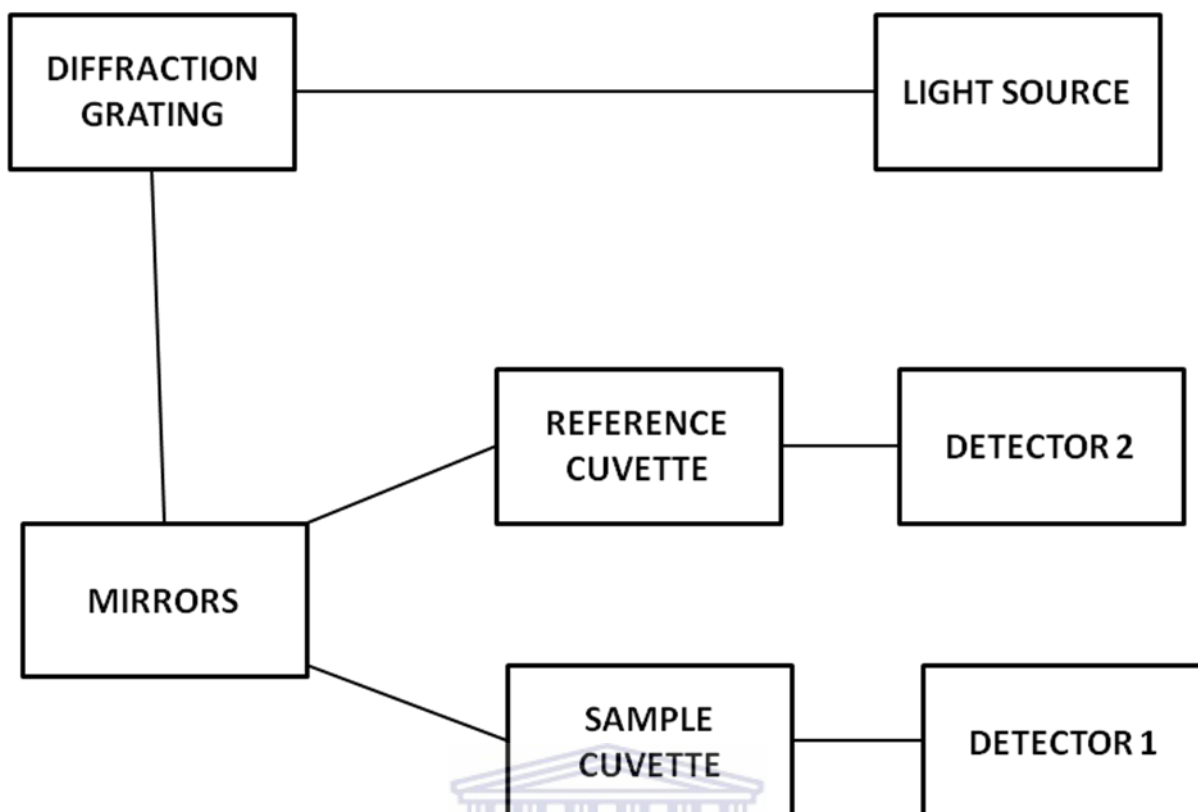


Figure 20: UV/Vis spectroscopy.

#### 2.1.4 Fluorescence spectroscopy

Fluorescence is the emission of light or other radiation from atoms or molecules that are bombarded by particles, such as electrons or by radiation from a separate source. The bombarding radiation produces excited atoms, molecules or ions and these emit photons as they fall back to the ground state. This emission rate of fluorescence is typically  $10^8 \text{ s}^{-1}$ , so that a typical fluorescence lifetime is near 10ns. Fluorescence spectral data are generally presented as emission spectra. Emission spectra vary widely and are dependent upon the chemical structure of the fluorophore and the solvent in which it is dissolved. A schematic portrayal of molecular electronic and vibrational energy levels, which shows the sequence of steps involved in fluorescence, is illustrated by Jablonski diagram (fig 22).

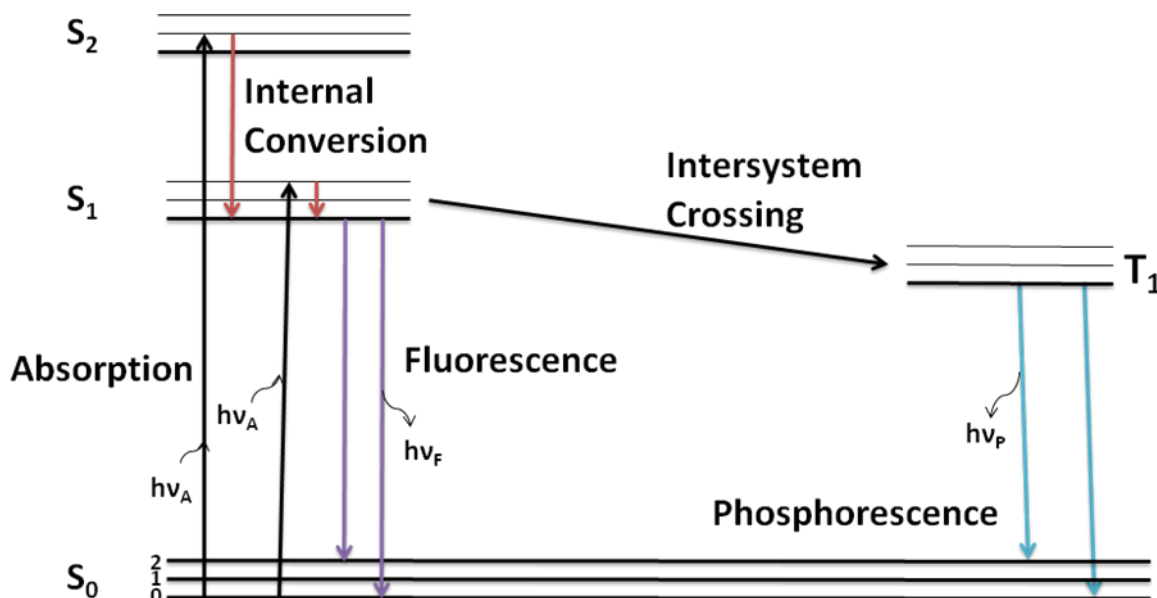


Figure 21: A simplified Jablonski diagram with absorbance, internal conversion, fluorescence, intersystem crossing and phosphorescence.

The ground, first and second electronic states are represented by  $S_0$ ,  $S_1$  and  $S_2$  correspondingly. The fluorophores can subsist in a number of vibrational energy levels (symbolized by 0, 1, 2) at each of these electronic energy levels. Transitions between states are represented as vertical lines to illustrate the instantaneous nature of light absorption. The initial absorption takes the molecule to an excited state, either  $S_1$  or  $S_2$  and it is subjected to collisions with the surrounding molecules and as it gives up the energy it steps down the ladder of vibrational levels. This process is called internal conversion, is nonradiative and takes place in  $10^{-12}$  s or less. The surrounding molecules, however, might be unable to accept the larger energy needed to lower the molecule to the ground electronic state. The excited state might therefore survive long enough to generate a photon and emit the remaining excess energy as radiation. The downward electronic transition is perpendicular, which means in agreement with the Franck – Condon principle, and the fluorescence spectrum has a vibrational structure characteristic of the lower electronic state. Fluorescence takes place at lower frequency. It occurs only after real excitation of the molecule in its excited state and if a molecule is not excited resonantly, it may still end up in an excited vibrational level of the ground state, this is a Raman scattering

process. The bright oranges and greens of fluorescent dyes are an everyday demonstration of this effect: they absorb in the ultraviolet and blue, and fluoresce in the visible.

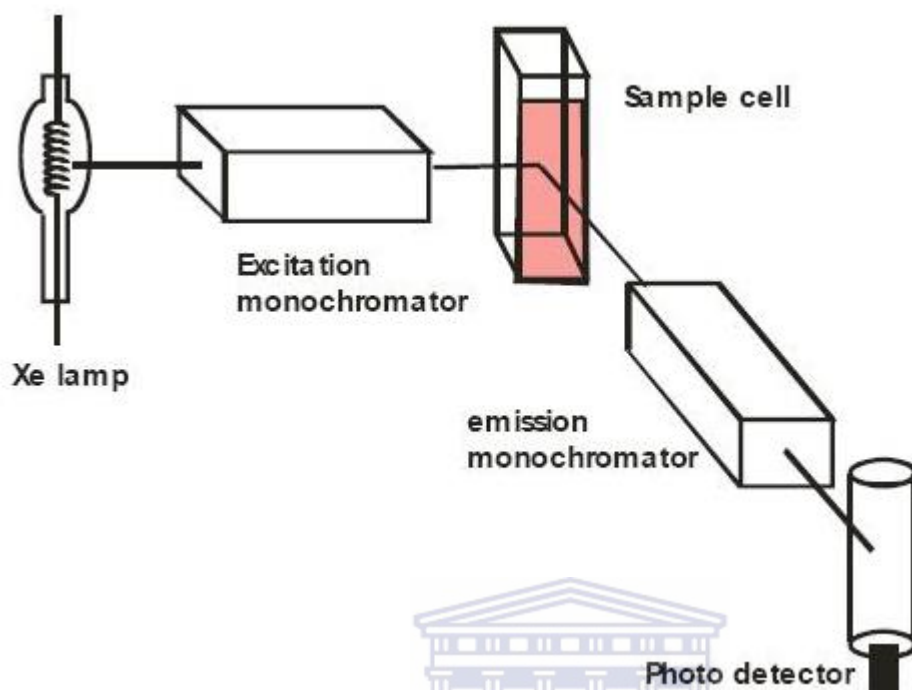


Figure 22: Fluorescence spectroscopy schematic diagram.

Uv light is used to excite the molecules in a solution and deuterium or xenon lamp is normally the excitation source. Broad – band excitation light from a lamp passes through a monochromator, which passes only the selected wavelength. Emission monochromator disperses the fluorescence and is detected by photomultiplier tube. Scanning the excitation monochromator gives the excitation spectrum and scanning the emission monochromator gives the fluorescence spectrum. Simple instruments sometimes use only a band pass filter to select the excitation wavelength.

### 2.1.5 Electrochemical techniques

Electrochemical techniques provide information on the processes taking place when an electric potential is applied to the system under study. They are predominantly utilized by researchers of different scientific fields due to the fact that the equipment used is of low cost, simple and easy to utilize and have the advantage of being *in situ* techniques, which allows monitoring the studied system in real time. The response of different surfaces such

as gold, graphite, carbon nanotubes, gold nanowires, gold nanoparticles, metallic oxide nanoparticles, spin-on glass surfaces, carbon paste which can be modified with different modifiers have been monitored using different electrochemical techniques. In this study cyclic voltammetry (CV), electrochemical impedance spectroscopy (EIS) and square wave voltammetry (SWV) have been used [47; 48].

### **2.1.5.1 Cyclic voltammetry (CV)**

Cyclic voltammetry is possibly the most versatile [48] electrochemical technique often used to get the first information on the nature of the electrode surface [47] such as its purity [49], stability [50], reproducibility, and repeatability [51], study of a compound and biological materials [48]. From time to time CV is used for cleaning the electrode surface [52], for activating [53] and for reconstructing the electrode surface and to determine the electrode active surface area for small molecules (hydrogen, methanol, ethanol etc) which adsorb on the electrode surface [54]. The use of CV results from its ability to rapidly monitor the redox behaviour over a wide potential range [48]. Its operation process is potential-controlled which involves cycling the potential of an electrode [48], which is immersed in an unstirred solution and measuring the resulting current. The potential of this working electrode is controlled versus a reference electrode such as a saturated calomel electrode (SCE) or a silver/silver chloride electrode (Ag/AgCl) [48]. The current response is plotted as a function of the applied potential a typical cyclic voltammogram is shown in fig 23.

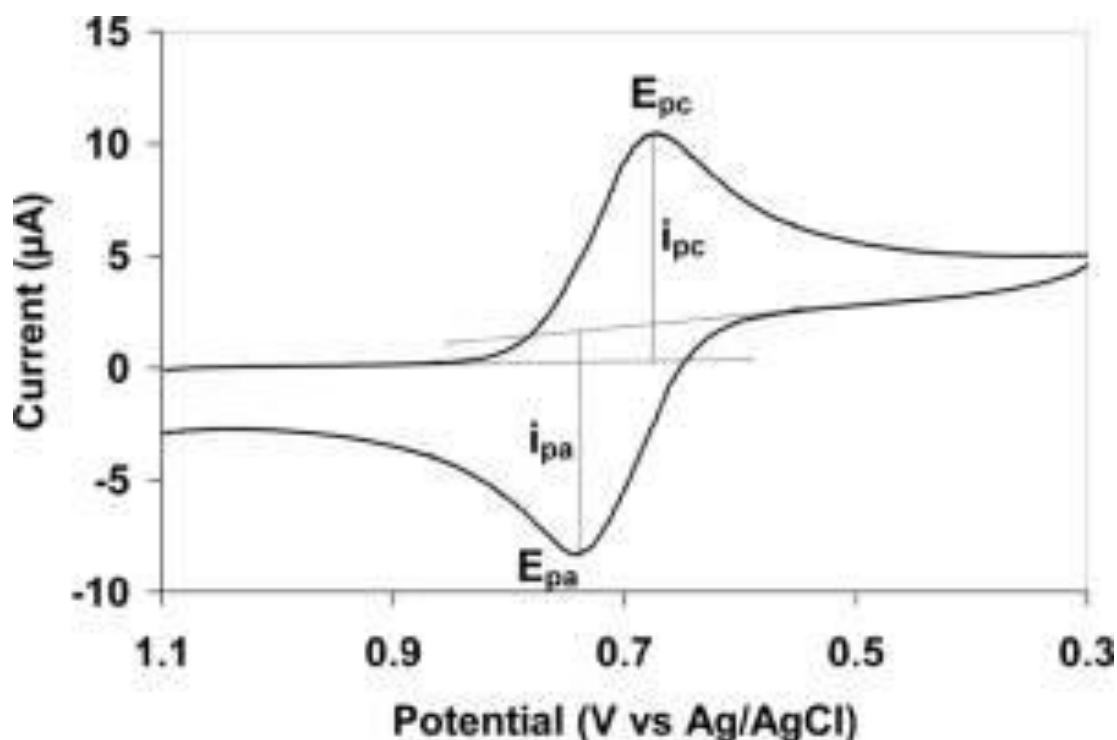


Figure 23: A typical cyclic voltammogram showing reduction and oxidation current peaks. [en.wikipedia.org/wiki/Cyclic\\_voltammetry](http://en.wikipedia.org/wiki/Cyclic_voltammetry).

A barrier may be formed on the electrode surface when it is modified with self-assembled monolayer or other modifiers which in some extension obstruct the charge transfer reaction. The changes in the electrochemical response of a reversible or quasi-reversible redox reaction of some electroactive species present in solution can be studied. An important and convenient tool for monitoring the barrier effect of the modified electrode since the electron transfer between the electrode and species in solution must occur by tunnelling either through the barrier or through the defects in the barrier is cyclic voltammetry of electroactive species such as  $\text{Fe}(\text{CN})_6^{3-/4-}$ , ferrocinium/ferrocene and others which can be used as markers. When the surface is completely covered by the modifier the tunnelling of electron transfer is expected to occur and an electron transfer via pinholes when it occurs at the defects of the modifier layer, situation where the microelectrode approach could be used. The surface coverage can be estimated from CVs resulting in a semi-quantitative analysis of this effect [47].

The magnitudes of the anodic peak current ( $i_{pa}$ ) and cathodic peak current ( $i_{pc}$ ) and the anodic peak potential ( $E_{pa}$ ) and cathodic peak potential ( $E_{pc}$ ) are the important parameters

of a cyclic voltammogram. An electrochemical reversible couple is a redox couple in which both species rapidly exchange electrons with the working electrode. The formal reduction potential ( $E^{\circ'}$ ) for a reversible couple is centered between  $E_{pa}$  and  $E_{pc}$ .

$$E^{\circ'} = \frac{E_{pa} + E_{pc}}{2} \quad \text{Equation (1)}$$

The number of electrons transferred in the electrode reaction ( $n$ ) for a reversible couple can be determined from the separation between the peak potentials

$$\Delta E_p = E_{pa} - E_{pc} \cong \frac{0.059}{n} \quad \text{Equation (2)}$$

Thus, a one-electron process such as the reduction of  $Fe^{3+}(CN)_6^{3-}$  to  $Fe^{2+}(CN)_6^{4-}$  exhibits a  $\Delta E_p$  of 0.059V. Slow electron transfer at the electrode surface, "irreversibility" causes the peak separation to increase. The peak current for reversible system is described by the Randles-Sevcik equation for the forward sweep of the first cycle

$$i_p = (2.69 \times 10^5) n^{3/2} A D^{1/2} C v^{1/2} \quad \text{Equation (3)}$$

where  $i_p$  is peak current (A),  $n$  is electron stoichiometry,  $A$  is electrode area ( $cm^2$ ),  $d$  is diffusion coefficient ( $cm^2/s$ )  $C$  is concentration ( $mol/cm^3$ ) and  $v$  is scan rate (V/s) [48].

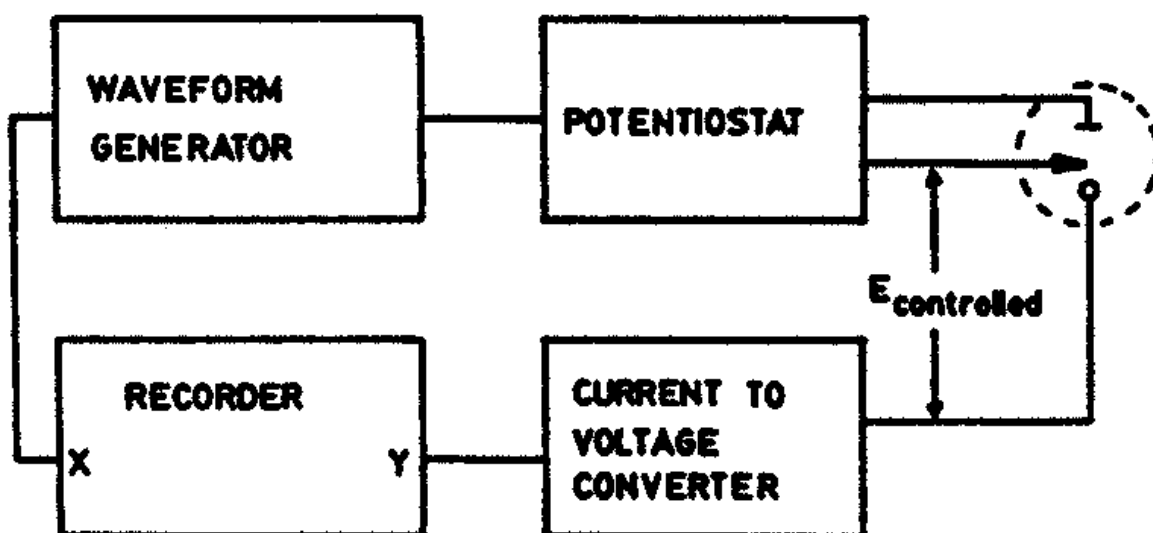


Figure 24: Instrumentation for cyclic voltammetry. Electrode designation  $\circ$ —working,  $\text{—}$  auxilliary,  $\leftarrow$  reference [48].

### 2.1.5.2 Squarewave voltammetry (SWV)

Square wave voltammetry (SWV) is a powerful electrochemical technique that can be applied in both electrokinetic and quantitative determination of redox couples strongly immobilized on the electrode surface. It is among the most sensitive techniques for the direct evaluation of concentrations and it can be widely utilized for the trace analysis. Osteryoung has developed the square wave technique which was invented by Ramaley and Krause and is the most common form of square wave technique [55]. The base potential increase by amplitude for each full cycle of the square wave and the current is measured at the end of each half cycle. SWV is normally applied to a stationary electrode or static mercury drop electrode whereby the time interval is arranged to allow the drop to grow to a predetermined size. The response consists of distinct current-potential points separated by the potential increment  $\Delta E$ . It is characterized by a pulse height  $\Delta E_p$ , measured with respect to the corresponding tread of the staircase and the pulse width  $t_p$  which is expressed in terms of the square wave frequency  $= 1/2t_p$ . The currents increase proportionally to the scan rate which is a number of current-potential points within a certain potential range determined by  $\Delta E$ . In this technique the net current is generally compared with theoretical predictions of a dimensionless current. SWV is employed more often than normal pulse voltammetry (NPV) and differential pulse voltammetry (DPV) techniques because response can be found at a high effective scan rate, thus reducing the scan time. NPV and DPV function with effective sweep rates between 1 and 10  $\text{mVs}^{-1}$ , SWV can reach 1  $\text{Vs}^{-1}$ . SWV uses forward current  $i_2$ , reverse current  $i_1$  or difference current ( $i = i_2 - i_1$ ) as the response [55; 56].

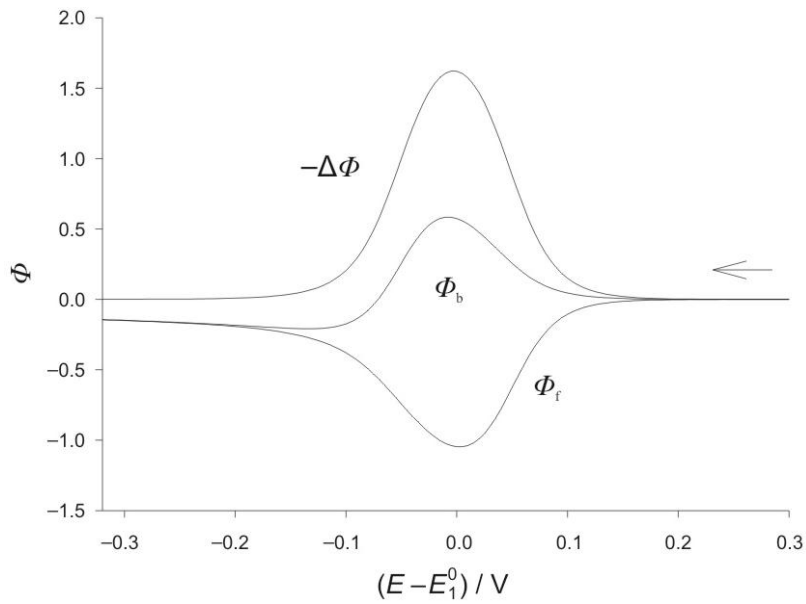


Figure 25: Dimensionless square wave voltammogram for the reversible oxidation-reduction case. [www.hindawi.com/journals/ijelc/2011/538341/fig1/](http://www.hindawi.com/journals/ijelc/2011/538341/fig1/).

Dimensionless representation of the voltammograms is shown in fig 25. The forward and reverse currents have a similar cyclic voltammogram and have much of the same diagnostic value, while the difference current resembles the response from DPV and has similar sensitivity. The difference current voltammogram attains a peak at  $E_{1/2} = E^{o'} + (RT/nF) \ln(D_R/D_O)^{1/2}$  and has a dimensionless peak current,  $\Delta\psi_p$  that depends on  $n$ ,  $\Delta E_p$  and  $\Delta E_s$ . The actual peak current,  $\Delta i_p$  is therefore [56]

$$\Delta i_p = \frac{nFAD_o^{1/2}C_o^*}{\pi^{1/2}t_p^{1/2}} \Delta\psi_p \quad \text{Equation (4)}$$

The experimental and dimensionless currents are related by Cottrell factor for the characteristic time [55]:

$$i = (nFAC^* \left(\frac{D}{\pi t_p}\right)^{\frac{1}{2}}) \varphi \quad \text{Equation (5)}$$

### 2.1.5.3 Electrochemical impedance spectroscopy (EIS)

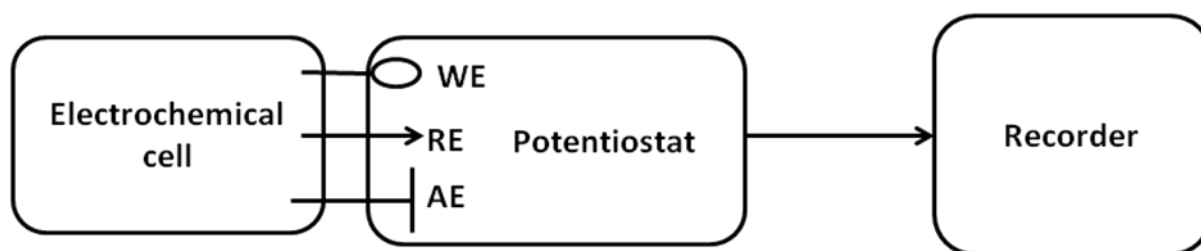


Figure 26: Electrochemical impedance spectroscopy instrument. WE-working electrode, RE-reference electrode, AE-auxiliary electrode.

Electrochemical impedance spectroscopy (EIS) can investigate over a large frequency range covering a vast interval of time constant value and that makes it a very useful technique to study almost all phenomena taking place at an interface. EIS is a powerful tool for investigating mechanisms of electrochemical reactions, measuring transport properties of materials, exploring properties of porous electrodes, investigating passive surfaces and modified electrodes, because it permits to separate different processes such as capacitive, charge transfer, mass transfer, adsorption/desorption and it has often been used to monitor the properties of SAMs, mainly in the presence of a redox couple in the electrolyte solution [47]. It does not allow the identification of chemical species, even though it is regarded as a powerful tool for studying many phenomena as in the case of other electrochemical techniques. The impedance or admittance consists of all the information that can be acquired from the system by linear electrical perturbation/response technique if an unlimited frequency range is investigated.

When a small amplitude of the sine wave (current or potential) is applied to perturb the system with respect to its equilibrium or steady state, a sinusoidal perturbation of certain frequency results in a sinusoidal response with the same frequency, while the amplitudes of the entry and exit signals may be different and may present a phase shift. Assuming a linear system, the theory of electrical circuits which can be represented by a proper arrangement of resistors, capacitors and inductors can be utilised to analyse the response if the perturbation is appropriate. Models developed to describe the electrochemical impedance data are equivalent electrical circuits (EEC) and they must obey at least two conditions: all elements of the EEC must have a clear physical meaning and associated to a property of the

system which should be able to produce electrical response; the EEC must be as simple as possible and generate impedance spectra which are different from the experimental one only by small defined quantity. A sufficient small perturbation in relation to the equilibrium or steady state is applied to the system, one needs to keep in mind that the electrochemical systems are not linear systems and their response can only approximate of linear system. some requirements must be followed or observed to have a trustful impedance experiment such as linearity, stability and causality [47].

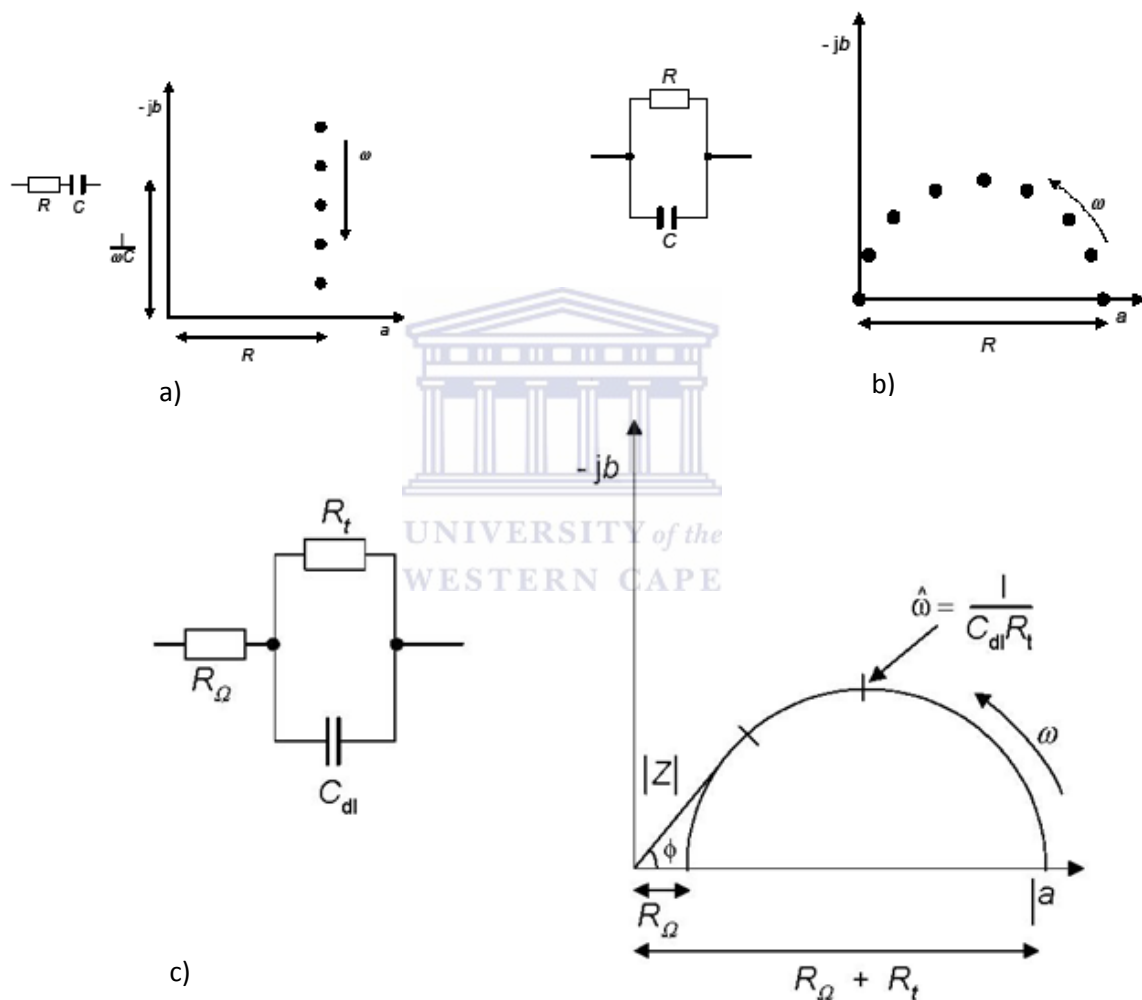
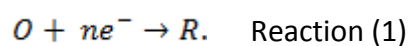


Figure 27: Complex plane impedance spectrum, series resistance, capacitance and parallel resistance capacitance.

No matter how well the measurement is made, the current flowing at an electrified interface due to an electrochemical reaction always contains nonfaradaic components



$n$  is the number of electrons transferred, O is the oxidant, and R is its reduced product (reductant). As illustrated in fig 30 the electron is transferred across the electrified interface and the charge transfer leads to both faradaic and nonfaradaic components. The faradaic component arises from the electron transfer via a reaction (6) across the interface by overcoming an appropriate activation barrier, that is charge transfer resistance  $R_{ct}$ , together with the uncompensated solution resistance  $R_s$  and the nonfaradaic current results from charging the double-layer capacitor  $C_{dl}$ . The mass transports of the reactant and product take on roles in determining the rate of electron transfer which depends on the consumption of oxidants and the production of reductant near the electrode surface when the charge transfer takes place at the interface [57].

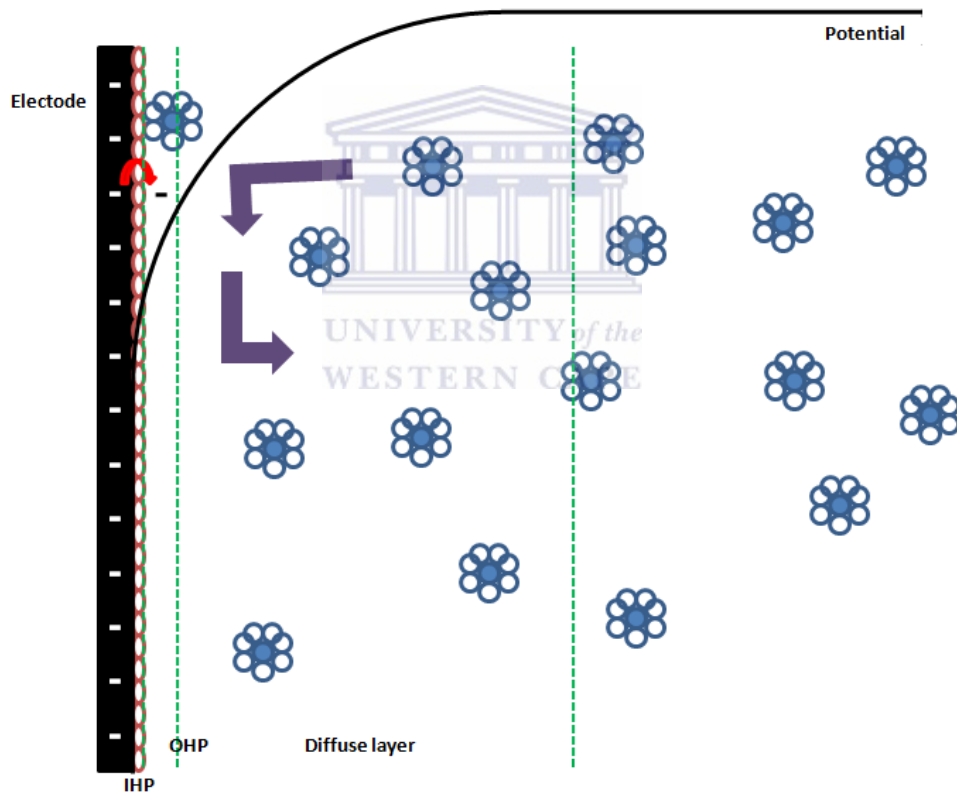


Figure 28: An electrified interface in which the electrode is negatively charged.

### 2.1.6 Powder x-ray diffraction (PXRD)

PXRD is utilised to monitor the phase changes and is a basic tool for the identification of compounds as each compound shows a unique pattern due to its particular structural

features [58]. Secondary "diffracted" beams of x-rays related to interplanar spacings in the crystalline powder according to a mathematical relation called "Braggs Law"

$$n\lambda = 2d \sin\theta \quad \text{Equation (6)}$$

are created when x-rays interact with the sample [59]. Where

$n$  is an integer

$\lambda$  is the wavelength of the x-ray

$d$  is the interplanar spacing generating diffraction and

$\theta$  is the diffraction angle

$\lambda$  and  $d$  are measured in the same unit, angstroms. The Bragg equation is the fundamental equation, valid only for monochromatic x-rays that is used to calculate interplanar spacings utilised in XRD analysis [58].



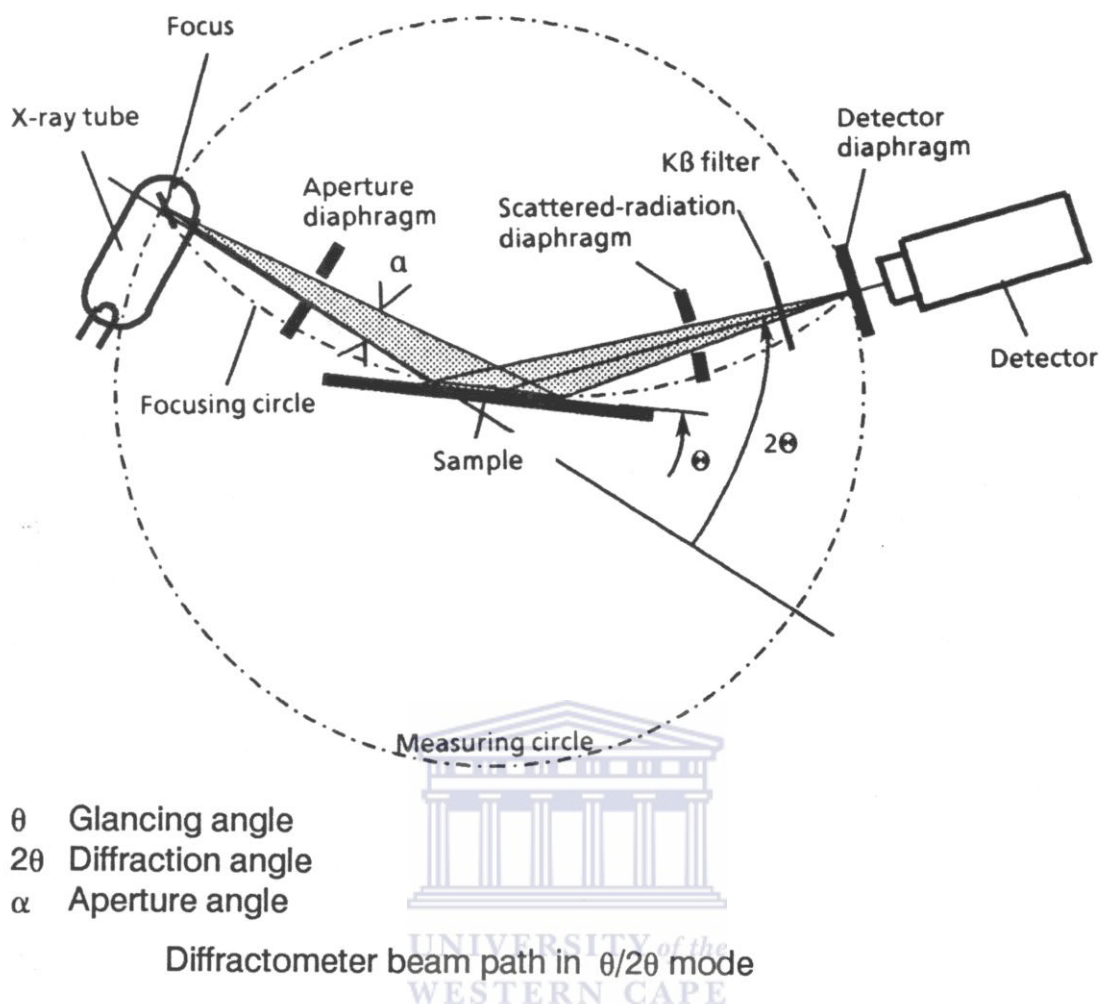
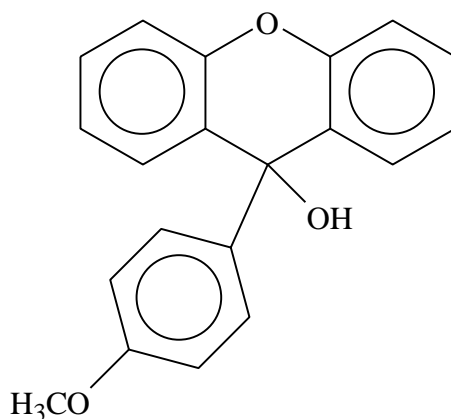


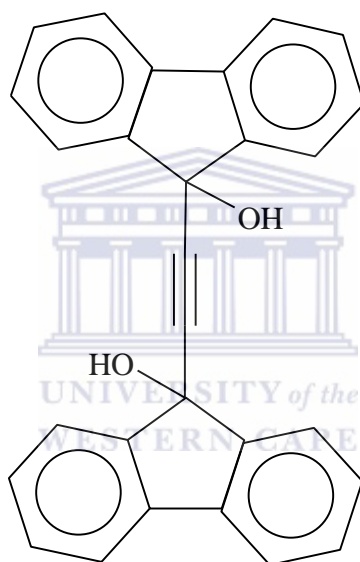
Figure 29: Diffractometer components and geometry [58].

## 2.2 Materials

Noncyclic organic molecules namely: 9-(4-methoxyphenyl)-9H-xanthen-9-ol and 9,9'-(ethyne-1,2-diyl)bis(flouren-9-ol) were selected for this study. These compounds were chosen for their ability to recognize and include other molecules as proven in the previous studies [60; 61; 62]. They are organic host compounds which conform to Weber's rule for host design that is, they are bulky, rigid and have hydroxyl moieties that can act as hydrogen-bond donors. 9-(4-methoxyphenyl)-9H-xanthen-9-ol has an ether oxygen which is a potential hydrogen-bond acceptor. There is no evidence that these two compounds have been used as immunosensor platforms before.



Scheme 3: 9-(4-methoxyphenyl)-9H-xanthen-9-ol



Scheme 4: 9, 9'-(ethyne-1,2-diyl)bis(fluoren-9-ol)

### 2.2.1 Synthesis of flourene derivative

A solution of ethylmagnesium bromide (150 ml) was added to dry THF (200 ml) saturated with concentrated sulphuric acid. The mixture was stirred for 0.5hour. A solution of flourenone (0.36 mol) in dry THF (300 ml) was added. The mixture was heated to reflux for 2 hours then cooled and quenched with saturated aqueous ammonium chloride solution. The ethereal phase was separated and the aqueous phase was extracted with diethyl ether. The combined organic phases were dried (anhydrous sodium sulphate) and the solvents were evaporated. The oily residue was extracted with refluxing *n*-hexane, the residue that did not

dissolve in *n*-hexane was extracted with refluxing THF and cooled to give crystals of the clathrate. Recrystallization from toluene yielded 2g of yellow powder [63].

### 2.2.2 Synthesis of xanthene derivative

Grignard reagent was prepared under nitrogen from 9g of magnesium turnings and 29 ml of anisole in 100 ml of dry THF. A small crystal of iodine and warming of the reaction mixture was required to initiate the reaction. The mixture was refluxed for 2.5 hours after addition of halide solution (potassium chloride) was complete. The Grignard reagent was transferred by syringe to the addition funnel on a dried nitrogen filled flask containing 75 ml of dry THF and 19.6g of xanthone. The Grignard solution was added rapidly dropwise to the ketone. The suspension formed was diluted with an additional 50 ml of dry THF and stirred at room temperature for 7 hours. It was then quenched with aqueous ammonium chloride and extracted with ether. The ethereal phase was washed, dried (magnesium sulphate) and condensed to yield 3.5g of white crystals [64].

### 2.2.3 Parvalbumin

It consists of 113 amino acid residue and one residue of glucose, resistant to heat, chemical denaturation and proteolytic enzymes making it a stable  $\text{Ca}^{2+}$  binding protein with low molecular weight (9 – 12 kDa). Parvalbumin is a hydrophilic protein that is found in high concentrations in the white muscle of aquatic vertebrates. It is broken into three domains, AB, CD and EF, each individual containing a helix – loop – helix motif. Lu and co-workers attempted to investigate the affinities of the MAb EG8-parvalbumin model system from different food using a SPR biosensor. They were successful in detecting the fish major allergen parvalbumin rapidly using MAb EG8 with the detection limit of 3.55 ug/L [65].

Dahlman-Höglund et al had developed a polyclonal sandwich ELISA against the salmon antigen parvalbumin to measure salmon allergen exposure among salmon processing workers. The detection limit was found to be 0.05 ng/ml. It was concluded that the workers were exposed to high levels of salmon major allergen at the filleting machine and at the filleting table. 186 ng/m<sup>3</sup> was found to be the highest exposure to airborne salmon from the person handling the filleting machine. This polyclonal antibody was able to detect both cod and pollack parvalbumin [66]. Monoclonal antibody have affinity for the same antigen, they

bind to the same epitope because they consist of monovalent affinity. Polyclonal antibody recognizes multiple epitopes on anyone antigen and can be batch to batch variability. In this study pierce anti-parvalbumin polyclonal rabbit was used.

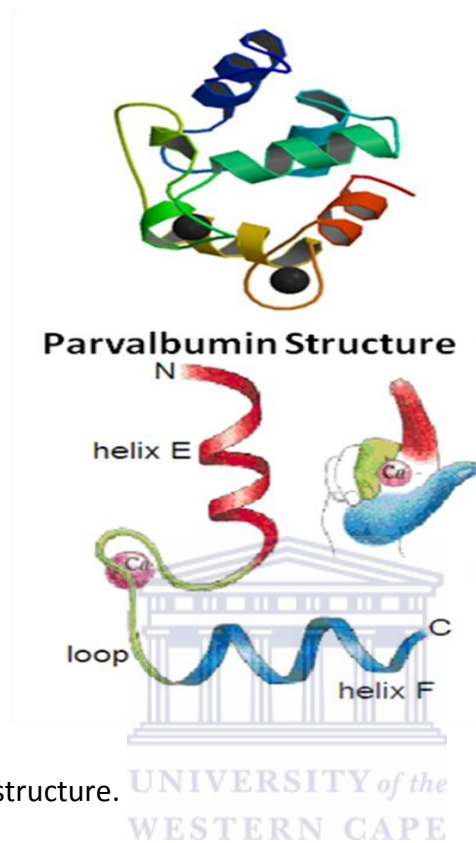
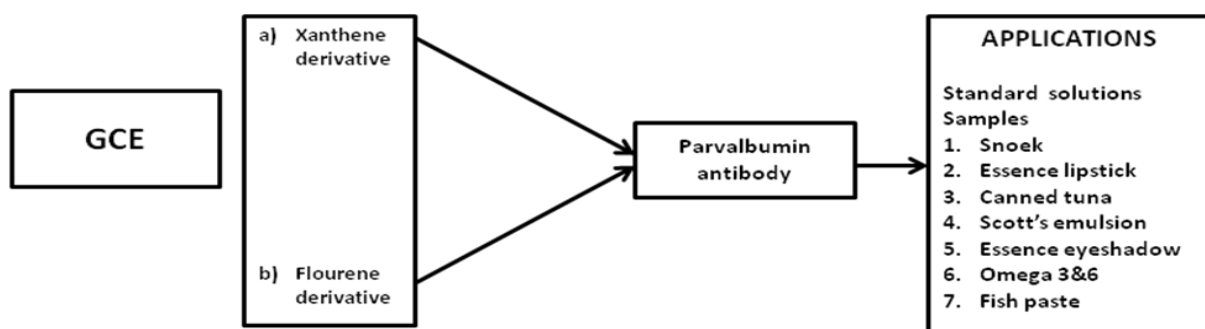


Figure 30: Parvalbumin structure.

The immunosensor was developed by drop-coating a layer of each compound onto the glassy carbon electrode. The modified electrode was incubated into antibody solution. The immunosensor was applied to standard solutions and seven samples for determination of parvalbumin content in real time.



Scheme 5: Immunosensor schematic.

## Chapter 3

*The sandwich ELISA was performed in collaboration with Neubrandenburg University, Department of Agriculture and Food Technology, through student exchange programme funded by NRF South Africa-Germany programme. It was possible to visit Neubrandenburg University and learn about immunoassay techniques in particular sandwich ELISA. In this chapter immunoassay, moulds causing mycotoxins, experimental work done at Neubrandenburg and results of sandwich ELISA will be discussed.*

### 3.1 Immunoassay

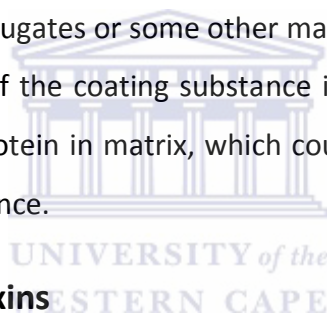
An immunoassay is a specific type of biochemical test that makes use of the binding between an antigen and its homologous antibody in order to identify and quantify the specific antigen or antibody in a sample. Antibodies are produced against a specific antigen beforehand and are used to capture molecules of the antigen samples. On the other hand antigens may be used to capture antibodies present in the sample. The specificity of the assay depends on the degree to which the analytical reagent is able to bind to its specific binding partner to the exclusion of all other substances that might be present in the sample to be analyzed and must have a sufficient high affinity for the analyte to permit an accurate measurement. Antibody contains in their structure recognition / binding sites for specific molecular structure of the antigen. An antibody interacts in a highly specific way with its unique antigen according to the 'key – lock' model. The interaction is reversible, as determined by the law of mass action, and is based on electrostatic forces, hydrogen bonding, hydrophobic and van der Waals interactions. Before assay development starts a good knowledge of the analytical target, its chemical structure, its stability and its degradation routes are required. ELISA formats are used for immunoassays.

#### 3.1.1 Optimisation of Immunoassay

Most importantly when developing an immunoassay is to produce a specific, sensitive and stable assay, which fulfils the demand of the target analyte detection. Many features have to be considered for assay optimisation due to numerous steps of assay and their inconsistency of material and methods. The natural occurrence of some targeting substances is in a very low concentration range e.g nano molar or pico molar therefore the

test systems require a very high sensitivity of assay. Freshly prepared reagents (all buffers, blocking solutions and standards) are strongly recommended for ELISA tests. The chemical or biological reagents should be carefully stored to avoid the changing or losing of their chemical or biological activity. Most of all a correct dilution of antibody plays an essential role on assay sensitivity.

According to the biological natures of the antibodies and enzymes a correct physiological condition is very important for ELISA. The buffers and blocking solutions also have drastic effect on ELISA not only the primary antibody, the secondary antibody, coating antigen and enzyme – tracer influences the assay sensitivity. Standard buffer, buffer for sample and conjugation dilution, wash buffer, coating and blocking buffer are important buffers and they must fulfil the criteria like pH, salt content, buffer range, and viscosity correspondingly to the assays. The surface of microtiter plate can be immobilised (coated) with antigens, antibodies, hapten – protein conjugates or some other materials like streptavidin depending on ELISA format. A high purity of the coating substance is required because the biological products might contain other protein in matrix, which could also bind on the plate surface besides the target coating substance.



### **3.2 Moulds causing mycotoxins**

Mycotoxins chemical characteristics and biology activities are very wide and able to cause different pathology and pathohistology changes in fish. They are vital toxins of environment. The amounts of these substances that can harm health are quite small; they enter organisms by ingestion and inhalation. Mycotoxins can cause cancerogenic, mutagenic and tetragenic effects. Their production depends on existence of toxin generating fungi, convenience of substrate for fungal growth and environmental conditions for fungal growth. The vital mycotoxicoses in fish are caused by aflatoxins, ochratoxins, zearalenone and trichotecenes. Toxic effects of certain mycotoxins differ according to age and species of fish. Younger fish are more sensitive.

### 3.2.1 Aspergillus

It is a group of fungi found in various climates world – wide, especially in the autumn and winter in the Northern hemisphere. Fungi is a spore bearing organisms lacking of chlorophyll, usually filamentous; naturally reproducing both sexually and asexually, living as parasites in plants, animals, or as saprobes on plant or animal remains, in aquatic, marine, terrestrial or sub aerial habitats. In humans and animals only a few of these fungi can cause illness but most people are protected in nature and do not develop disease caused by aspergillus. Aspergillus species grow as mould in oxygenated environments on the surface of a substrate and they are toxins of starchy foods (such as bread and potatoes).



Figure 31: Aspergillus moulds growing on maize.

Their species are vital medically (more than 60 aspergillus species) and commercially (microbial fermentations) but some can cause infection (to the external ear, skin lesions and ulcers classed as mycetomas) in humans and other animals. Aspergillus fumigates and aspergillus flavus are common causing pathogenic species. Aflatoxin is produced by aspergillus flavus and is both toxin (acute liver damage) and a carcinogen and which can contaminate foods such as nuts. Disease on many grain crops, especially maize (fig 31) are caused by aspergillus spp. and it also synthesise mycotoxins including aflatoxin. Aflatoxin reduces polymerase enzyme and RNA synthesis that leads to cell changes by penetrating into the cells and binds to the DNA molecules.

### 3.2.2 Penicillium

Penicillium is a group of green or blue ascomycetous fungi of major importance in the natural environment as well as food and drug production. It produces penicillin, an

antibiotic which kills or stops the growth of certain kinds of bacteria inside the body and is also helpful in the ripening of cheeses. Penicillium has a brush – like asexual fruiting structure (fig 32). They prefer cool and moderate climates, commonly present wherever organic material is available. Highly toxic mycotoxins are produced by their species and they cause food spoilage. Penicillium species are present in the air and dust of indoor environments, such as homes and public buildings.

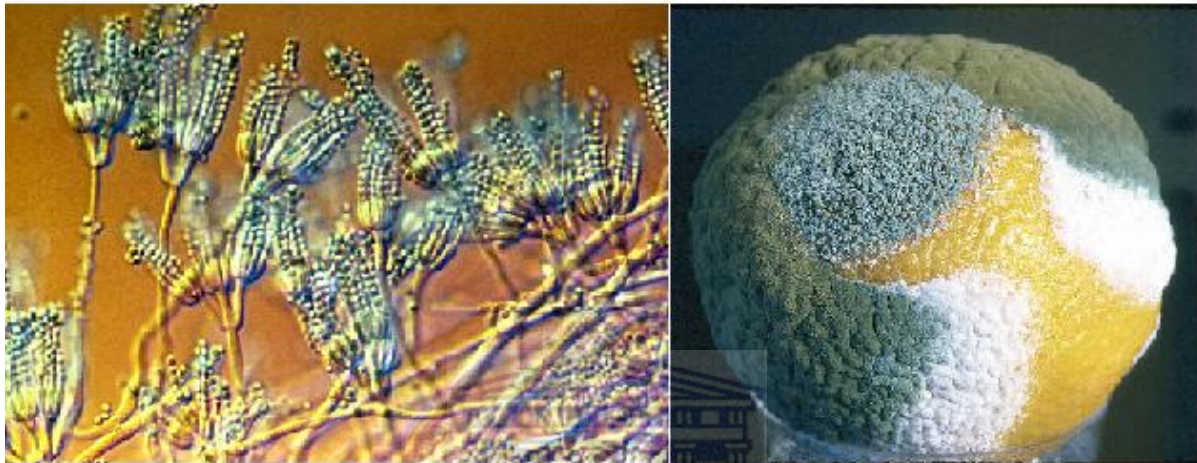


Figure 32: Penicillium moulds grown on oranges.

Human foods (wheat, rice, corn, barley, oats, and rye) are affected by some penicillium species. Quite a few species of the group penicillium play an important role in the production of cheese (blue cheese) and of various meat products (improve taste of sausages and hams). Penicillium produces citrinin, ochratoxin A and patulin mycotoxins. Their contamination increases during storage. Ochratoxin A is potentially carcinogenic to humans and has a strong affinity for the brain. The toxin has been found in the tissues and organs of animals including human blood and breast milk. Introduction of ochratoxin A into human can take place through consumption of contaminated food products, particularly contaminated grain and pork products as well as coffee, wine grapes and dried grapes.

Fish species are plentiful and exist in multiple eatable forms that are consumed in most countries of the world. Fish plays a vital role in the human food providing a valuable source of proteins, used as medicine, ground into vitamins or processed into cosmetics and perfumes, lubricants varnishes, soap and margarine. It also causes food allergies common in children and young adults with a variety of symptoms (urticaria, allergic contact dermatitis,

rhinoconjunctivitis, asthma, oral allergy syndrome, diarrhea or anaphylaxis). Humans are affected by fish allergens through inhalation of airborne allergens during outdoor drying, skin contact while filleting and cooking fish or ingestion of fish meals.

Cod (group *Gadus*) is a cold – water fish belonging to the family Gadidae. Atlantic cod (*Gadus morhua*) and Pacific cod (*Gadus macrocephalus*) are the two most important species of cod. Cod is valuable for its eatable flaky white flesh with a mild flavour, the oils of its liver, an important source of vitamin A, vitamin D, vitamin E and Omega – 3 fatty acids. These may be extracted to produce nutrient supplements such as Scott’s emulsion and omega 3&6 oils [67].



Figure 33: Atlantic cod.

Allergen M (*Gad c 1*) is the major allergen of codfish and has been found to be a parvalbumin. It consists of 113 amino acid residue and one residue of glucose. Fish muscle parvalbumin is resistant to heat, chemical denaturation and proteolytic enzymes making it a stable acidic  $\text{Ca}^{2+}$  binding protein (12 kd). In white muscles of lower vertebrates parvalbumins are present in high amounts and in fast twitch muscles of higher vertebrates they are present in lower amounts. Patients allergic to codfish can consume some other species without risk of allergic symptoms.

Alaska Pollock (*Theragra chalcogramma*) is a relatively fast growing and short – lived species of the cod family Gadidae. It has a white soft flesh, milder in flavour and lower oil content. At McDonald’s (fast food restaurant franchise worldwide) Alaska Pollock is used in the Filet

– O – Fish sandwich. Parvalbumin beta – 1 (allergen the c 1) is the major allergen of Alaska Pollock fish. Parvalbumin is thought to be involved in relaxation after contraction in muscle.



Figure 34: Alaska Pollock

Alaska Pollock and Atlantic codfish, they both have similar flavour, odour and texture. The Alaska Pollock is a relative of the Atlantic cod but is smaller averaging 4 – 12 pounds as compared with average of 10 – 22 pounds codfish.

### 3.3 Standard sandwich ELISA

An enzyme is used to detect the binding of antigen (Ag) antibody (Ab). It converts a colourless substrate to a coloured product, signifying the presence of Ag:Ab binding. The procedure has mainly five steps followed by the evaluation of results. After each steps the micro titer plate is washed with an ELISA – washer using a washing buffer (phosphate buffered saline, 8 mmol/L, pH 7.6 + 0.05 % Tween 20). Program number four of the ELISA – washer was chosen, because it has three washing periods. It is a recommendation to protect the micro titer plate by using aluminium foil as a cover during the whole experiment. When filling the micro titer plate, it is wise to use the same order with different substances. Coating of the micro titer plate with the primary monoclonal antibody (3D12G7) was the first step. A 1:1000 dilution with coating buffer (1.70g  $\text{Na}_2\text{CO}_3$ , 2.86g  $\text{NaHCO}_3$  in 1L) was prepared, and 150  $\mu\text{L}$  was added into each well of the micro titer plate. The plate was covered with a foil and incubated at 4°C over night. After incubation, micro titer plate was washed followed by the blocking step to prevent cross reactions or false binding. 1% solution of bovine serum albumin (BSA) in phosphate buffered saline (1.265g  $\text{NaH}_2\text{PO}_4\cdot\text{H}_2\text{O}$ , 12.1g  $\text{Na}_2\text{HPO}_4\cdot\text{H}_2\text{O}$ , 8.5g  $\text{NaCl}$  in 1L) was prepared. Into each well 200  $\mu\text{L}$  of this solution

was added and the micro titer plate was incubated at room temperature for an hour. After washing, 1mg of fish antigen diluted with 1 mL PBS was prepared and 150  $\mu\text{L}$  of this solution was added into each well, it was then incubated for an hour in room temperature. The plate was again washed and the secondary monoclonal antibody (4B10CG fr.3 POD) was prepared, the procedure was the same as the one for the primary monoclonal antibody. 150  $\mu\text{L}$  of this solution was added into each cavity of the micro titer plate and incubated for an hour at room temperature. Fifth step, after washing 200  $\mu\text{L}$  substrate solution (400  $\mu\text{L}$  tetramethylbenzidin, 100  $\mu\text{L}$  1%  $\text{H}_2\text{O}_2$  in 25 mL substrate buffer [8.2 g/L  $\text{CH}_3\text{COONa}$ , pH 5.5 with citric acid]) was added into each cavity freshly prepared before use. The micro titer plate was incubated at room temperature for 30 min, blue colour was observed. The reaction was stopped with 50  $\mu\text{L}$  4N  $\text{H}_2\text{SO}_4$  into each cavity, the colour changed from blue to yellow. The ELISA – reader was used to measure the intensity at 450 nm.



Figure 35: ELISA – washer, program number four with three washing periods was chosen.



Figure 36: Fifth step of the sandwich – ELISA, colour change after the addition of the substrate solution indicating positive results.

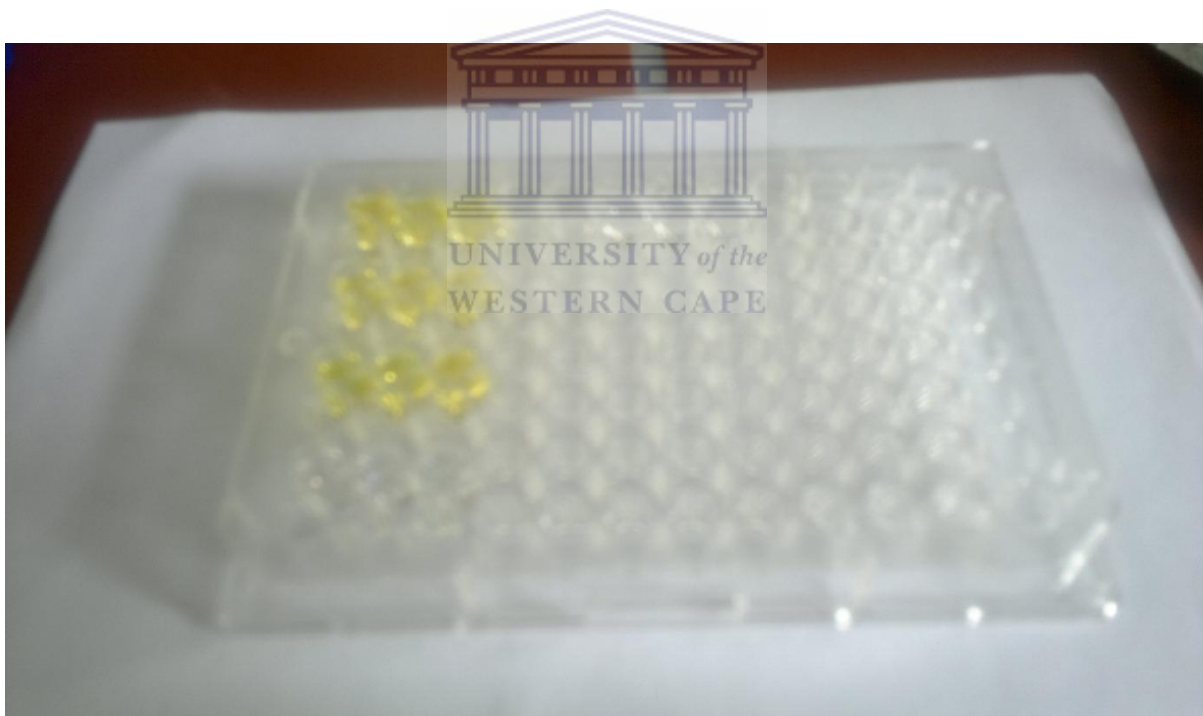


Figure 37: Shows the colour change from blue to yellow after the addition of the stopping solution (4N H<sub>2</sub>SO<sub>4</sub>).

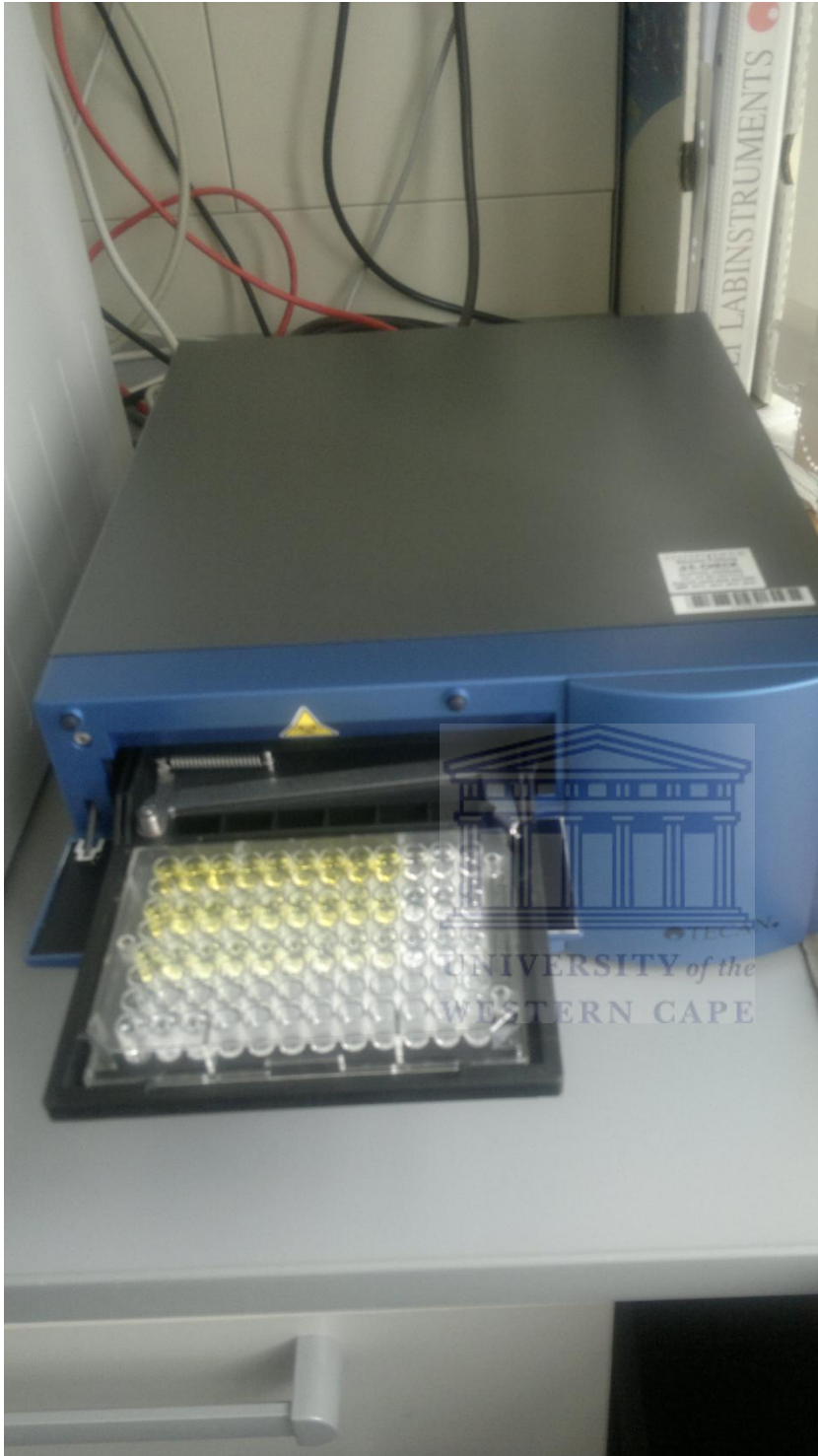


Figure 38: ELISA – reader, wavelength set at 450 nm.

### 3.3.1 Results

The detection of allergen in fish is vital. A sandwich ELISA was used to determine the right pair of antibodies to be utilised. Table 2 shows the absorption measured with the ELISA – reader, concentration ranged from 1  $\mu\text{g}/\text{mL}$  – 1000  $\mu\text{g}/\text{mL}$ . Figure 39 is a plot of absorption against concentration. These results prove the combination of 3D12G7 (primary antibody) and 4B10C9 Fr. 3 (secondary antibody) is able to detect the fish antigen. For codfish from low concentration to high concentration absorbance between 0.012 – 1.241 was observed and the sensitivity of 0.27 was estimated with detection limit of 0.18  $\mu\text{g}/\text{ml}$ . And for Alaska Pollock absorbance between 0.0447 – 0.906 was observed and the sensitivity of 0.44 was calculated with detection limit of 0.012  $\mu\text{g}/\text{ml}$ . New experiments can be done with these antibodies for fish samples. The control sample containing PBS only showed absorption results very close to zero indicating the positive binding of antibody combination with the fish antigen and their sensitivity. Faster detection methods for fish allergens are to be developed, because they are in demand in the food industry, sandwich ELISA is time consuming. This experiment was performed as a guideline as to which antibody can be utilized in the immunosensor preparation.

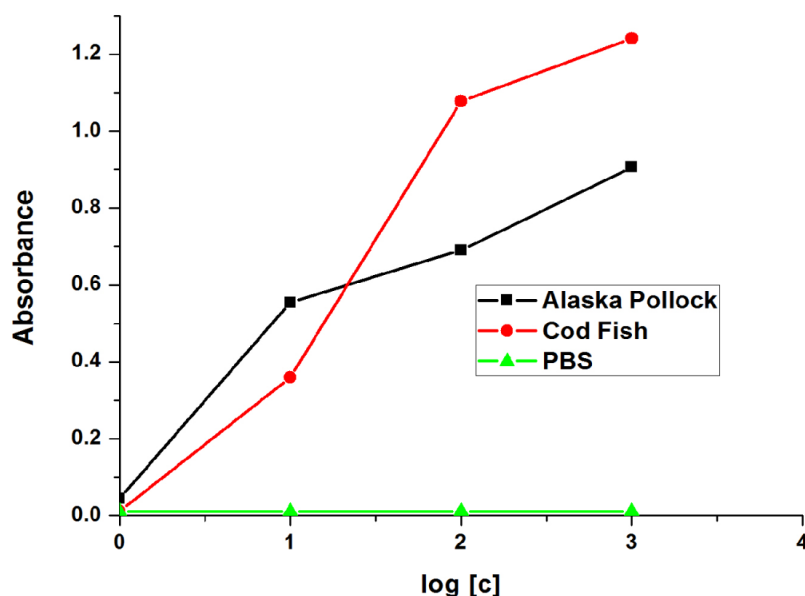


Figure 39: Absorbance versus concentration of fish allergens with PBS as the control sample. Data from table 2.

|                | Concentration | ALASKA POLLOCK       |       |       | CODFISH             |       |       |
|----------------|---------------|----------------------|-------|-------|---------------------|-------|-------|
| 1.             | 1 µg/mL       | 0.026                | 0.053 | 0.055 | 0.01                | 0.013 | 0.013 |
|                |               | <b>Mean = 0.0447</b> |       |       | <b>Mean = 0.012</b> |       |       |
|                |               | <b>SD = 0.0087</b>   |       |       | <b>SD = 0.0011</b>  |       |       |
| 2.             | 10 µg/mL      | 0.527                | 0.585 | 0.550 | 0.355               | 0.374 | 0.349 |
|                |               | <b>Mean = 0.554</b>  |       |       | <b>Mean = 0.359</b> |       |       |
|                |               | <b>SD = 0.0146</b>   |       |       | <b>SD = 0.0070</b>  |       |       |
| 3.             | 100 µg/mL     | 0.671                | 0.641 | 0.758 | 1.06                | 1.077 | 1.098 |
|                |               | <b>Mean = 0.690</b>  |       |       | <b>Mean = 1.078</b> |       |       |
|                |               | <b>SD = 0.032</b>    |       |       | <b>SD = 0.0092</b>  |       |       |
| 4.             | 1000 µg/mL    | 0.821                | 0.991 | 0.906 | 1.213               | 1.238 | 1.271 |
|                |               | <b>Mean = 0.906</b>  |       |       | <b>Mean = 1.241</b> |       |       |
|                |               | <b>SD = 0.060</b>    |       |       | <b>SD = 0.014</b>   |       |       |
| <b>CONTROL</b> |               | 0.009                | 0.008 | 0.013 |                     |       |       |
|                |               | <b>Mean = 0.010</b>  |       |       |                     |       |       |
|                |               | <b>SD = 0.0014</b>   |       |       |                     |       |       |

Table 2: Absorption results from the ELISA – reader with calculated mean and standard deviation.

## Chapter 4

Flourene derivative and xanthene derivative were synthesized by reflux method and through stirring at room temperature. The products were obtained as solid powder materials and its characterization using spectroscopic and electrochemical techniques is presented in this chapter.

### 4.1 Characterization of Flourene derivative

Flourene derivative compound was characterized using differential scanning calorimetry for enthalpy of melting and the compound purity, Infra-red spectroscopy to confirm the structure by identifying functional groups, Ultra violet visible spectroscopy to determine if the compound absorbs light in solution, flourescence spectroscopy to determine if the compound fluoresce in solution. Squarewave voltammetry and cyclic voltammetry was used to study the compound's electroactivity and Powder X-Ray Diffraction was used to identify the compound.

#### 4.1.1 Differential Scanning Calorimeter

We investigated the thermal profile of the powder synthesized by DSC. Flourene derivative yielded a single broad endotherm corresponding to its melting point (fig 40). The endotherm is broad due to the fact that the powder is impure and that is confirmed by the lower melting point. Weber and co-workers [63] has found the melting point to be in the range of 244 - 245 °C. The purity of the synthesized compound was not our concern, we were focussing on getting a product that is compatible with antibody.

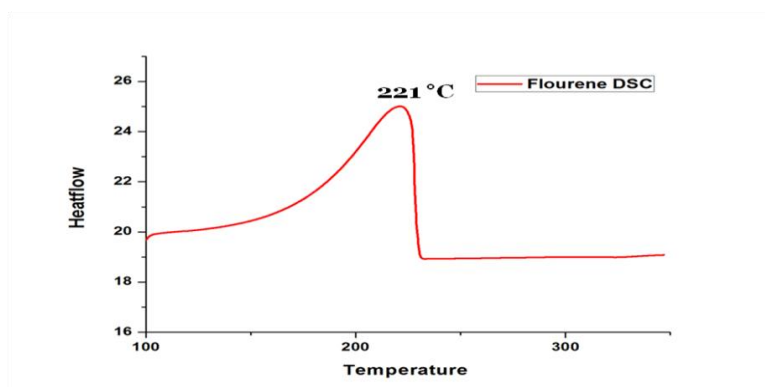


Figure 40: DSC curve showing melting point of flourene derivative.

### 4.1.2 Fourier transform infrared spectroscopy

The sample holder was cleaned using acetone, the sample was then transferred onto the sample holder and it was pressed, then the spectrum was recorded. FTIR spectra of the flourene derivative compound supported its structure. Fig 41 shows characteristics absorption bands around 3200  $\text{cm}^{-1}$  due to O-H stretching, 2169  $\text{cm}^{-1}$  due to  $\text{C}\equiv\text{C}$  stretching, around 1603-1447  $\text{cm}^{-1}$  due to  $\text{C}=\text{C}$  aromatic stretch and around 1149-922  $\text{cm}^{-1}$  corresponding to C-O stretch from alcohol.

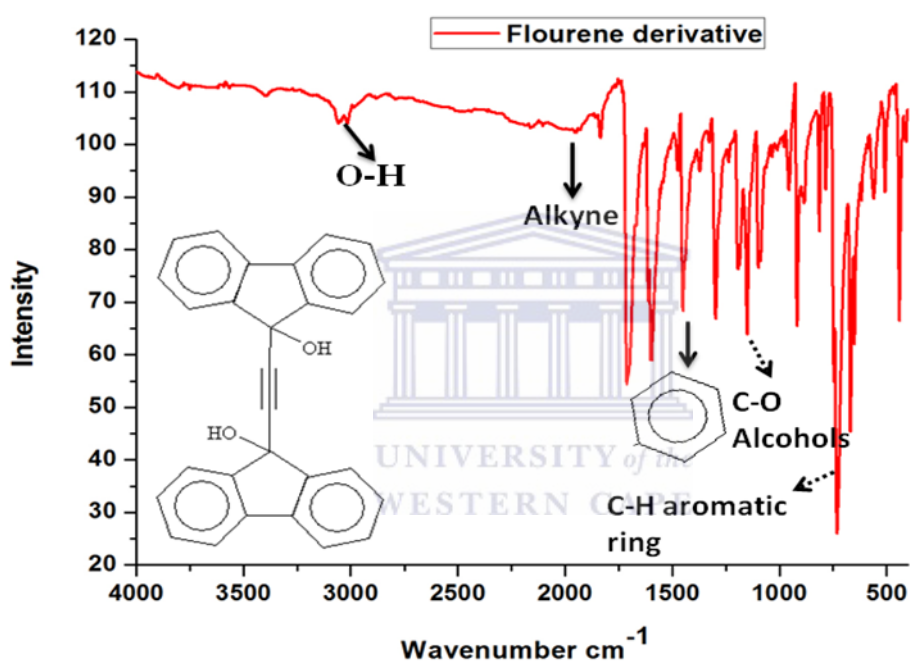


Figure 41: IR spectrum showing flourene derivative functional groups.

### 4.1.3 Ultraviolet visible spectroscopy

UV/Vis analysis was performed by dissolving flourene derivative in methanol. A yellow solution was observed. Fig 42 shows a broad peak with absorption maxima of 400 nm which is attributed to the  $\pi\text{-}\pi^*$  transition with the band gap of 3.1 eV. The band gap was calculated using the formula

$$EG = 1240/\lambda \quad \text{Equation (7) [68].}$$

Similar absorption spectra was observed for difluorene substituted carbazole [69] and poly[2,7'-(ethyl 9,9-dioctyl-7,2'-bifluorene-9-carboxylate)][70].

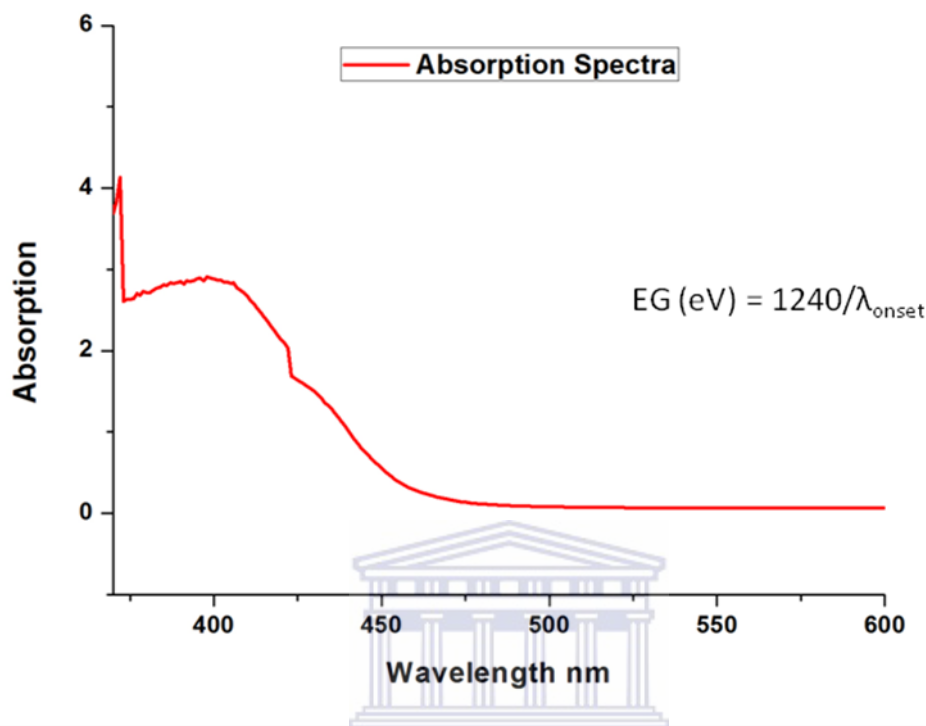


Figure 42: UV – Vis Spectra. Absorption maxima of flourene derivative in methanol is 400 nm which is attributed to the  $\pi$ - $\pi^*$  transition with energy gap of 3.1eV. Flourenyl is rigid and bulky.

#### 4.1.4 Flourescence spectroscopy

Figure 43 reveals the excitation and emission spectra of flourene derivative with excitation maxima of 433 and emission maxima of 441 nm. It also reveals a vibronic structure which is correlated with a coupled C=C stretching mode ( $1603\text{-}1447\text{ cm}^{-1}$ ) and small Stokes shift of 8nm[71]. Well-defined vibronic structure specifies a rigid and well-defined backbone [70]. Small stokes shift is a result of J-aggregates whereby molecular arrangement in which the transition moment of individual monomers are aligned parallel to the line joining their centers. A similar spectra has been observed for poly[(1,4-phenylene)-2,7-(9,9-dioctylfluorene)][70].

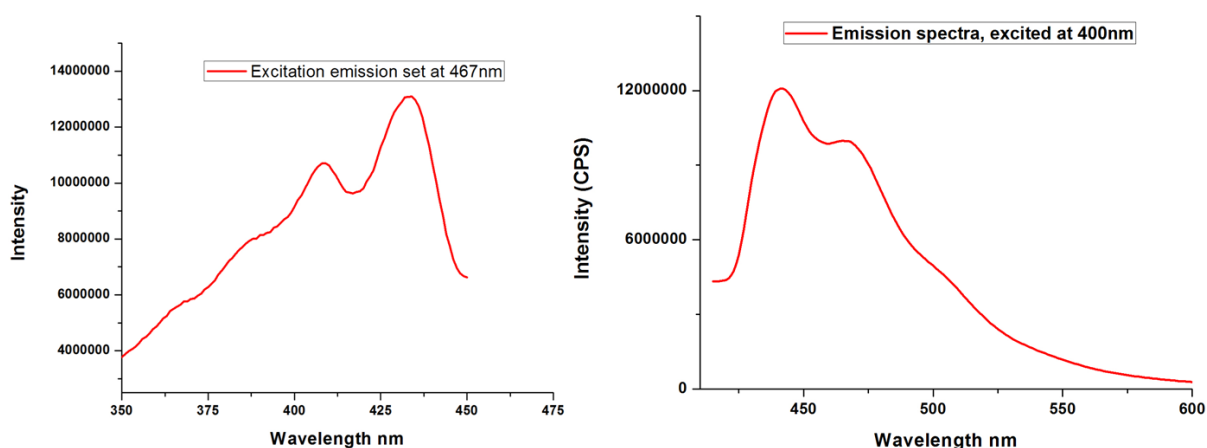


Figure 43: Emission and excitation spectra for flourene derivative.

#### 4.1.5 Cyclic voltammetry and Squarewave voltammetry

Electrochemistry of flourene derivative was investigated. The preparation was the same for CV and SWV analysis. A layer flourene derivative compound was deposited by drop-coating on the glassy carbon electrode and the electroactivity was evaluated. The measurements were carried out in pH 7.12, 0.2 M phosphate buffer at the potential window; -700 mV to 800 mV at scan rates of 20, 40, 60, 80 and 100 mVs<sup>-1</sup> for CV and at scan rates of 75, 150 and 300 mVs<sup>-1</sup> for SWV. Fig 44 shows a typical cyclic voltammogram of flourene derivative respectively. Reversible oxidation-reduction peaks were observed with peak separation of 75.4 mV for one electron redox which means that the system is quasi reversible. Peak separation of 80 mV for the reversible wave of flourene derivative FDF was observed [72]. The peak current magnitude was observed to increase upon increment of the scan rate signifying the peak currents are diffusion controlled. Diffusion coefficient and surface concentration were calculated from plots of current versus square root of scan rate from CV data and based on the slope of peak current versus dimensionless peak current plot from SWV data (fig 45). The calculated diffusion coefficient for flourene derivative was found to be 1.37x10<sup>-21</sup> cm<sup>2</sup>s<sup>-1</sup> from CV data and 1.78x10<sup>-16</sup> cm<sup>2</sup>s<sup>-1</sup> from SWV data with the formal potential of -134 mV and the surface concentration was estimated to be 1.55x10<sup>-13</sup> molcm<sup>-2</sup>.

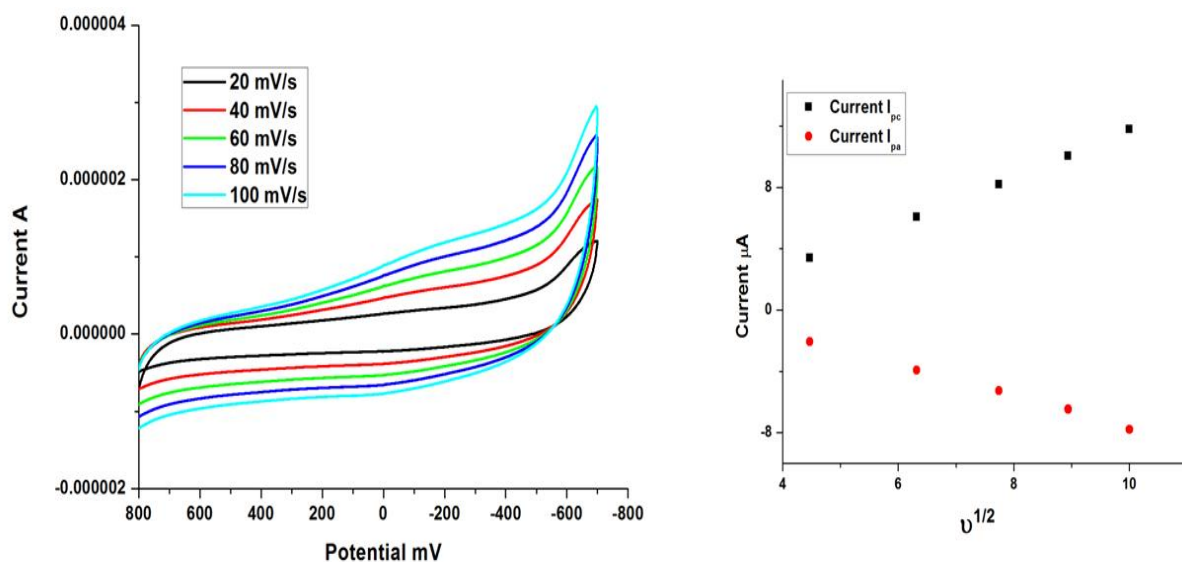


Figure 44: Cyclic voltammograms flourene derivative on GCE in 0.2 M PBS pH 7.12. Scanrate ( $v^{1/2}$ ). Plot of  $i_{pc}/i_{pa}$  versus scanrate $^{1/2}$  from voltammograms.

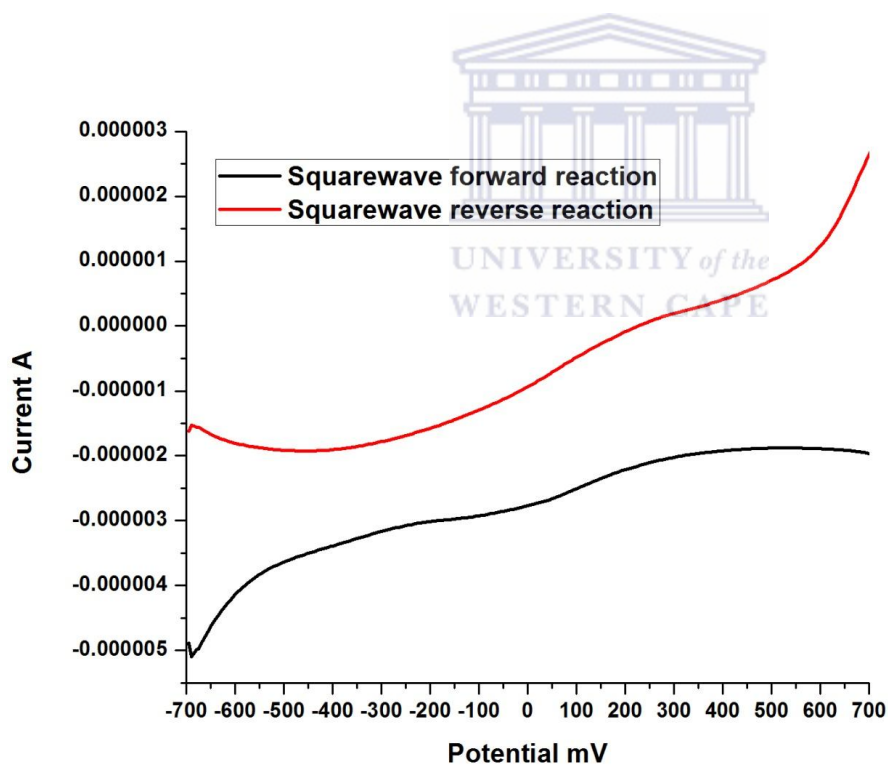


Figure 45: SWV data with the formal potential of -134 mV.

### 4.1.6 Powder x-ray diffraction

PXRD was used to observe the phase changes (size, shape and symmetry of the unit cell). Manually ground powdered samples were placed on X-ray insensitive Mylar film. The intensities of the diffraction spots were measured using BRUKER D8-ADVANCE diffractometer CuK $\alpha$ 1 (1.54 Å) radiation produced at 40 kV and 40 mA. PXRD experiments were completed at iThemba labs. Fig 46 shows a powder pattern for 9,9'-(ethyne-1,2-diyl)bis(flouren-9-ol) referred to as flourene derivative. Similar powder pattern were observed for 9,9-bis(4-(2-hydroxyethoxy) phenyl) fluorene and 9,9-bis(4-hydroxyphenyl) fluorene [73].

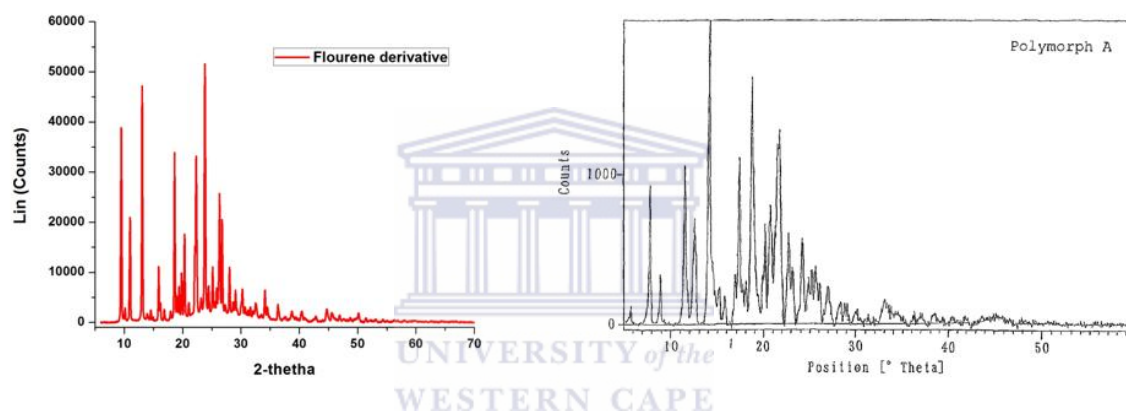


Figure 46: Powder pattern for 9,9'-(ethyne-1,2-diyl)bis(flouren-9-ol) (red) and 9,9-bis(4-(2-hydroxyethoxy) phenyl) fluorene (black) .

## 4.2 Xanthene derivative characterization

Xanthene derivative compound was characterized using the same techniques as for flourene derivative. The preparation was also done the same way for all the techniques.

### 4.2.1 Differential scanning calorimeter

Figure 47 reveals two endotherms, first endotherm is due to the melting point of xanthene derivative at 176 °C and the second endotherm is due to the decomposition of the compound. The melting point is 2 °C higher than that of starting material (xanthone) and 50 °C higher than the expected melting point. The compound from synthesis was used as produced. The influence of the impurities could be seen in the DSC melting point which was

not equivalent to the literature. Clathrate formed was confirmed using spectroscopic methods and the electrochemistry of the synthesized product followed. Now that we know that these clathrates are compatible with antibody purification is recommended.

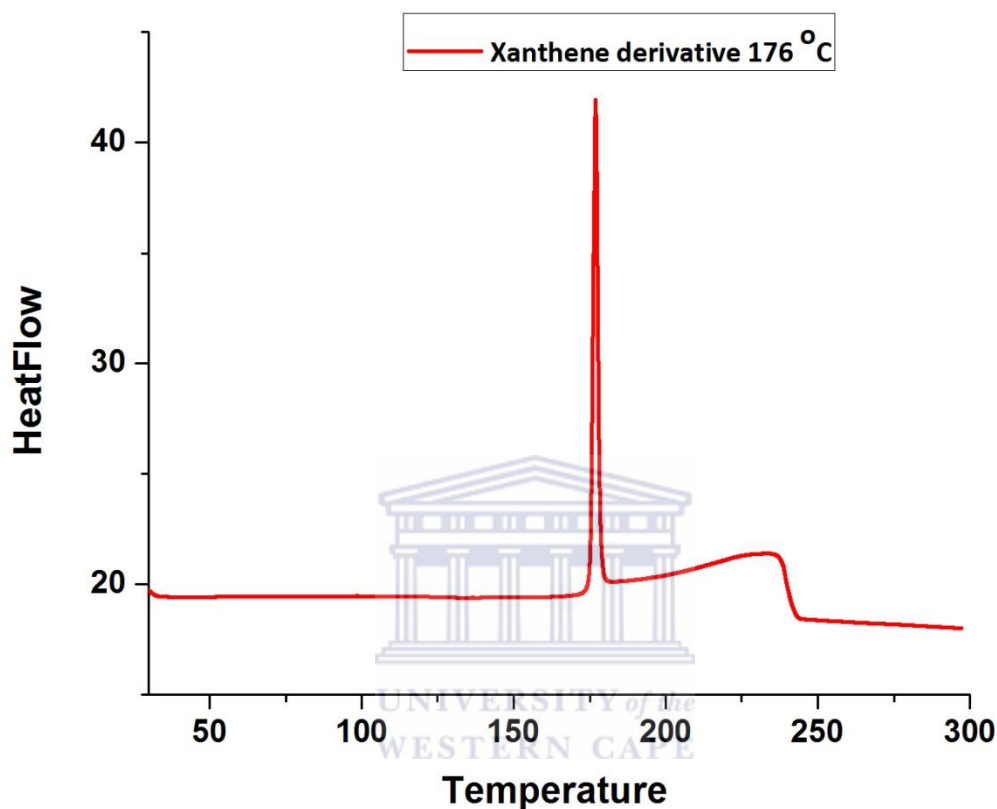


Figure 47: DSC curve showing melting point of xanthene derivative.

#### 4.2.2 Fourier transform infrared spectroscopy

FTIR spectra supported the structure of xanthene derivative. It exhibited characteristics absorption bands around  $3750\text{ cm}^{-1}$  corresponding to O-H stretch, around  $2669\text{ cm}^{-1}$  due to C-H stretch from aromatic ring, around  $1656\text{--}1447\text{ cm}^{-1}$  due to C=C stretch aromatics and around  $1339\text{--}1147\text{ cm}^{-1}$  corresponding to C-O-C stretch. Even though the melting points are not that different the IR spectra are different proving that a new compound was synthesized (fig 48).

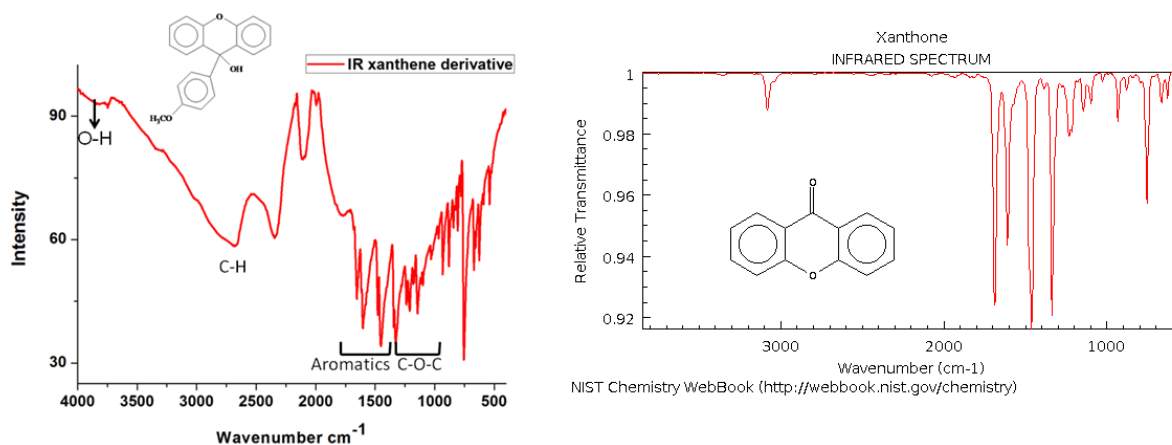


Figure 48: IR spectrum showing functional groups of xanthene derivative and spectra for xanthone starting material.

### 4.2.3 Ultraviolet visible spectroscopy

UV/Vis analysis was performed by dissolving xanthene derivative in ethanol. For xanthene derivative absorption spectra (fig 49) showed a narrow peak with a little shoulder and the absorption maxima of 337 nm due to  $\pi\text{-}\pi^*$  transition with energy gap of 3.6 eV calculated using equation 7. Rhodamine B also showed similar absorption spectra with the maxima of 555 nm [74]. Xanthenes form aggregates that modify the absorption spectrum and photophysical properties that affect the ability to emit. Band splitting is always observed for the xanthenes indicating that these aggregates are neither parallel nor linear but have intermediate geometry [75].

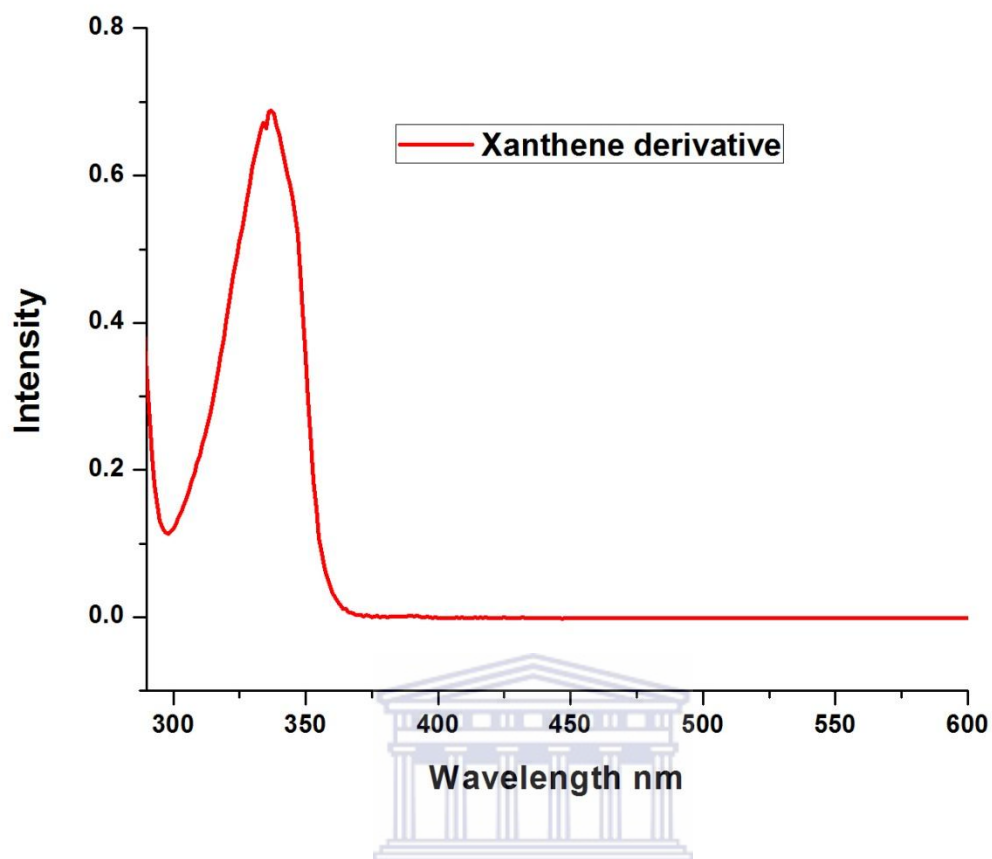


Figure 49: UV – Vis Spectra. Absorption maxima of xanthene derivative in ethanol is 337 nm which is attributed to the  $\pi\text{-}\pi^*$  transition with energy gap of 3.6 eV.

#### 4.2.4 Fluorescence spectroscopy

Fig 50 shows excitation and emission spectra of xanthene derivative. The maximum emission band is located at 380 nm and the excitation maxima is 344 nm with a Stokes shift of 36 nm.

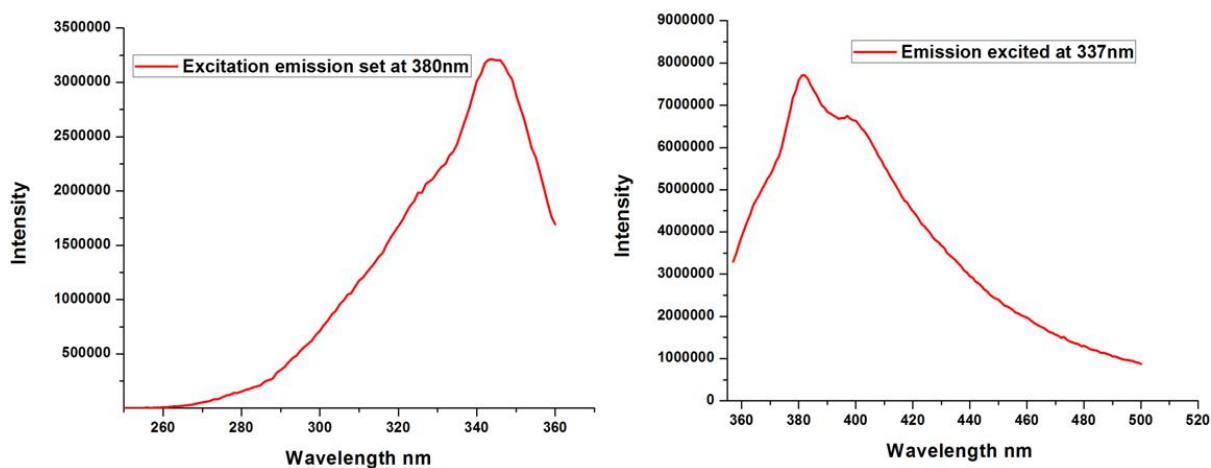


Figure 50: Emission and excitation spectra for xanthene derivative.

#### 4.2.5 Cyclic voltammetry and Squarewave voltammetry

Electrochemistry of xanthene derivative was investigated. The preparation was the same for CV and SWV analysis. A layer of each compound was deposited by drop-coating on the glassy carbon electrode and the electroactivity was evaluated. The measurements were carried out in pH 7.12, 0.2 M phosphate buffer at the potential window; -1000 mV to 1000 mV at scan rates of 10, 20, 40, 60, 80 and 100 mVs<sup>-1</sup> for CV and at scan rates of 75, 150 and 300 mVs<sup>-1</sup> for SWV. Reversible oxidation-reduction peaks were observed with peak separation of 59.95 mV for one electron redox which means that the system is fully reversible. The peak current magnitude was observed to increase upon increment of the scan rate signifying the peak currents are diffusion controlled. Diffusion coefficient and surface concentration were calculated from plots of current versus square root of scan rate from CV data and based on the slope of peak current versus dimensionless peak current plot from SWV data (fig 52). The calculated diffusion coefficient for xanthene derivative was estimated to be  $9.79 \times 10^{-21} \text{ cm}^2 \text{ s}^{-1}$  from CV data and  $4.02 \times 10^{-16} \text{ cm}^2 \text{ s}^{-1}$  using SWV data with the formal potential of -73.5 mV. The surface concentration was estimated to be  $2.00 \times 10^{-13} \text{ mol cm}^{-2}$ .

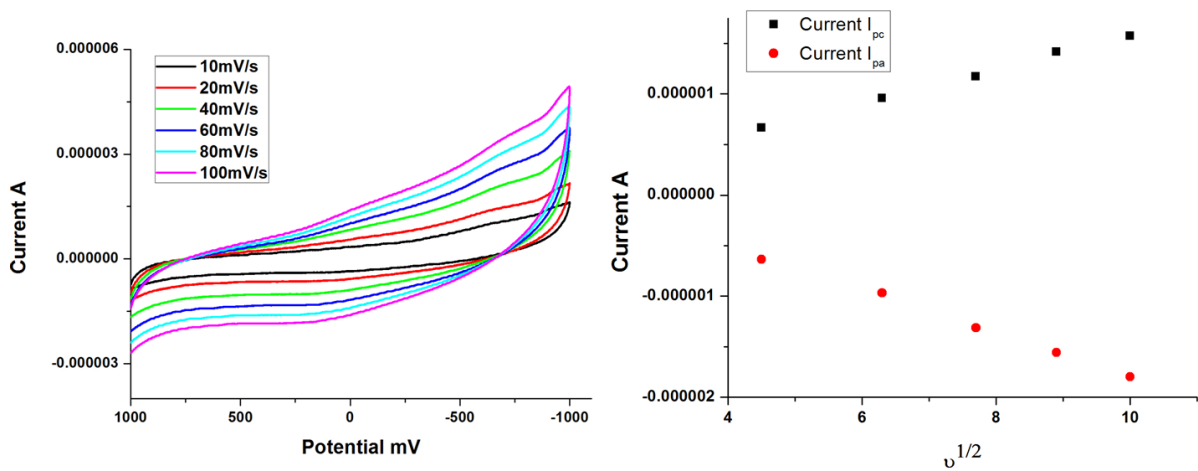


Figure 51: Cyclic voltammograms of xanthene derivative on GCE in 0.2 M PBS pH 7.12. Scanrate ( $v^{1/2}$ ). Plot of  $i_{pc}/i_{pa}$  versus scanrate $^{1/2}$  from voltammograms.

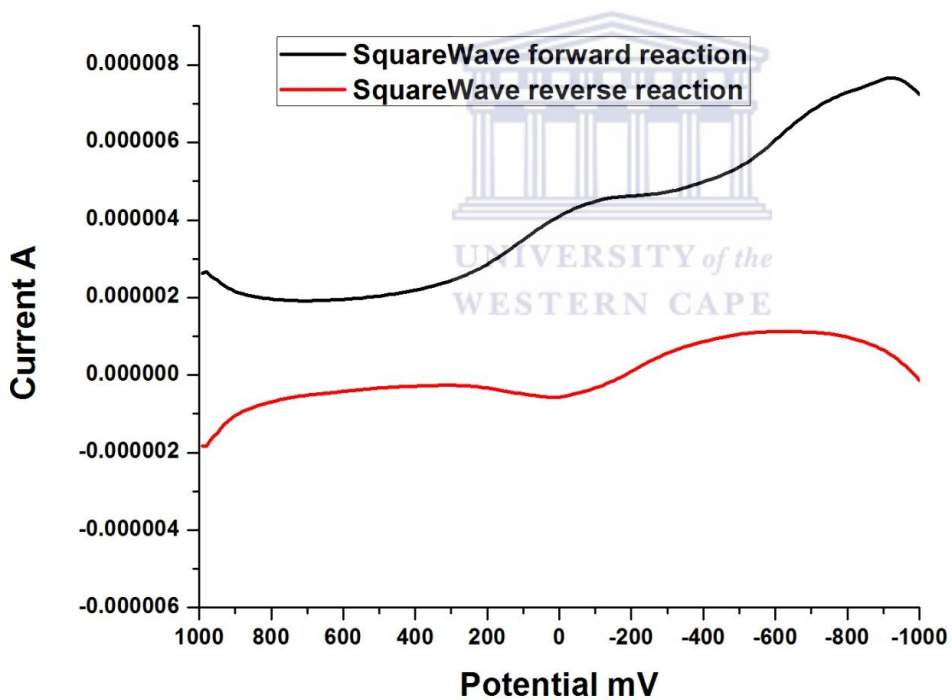


Figure 52: SWV data with the formal potential of -134 mV.

## 4.2.6 Powder x-ray diffraction

Fig 53 reveals a powder pattern for xanthene derivative which is different from that of the starting material xanthone [76]. This confirms that 9-(4-methoxyphenyl)-9H-xanthen-9-ol was indeed synthesized.

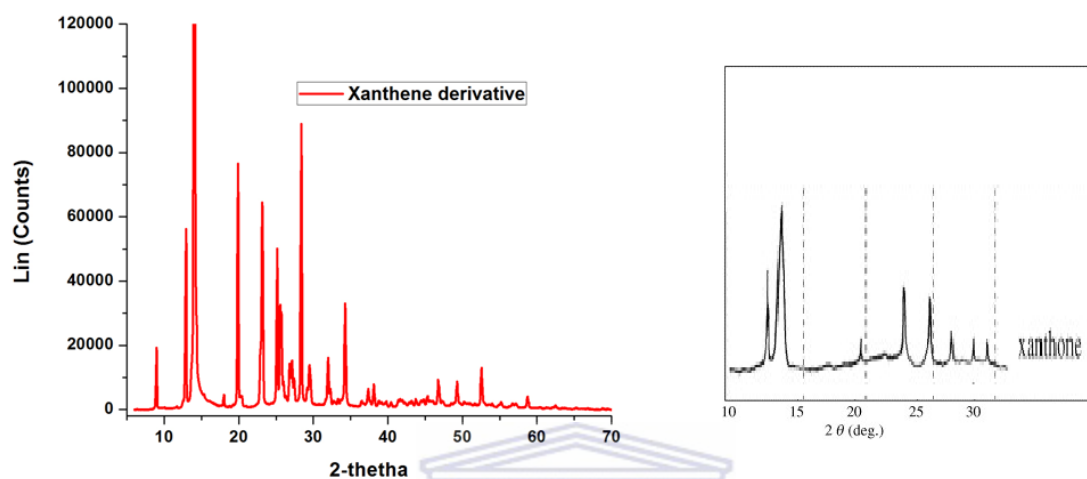


Figure 53: Xanthene derivative powder pattern (red) and xanthone powder pattern (black).

Clathrate compounds are chemical substances consisting of a lattice of one type of molecule trapping or containing a second type of molecule. The name clathrate complex has been adopted for many weak composites which consist of a host molecule (forming the basic frame) and a guest molecule (held in the host molecule by inter-molecular interaction). Cyclodextrins are cyclic oligosaccharides comprising of glucopyranose units linked by  $\alpha$ -(1,4) bonds soluble in water [77; 78].  $\alpha$ -,  $\beta$ -,  $\gamma$ -cyclodextrins are commonly available and have a torus shape cavity with internal cavity diameters of 4.2, 7.8 and 9.5 Å [77] respectively.  $\beta$ -cyclodextrin is the mostly used, it is easily accessible [78]. They are widely used due to their structural characteristics [79] and special functions. They can form host – guest complexes with a large variety of solid, liquid and gaseous organic compound by inclusion phenomena (host-guest systems such as molecular recognition, enzyme modelling, catalysis by inclusion compounds, macrocyclic ligands and crystallography). In cyclodextrin the guest molecules are temporarily locked or caged within the host cavity and that makes cyclodextrins carriers for biologically active substances, as enzyme model, sensor or solubilising agent for volatile organic compounds, protection agents for perfumes and also intermediates in organic

chemistry [78]. Fang et al. [79] have studied voltammetric responsive sensor for organic compounds based on organized self assembled lipoyl- $\beta$ -cyclodextrin derivate monolayer on gold electrode and concluded that  $\beta$ -cyclodextrin SME could be used as a electrochemical sensor for organic guest compounds, providing a method of electrochemical detection for electroinactive organic species. Sol – gel is chemically inert biocompatible, resistant to microbial attack, mechanical strength and negligible swelling in aqueous or organic solvent preventing leaching of biomolecules [80]. Wang and co – workers [81] have demonstrated that sol – gel processing can be used for the preparation of electrochemical immunosensors coupled with the screen – printing technology to allow one step mass production of low – cost antigen containing strips. It has been reported that the main disadvantage of the preparation of sol-gel glass-based immunoaffinity supports is the lack of standardization. The crushing and sieving of glass monoliths is not easily controllable.

Flourene derivative and xanthene derivative are both rigid and bulky conforms to Weber's host design rule. Yellow solution was observed for both clathrate compounds. Flourene derivative absorbs light at 400nm with the energy gap of 3.1 eV and xanthenes derivative absorbs light at 337 nm with the energy gap of 3.6 eV. This is due to  $\pi$ - $\pi^*$  transition in both flourene derivative and xanthenes derivative. Reversible oxidation-reduction peaks were observed for both clathrates compounds with similar diffusion coefficient ( $D_e$ ) from both CV and SWV data.  $D_e$  was found to be  $1.37 \times 10^{-21} \text{ cm}^2 \text{ s}^{-1}$  from CV data and  $1.78 \times 10^{-16}$  from SWV data and  $9.79 \times 10^{-21} \text{ cm}^2 \text{ s}^{-1}$  from CV data and  $4.02 \times 10^{-16} \text{ cm}^2 \text{ s}^{-1}$  from SWV data. Both clathrates compounds behaved in almost same manner.

We were able to synthesize the flourene derivative in one day. The xanthene derivative was synthesized over two days. The DSC showed a broad endotherm for flourene derivative due to impurities. FTIR and PXRD confirmed both clathrate structures. Mass spectroscopy was also performed but there were no conclusive results (see appendix 1). Nuclear magnetic resonance studies will be pursued in order to conclude the structures. Previously porous macrocyclic compounds with cavity have been used whereby the guest molecule is temporarily locked or caged within the host cavities. Gold nanoparticles have been used in the immunosensor development for these macrocyclic compounds, they act as tiny conducting centres facilitating normal electron transfer kinetics. Flourene derivative and

xanthene derivative are porous noncyclic compounds with highly hydrophobic surface. Small Stokes shift have been observed from the fluorescence which confirmed that these compounds are rigid and have a well-defined backbone. Both compounds are electroactive confirmed by SWV and CV. Fluorene derivative and xanthene derivative were utilized in the immunosensor development whereby a conductive transducer (glassy carbon electrode) was used. The antibody was immobilized directly onto these clathrate compounds.



## Chapter 5

The clathrate materials xanthene derivative and flourene derivative were employed as electrochemical platforms in the design of novel immunosensors for parvalbumin. In this chapter we will present the immunosensor design.

### 5.1 Immunosensor development

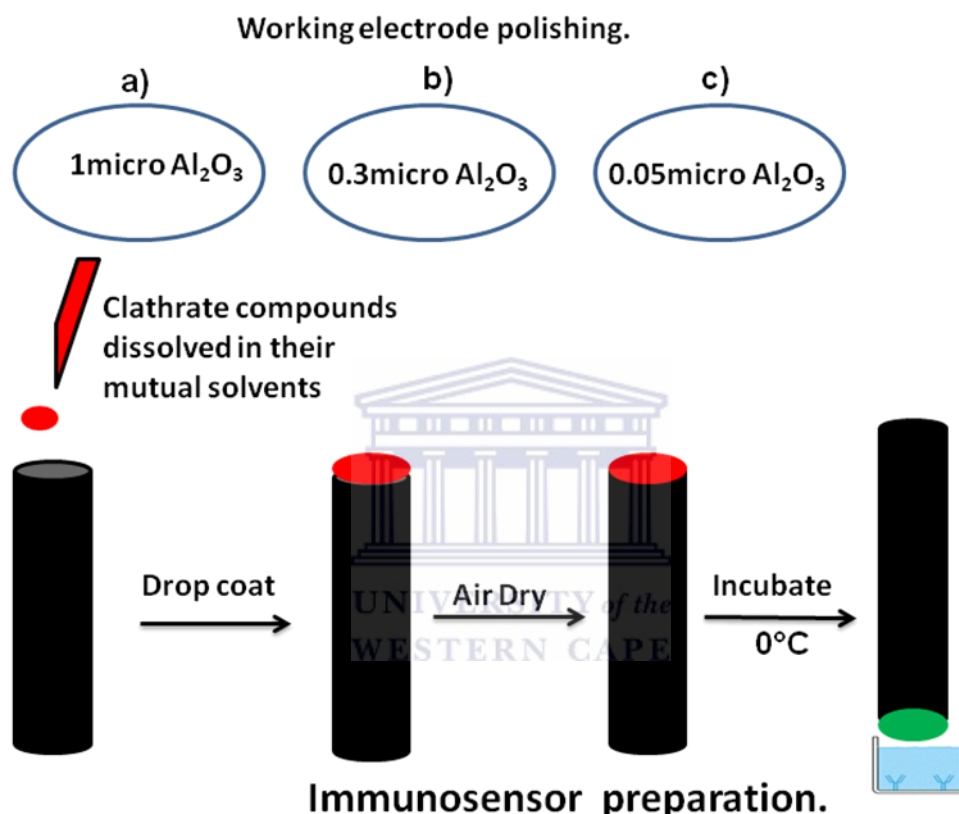


Figure 54: Immunosensor development.

Working electrode (glassy carbon electrode GCE) was polished using  $1\mu$ ,  $0.3\mu$  and  $0.05\mu$  alumina powder. After each polishing the electrode was rinsed with distilled water. It was then sonicated in ethanol and in water and finally air dried. Immunosensor was prepared by dissolving the xanthene derivative in ethanol and the flourene derivative was dissolved in methanol. The  $5\mu\text{L}$  of the respective solutions was drop-coated onto the GCE working electrode leaving it to dry for 20 minutes. The clathrate modified GCE was used as the immunosensor platform. The GCE/X and GCE/F respectively, was then incubated in antibody solution for 30 minutes at  $0^\circ\text{C}$ . The final immunosensor format may be abbreviated as

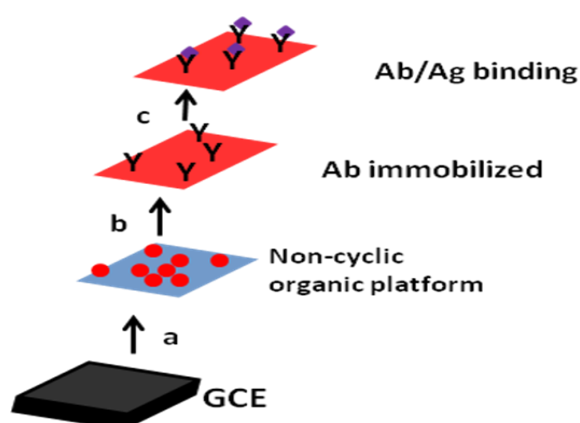
GCE/X/Ab when using the xanthene derivative and GCE/F/Ab when using the flourene derivative. The parvalbumin immunosensor was freshly prepared for each analysis. However Lu et al. [65] and co-workers have regenerated their parvalbumin immunosensor by washing twice with 20 mM HCl for 2 minutes, followed by a 5 minutes PBS/T re-equilibration before re-use. The immunosensor prepared was intended to be utilised in disposable screen printed electrodes. At this point in time we were not interested in the lifetime of the immunosensor, we focussed on developing an immunosensor that will detect parvalbumin rapidly.

## 5.2 Immunosensor characterization

### 5.2.1 Flourene derivative immunosensor

#### 5.2.1.1 Atomic force microscopy (AFM)

AFM was used in the stepwise immunosensor development process with non-contact mode. Scheme 6 illustrate the stepwise development process of the immunosensor and figure 57 shows the equivalent surface topographic images of films of the corresponding stepwise immunosensor development process. AFM confirmed that the antibody was indeed attached to the clathrate compound by studying morphology of the electrode surface after modification (fig 55A) and after incubation (fig 55B). Fig 55B showed a different morphology from fig 55A proving that the antibody is attached to the clathrate compound.



Scheme 6: Schematic illustration of the stepwise immunosensor development process.

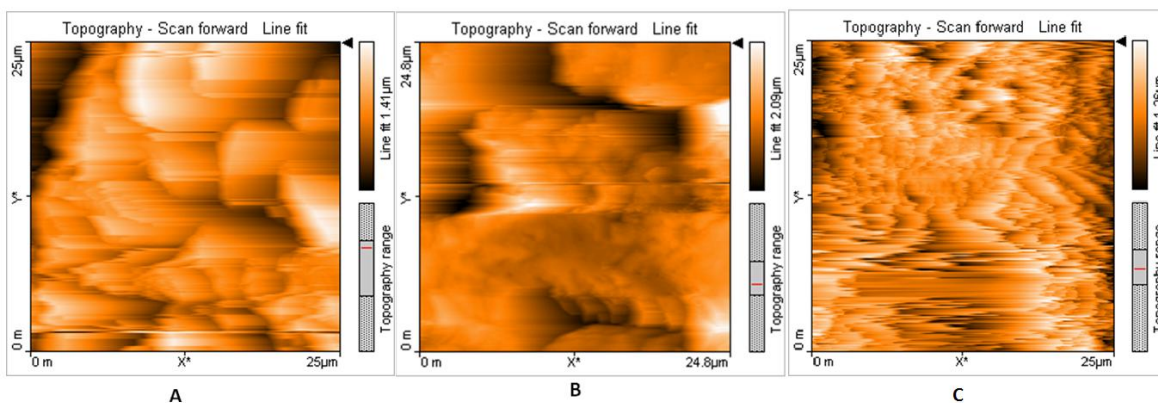


Figure 55: AFM. A = Topography of flourene derivative, B = Topography of flourene derivative plus antibody, C = Topography of flourene derivative Ab/Ag.

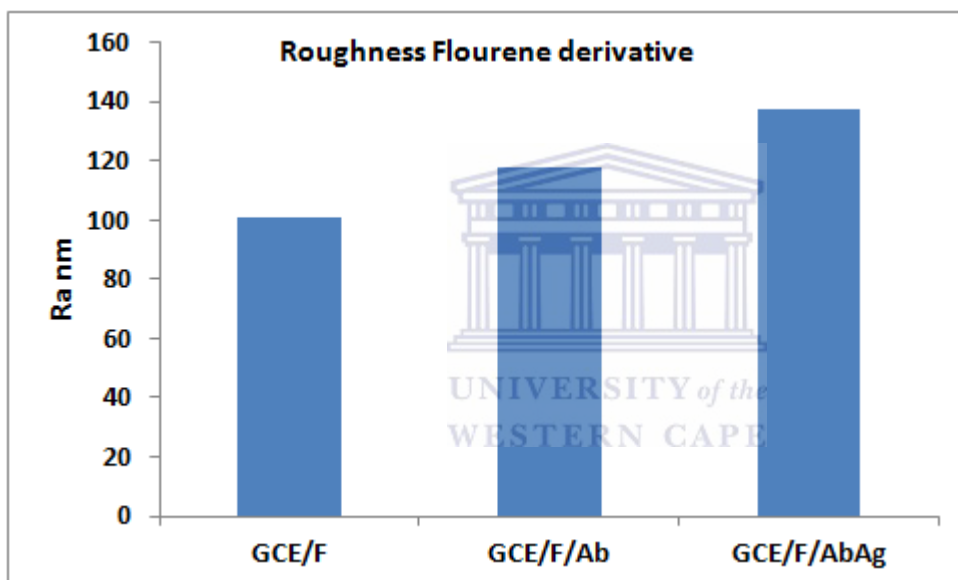


Figure 56: Flourene derivative and immunosensor surface roughness.

### 5.2.1.2 Electrochemical impedance spectroscopy

EIS measurements were carried out in 0.2 M pH 7.12 PBS at a fixed potential of -134 mV for flourene derivative where clathrate platform and immunosensor interfacial parameters were investigated. The change in electron transfer resistance that occurred after each surface modification step was investigated and represented as Nyquist diagrams as indicated in fig 57. The impedance data was modelled as a simple Randles circuit with a single RC loop. The parameter resulting from circuit fitting study are listed in table 3 such as solution resistance  $R_s$ , double layer capacitance  $C_{dl}$  and charge transfer resistance  $R_{ct}$ . These

parameters were used to calculate the time constant ( $\tau$ ) using equation 9, the exchange current ( $i_0$ ) using equation 10 and homogeneous rate constant using equation 11. The results are listed in table 3.

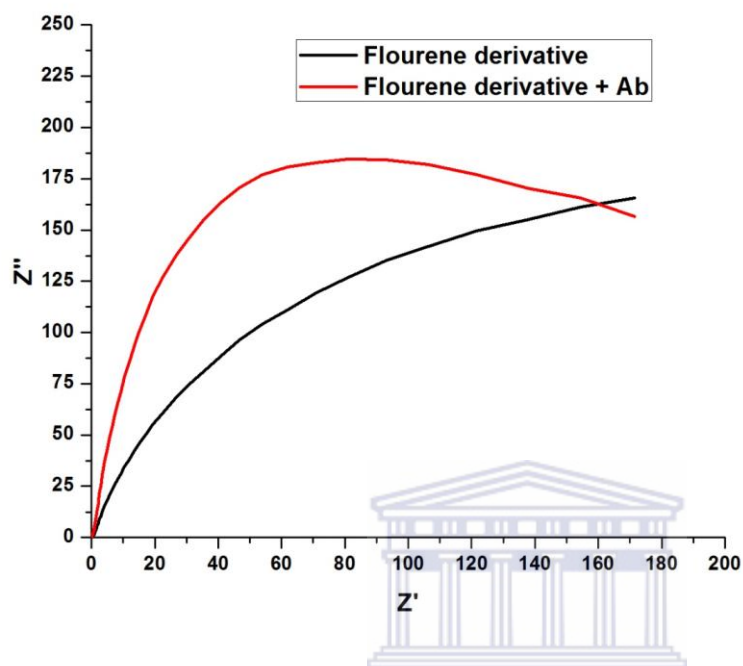


Figure 57: Nyquist diagram to illustrate clathrate and immunosensor response for flourene derivative.

| Parameter  | GCE/F               | GCE/F/Ab           |
|--|---------------------|--------------------|
| Electrolyte resistance ( $R_s$ ) Ohms            | 12.56               | 59.72              |
| Charge transfer resistance ( $R_{ct}$ ) Ohms     | $9.128 \times 10^6$ | $1.23 \times 10^6$ |
| Double layer capacity ( $C_{dl}$ ) $\mu\text{F}$ | 35.45               | 77.94              |

Table 3: EIS parameters obtained from the circuit fitting of impedance data for GCE/F and GCE/F/Ab.

A decrease in  $R_{ct}$  was observed after Ab immobilization, which means that immunosensor was more electroactive compared to GCE/F.

| Element  | GCE/F                  | GCE/F/Ab               |
|--|------------------------|------------------------|
| Time constant ( $\tau$ ) s rad <sup>-1</sup>             | 3.24                   | 9.59x10 <sup>-1</sup>  |
| Exchange current ( $i_0$ ) A                             | 1.41x10 <sup>-9</sup>  | 1.04x10 <sup>-8</sup>  |
| Homogeneous rate constant ( $K_{et}$ ) cms <sup>-1</sup> | 1.03x10 <sup>-12</sup> | 7.62x10 <sup>-12</sup> |

Table 4: Calculated results for time constant, exchange current and homogeneous rate constant for GCE/F and GCE/F/Ab.

The double layer capacitance was observed to increase upon Ab immobilization to two times the capacitance of GCE/F platform only. This confirms that the immobilized Ab provides an increase in the surface band charge transfer region.

$$\tau = R_{ct}C_{dl}$$

Equation (8)

$$i_0 = \frac{RT}{nFR_{ct}}$$

Equation (9)

$$i_0 = nFAK_{et}C^*$$

Equation (10)



## 5.3 Xanthene derivative immunosensor

### 5.3.1 Atomic force microscopy

Morphology of the modified electrode with xanthene derivative solution and the incubated electrode in antibody solution was investigated using AFM. Fig 58B is similar to fig 55B indicating that the antibody is attached to the xanthene derivative.

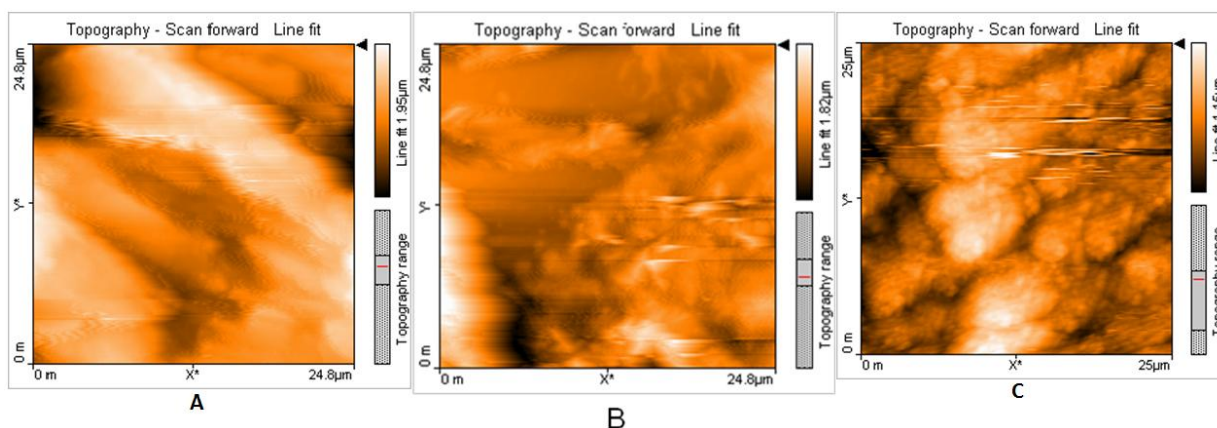


Figure 58: AFM. A = Topography of xanthene derivative, B = Topography of xanthene derivative plus antibody, C = Topography of xanthene derivative Ab/Ag.

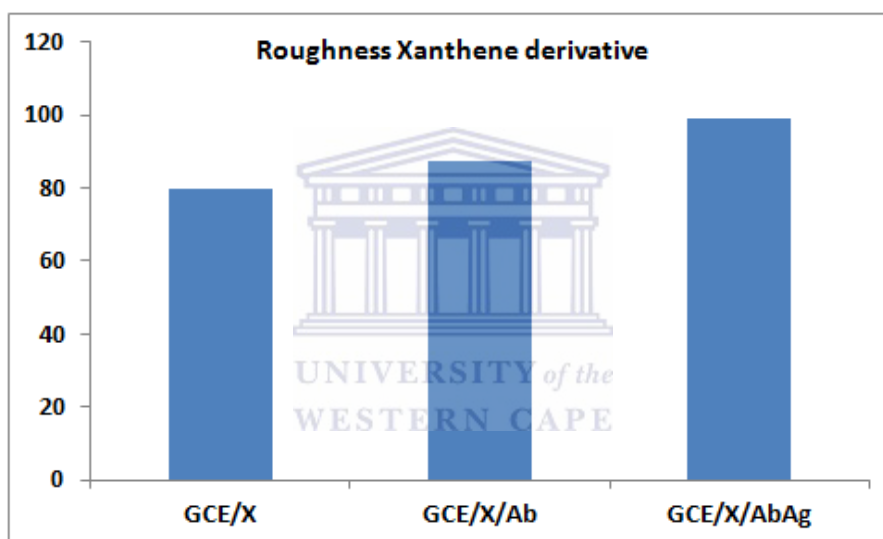


Figure 59: Xanthene derivative and immunosensor surface roughness.

### 5.3.2 Electrochemical impedance spectroscopy

EIS measurements were carried out in 0.2 M pH 7.12 PBS at a fixed potential of -73 mV for xanthene derivative where clathrate and immunosensor was investigated. The change in electron transfer resistance that occurred after each surface modification step was investigated and represented as Nyquist diagrams as indicated in fig 60. The parameter resulting from the EIS study are listed in table 5 such as solution resistance  $R_s$ , double layer capacitance  $C_{dl}$  and charge transfer resistance  $R_{ct}$ . These parameters were used to calculate the time constant ( $\tau$ ), the exchange current ( $i_0$ ) and homogeneous rate constant as before.

The results are listed in table 6. The same behaviour with respect to  $R_{ct}$  and double layer capacitance was observed for both immunosensor systems.

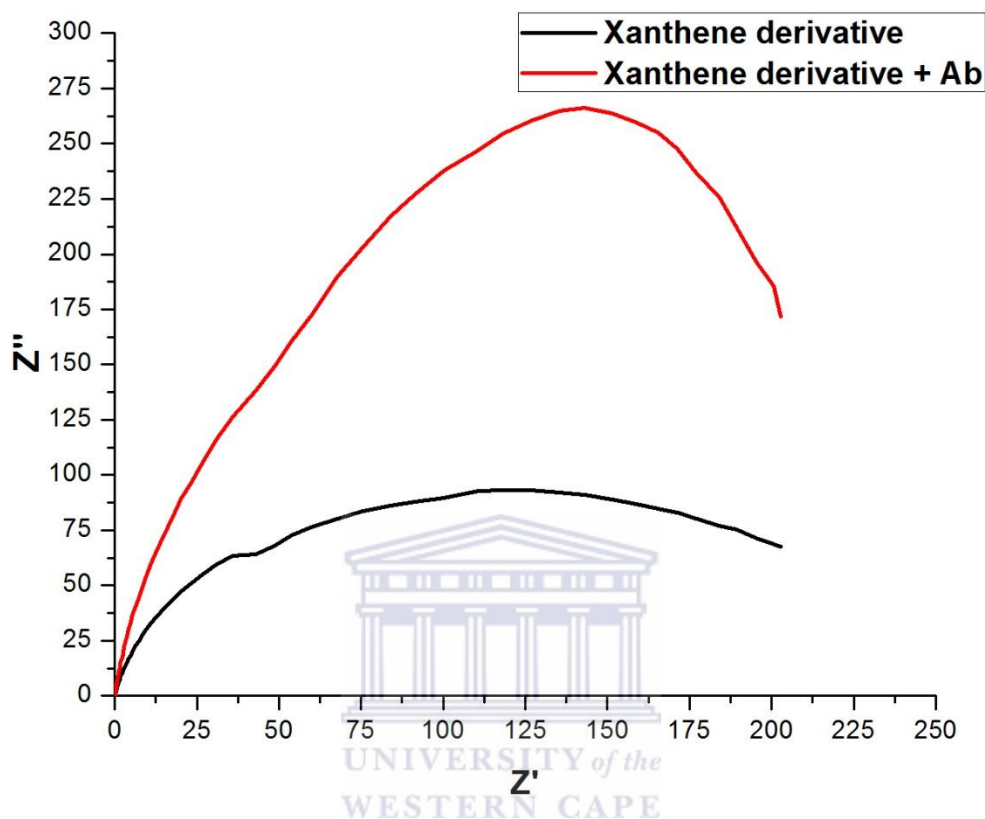


Figure 60: Nyquist diagram to illustrate clathrate and immunosensor response for xanthene derivative.

| Parameter  | GCE/X              | GCE/X/Ab           |
|--|--------------------|--------------------|
| Electrolyte resistance ( $R_s$ ) Ohms            | 206.2              | 75.31              |
| Charge transfer resistance ( $R_{ct}$ ) Ohms     | $4.40 \times 10^6$ | $4.29 \times 10^6$ |
| Double layer capacity ( $C_{dl}$ ) $\mu\text{F}$ | 26.9               | 42.7               |

Table 5: EIS parameters obtained from the circuit fitting of impedance data for GCE/X and GCE/X/Ab.

| Element  | GCE/X                  | GCE/X/Ab               |
|--|------------------------|------------------------|
| Time constant ( $\tau$ ) s rad <sup>-1</sup>             | 1.18                   | 1.83                   |
| Exchange current ( $i_0$ ) A                             | $2.92 \times 10^{-9}$  | $2.99 \times 10^{-9}$  |
| Homogeneous rate constant ( $K_{et}$ ) cms <sup>-1</sup> | $2.13 \times 10^{-12}$ | $2.18 \times 10^{-12}$ |

Table 6: Calculated results for time constant, exchange current and homogeneous rate constant for GCE/X and GCE/X/Ab.

As observed before for flourene derivative, a decrease in  $R_{ct}$  after Ab immobilization and an increase in double layer capacitance were also observed for xanthene derivative.

Previous studies has shown that gold nanoparticles had been used to covalently bind to the self-assembly monolayer surface through its functional groups and can be prepared by self-assembly on the polymer-coated substrate [82]. The antibody was directly immobilized on to the clathrates platforms without utilizing a cross-linker to enable the covalent binding between antibody and the platform. This means that the mechanism of adsorption is controlled by physical forces. However for all experiments conducted the strength of the adsorption was able to keep the working interface intact. A slightly higher charge transfer resistance was observed for GCE/X/Ab with a value of  $4.29 \times 10^6$  Ohms when compared to GCE/F/Ab with a value of  $1.23 \times 10^6$  Ohms. These values revealed the hindering ability of xanthene derivative and antibody on the electrode surface thus impeding electron transfer. The exchange current value obtained for the GCE/F/Ab further confirmed its ability to transfer electrons fast when compared to GCE/X/Ab. GCE/F/Ab was found to have a higher surface roughness than GCE/X/Ab meaning that it has a high surface area that leads to faster kinetics. Flourene derivative immunosensor has better electrokinetics.

The clathrates materials xanthene and flourene that were synthesized by chemical methods were successfully drop-coated onto glassy carbon transducer as evidenced by AFM images and surface roughness calculations. The glassy carbon electrodes modified in this way produced good electrocatalytic platforms as indicated by charge transfer resistance measured by EIS. The immobilization of the antibody was effected by incubation in antibody stock solution at 4 °C. The antibody activity was not destroyed during the incubation step

since the charge transfer resistance was only slightly reduced. The immunosensor produced in this way was used to evaluate parvalbumin calibration curves and the measurement of parvalbumin in selected real samples.

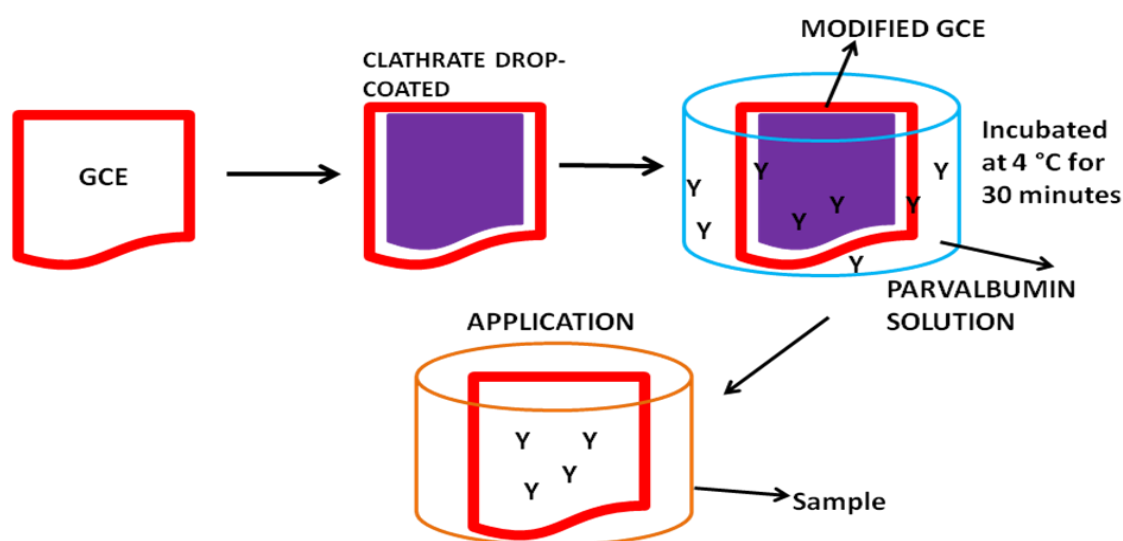


## Chapter 6

The flourene derivative and xanthene derivative were used as a conductive platform in the preparation of the immunosensor. Immunosensor response to parvalbumin standard solution is described in this chapter.

### Introduction

Pierce anti-parvalbumin polyclonal rabbit supplied by Sigma purified was diluted using coating buffer of pH 9.6. The development of immunosensor followed a direct assembly approach. Non-labelled and labelled self-assembled nanoparticles immunosensor have been developed. Liang et al have used a non-labelled self-assembled nanoparticles immunosensor for the determination of hepatitis B surface antigen in human serum constructed by combining sol-gel and self-assembly techniques on gold electrode. This technology demonstrates the benefits of self-assembly, nanoparticles and increased surface area of three dimensional electrodes [83]. Ju et al have developed a novel nano-Au/sol-gel composite structure for encapsulating HRP-labelled hCG antibody on glassy carbon electrode showing good hydrophilicity and effective for tunnelling electrons between immobilized HRP and electrode surface and retaining bioactivity of immobilized biomolecules. In this work immunosensor preparation was done in an easy and quick manner using non-labelled antibody [84].



Scheme 7: Immunosensor application.

## 6.1 Immunosensor response

Antibody/Antigen binding events were investigated in solution using EIS. The antibody was immobilized onto the modified electrode (GCE/F) by incubating the electrode in an antibody solution for 30 minutes at 0 °C. The GCE/F/Ab immunosensor was allowed to dry before being immersed in 3 ml of 0.2 M pH 7.12 PBS. 2000 pg/ml of antigen solution was added in increments of 2  $\mu\text{L}$ , the solution was stirred for 3 minutes before each run. A decrease in  $R_{ct}$  after antibody immobilization and a further decrease in  $R_{ct}$  after each addition of antigen solution was observed (fig 61 & 62). This indicates that the more the antibody binds the antigen the system becomes more conductive. The affinity binding between Ab/Ag was observed as an increase in Caps with each addition of Ag. The detection limit is the lowest amount of analyte in a sample that can be detected, but not necessarily quantitated as an exact value.

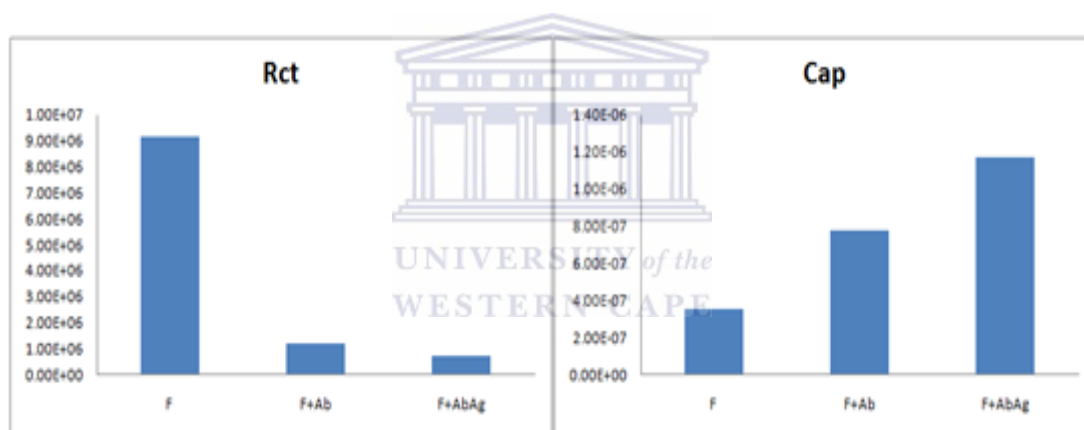


Figure 61: A graph showing decrease in  $R_{ct}$  and an increase in capacitance in fluorene derivative immunosensor response.

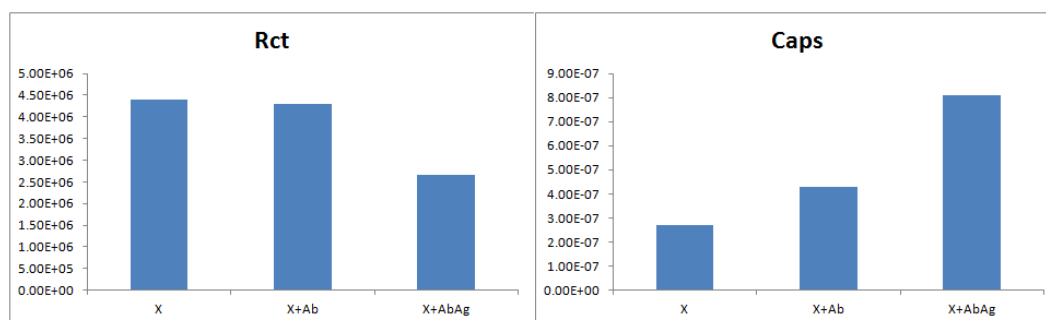


Figure 62: A graph showing decrease in  $R_{ct}$  and an increase in capacitance in xanthene derivative immunosensor response.

An increase in capacitance with an increase in concentration was observed. The flourene derivative immunosensor response showed sigmoidal fit indicating cooperative binding between analyte and antibody, because the binding of analyte to one of the subunits modifies affinity of other subunits for analyte. The analyte-binding sites of antibody interact with each other such that the binding of one molecule of analyte to one antibody facilitates binding of other analyte molecules to other antibody sites. A plot of capacitance vs concentration is presented in fig 65 and the values are listed in table 7. The sensitivity was calculated from the linear range and was found to be  $5.36 \times 10^4$ . The analysis was repeated three times and the average sensitivity was determined. The detection limit was estimated to be 1.50 pg/ml. However the xanthene derivative immunosensor showed a hyperbolic fit, signifying no cooperative binding of the antibody. The antibody concentration is independent of the analyte molecule that binds to the active site of the antibody. A plot of capacitance vs concentration is presented in fig 67 and the values are listed in table 8. The sensitivity was calculated from the linear range and was found to be  $4.82 \times 10^4$ . The detection limit was calculated to be 2.42 pg/ml. Flourene derivative immunosensor was found to be more sensitive and stable than xanthene derivative immunosensor.

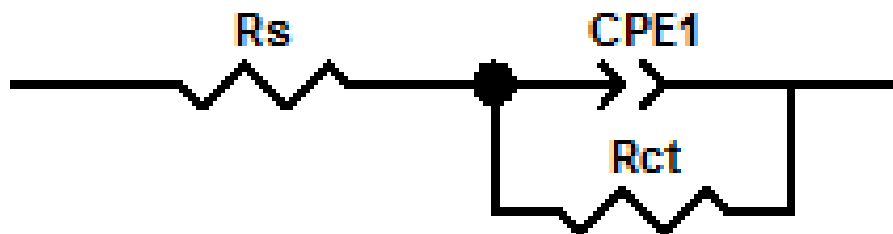


Figure 63: Equivalent circuit used for all impedance analysis.

Solution resistance  $R_s$  is the resistance between the working electrode and the reference electrode. This is shown by a small offset on the real impedance axis. It is measured at high frequency intercept near the origin of the nyquist plot.

Charge transfer resistance  $R_{ct}$  is the resistance associated with the charge transfer mechanism for the electrode reactions. It is the resistance to electron transfer at the electrode interface.

Constant phase element **CPE** is a non-intuitive circuit element that was invented while looking at the response of real-world system. Normally it is used in a model in place of a capacitor due to deviation of capacitance parameters from expected values (inhomogeneities at the interface).

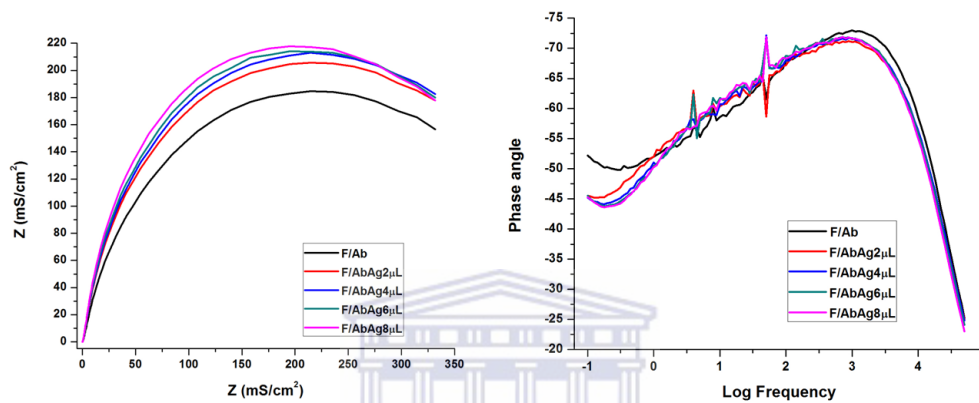


Figure 64: EIS complex plot for analyte additions and bode plot using flourene derivative immunosensor.

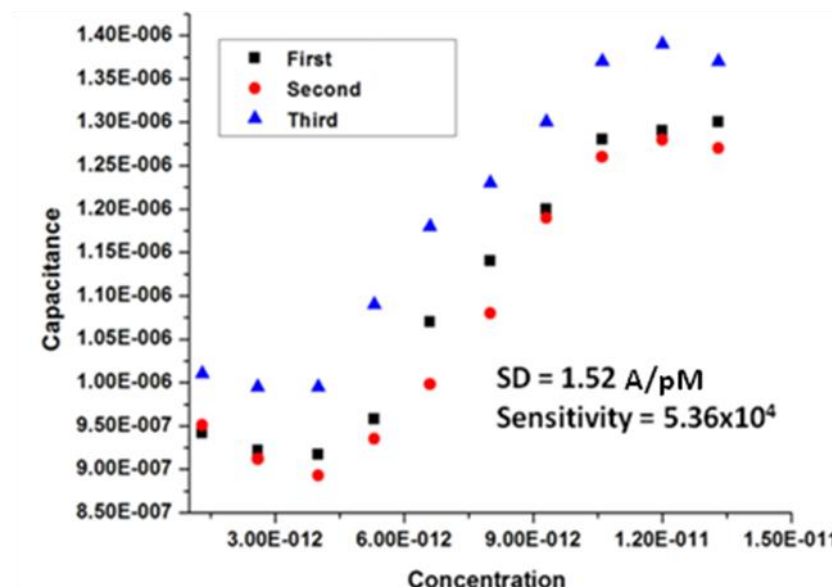


Figure 65: A plot of capacitance vs concentration for flourene derivative immunosensor response.

| <b>Conc</b>        | <b>First result</b> | <b>Second result</b> | <b>Third result</b> |
|--------------------|---------------------|----------------------|---------------------|
| 1.3E-12            | 9.42E-7             | 9.51E-7              | 1.01E-6             |
| 2.6E-12            | 9.22E-7             | 9.12E-7              | 9.95E-7             |
| 4E-12              | 9.17E-7             | 8.93E-7              | 9.95E-7             |
| 5.3E-12            | 9.58E-7             | 9.35E-7              | 1.09E-6             |
| 6.6E-12            | 1.07E-6             | 9.98E-7              | 1.18E-6             |
| 8E-12              | 1.14E-6             | 1.08E-6              | 1.23E-6             |
| 9.3E-12            | 1.2E-6              | 1.19E-6              | 1.3E-6              |
| 1.06E-11           | 1.28E-6             | 1.26E-6              | 1.37E-6             |
| 1.2E-11            | 1.29E-6             | 1.28E-6              | 1.39E-6             |
| 1.33E-11           | 1.3E-6              | 1.27E-6              | 1.37E-6             |
| <b>Sensitivity</b> | 53663               | 53666                | 53664               |

Table 7: Concentration and capacitance results obtained for flourene derivative immunosensor.

The conventional immunosensing based on solid supports has been limited due to the lack of a simple protein immobilization approach that might avoid denaturation of the bound redox enzymes. Stability and activity of the immobilized biocomponents on solid support have been a long standing. We were able to develop an immunosensor with better antibody orientation resulting to high sensitivity. The measurements were repeated three times, for each measurement the flourene derivative immunosensor was freshly prepared. The solution was stirred for three minutes after each addition of analyte. The standard deviation of sensitivity average was found to be 1.52 A/pM (n=3) indicating good repeatability and reproducibility of results.

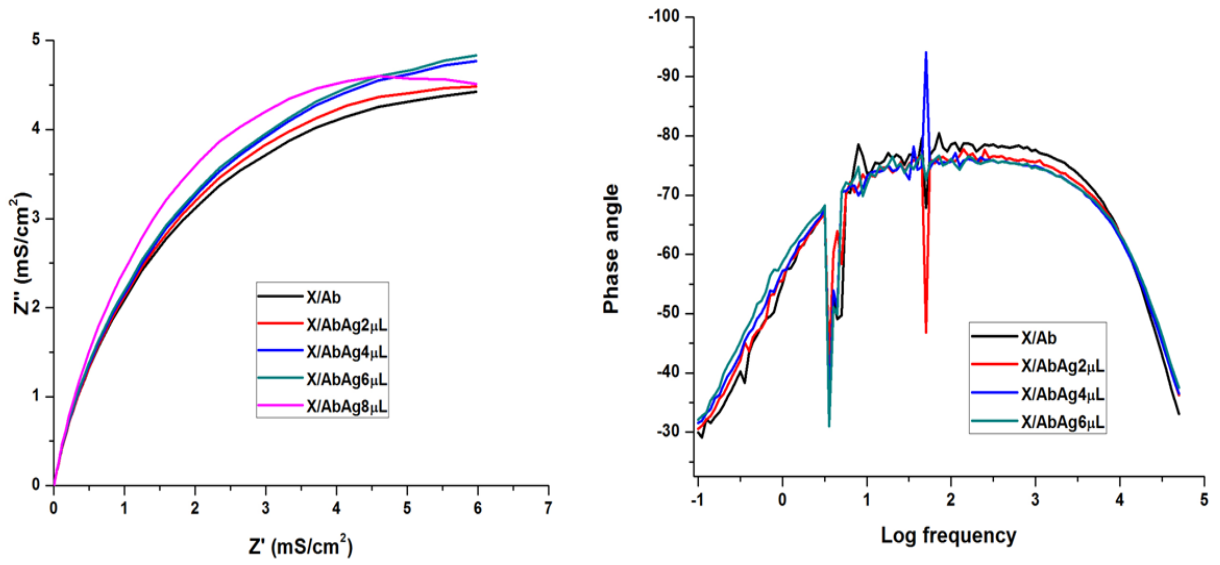


Figure 66: EIS complex plot for analyte additions and bode plot using xanthene derivative immunosensor.

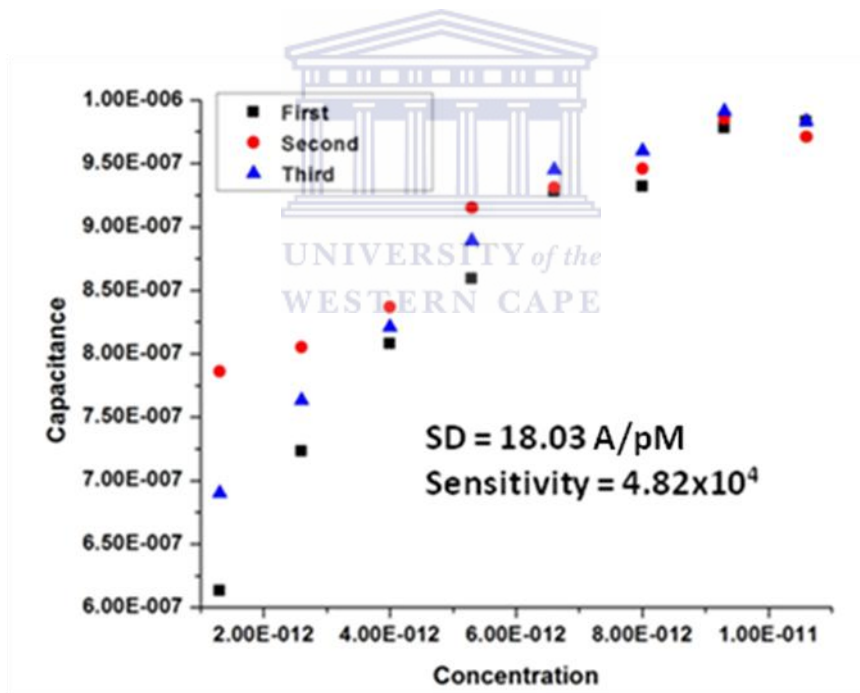


Figure 67: A plot of capacitance vs concentration for xanthene derivative immunosensor response.

| Conc               | First result | Second result | Third result |
|--------------------|--------------|---------------|--------------|
| 1.30E-12           | 6.13E-07     | 7.26E-07      | 6.90E-07     |
| 2.60E-12           | 7.23E-07     | 8.05E-07      | 7.63E-07     |
| 4.00E-12           | 8.08E-07     | 8.37E-07      | 8.21E-07     |
| 5.30E-12           | 8.59E-07     | 9.15E-07      | 8.89E-07     |
| 6.60E-12           | 9.28E-07     | 9.31E-07      | 9.45E-07     |
| 8.00E-12           | 9.32E-07     | 9.46E-07      | 9.60E-07     |
| <b>Sensitivity</b> | 48299        | 48278         | 48263        |

Table 8: Concentration and capacitance results obtained for flourene derivative immunosensor.

The measurements were performed in the same manner as for flourene derivative immunosensor. The standard deviation of sensitivity was found to be 18.03 A/pM indicating that repeatability and reproducibility is not as good as that of flourene derivative immunosensor.

## 6.2 Antibody/Antigen binding UV/Vis analysis

In UV/Vis a sample is irradiated with light of a particular wavelength, if the compound absorbs the light the detector will record the amount of the absorbance. In UV/Vis spectrum the light is absorbed between 200nm – 700nm whereby 200nm – 370nm is the UV range and 370nm – 700nm is the visible light range. UV/Vis light causes electronic excitations.

UV/Vis analysis was carried out to confirm Antibody/Antigen binding in solution. The antibody solution was prepared in phosphate buffer pH 7.12 and recorded for observation of antibody before and after successive additions of the respective analyte. An increase in the absorption intensity upon addition of different concentrations of analyte was observed, indicating that the environment of the antibody had changed the conjugation has increased. The UV/Vis spectra revealed a slight shift in both intensity and wavelength. This shift is most likely caused by the change in antibody structure. The shift observed is the red shift from 217nm – 220nm longer wavelengths which result to lower frequency and lower energy. This was understood as confirmation of analyte binding to the indigenous antibody in

solution. The plot of absorbance vs concentration showed the same response behaviour as the flourene derivative immunosensor response, sigmoidal response. The sensitivity calculated from the slope of this plot, was more than two time higher than that of the flourene derivative and xanthene derivative immunosensor  $1 \times 10^{11}$ . This is due to the fact that antibody molecule are free in solution whereas for the clathrates they are attached to a platform. The immobilization of antibody restricts its affinity binding capacity because binding sites are restricted.

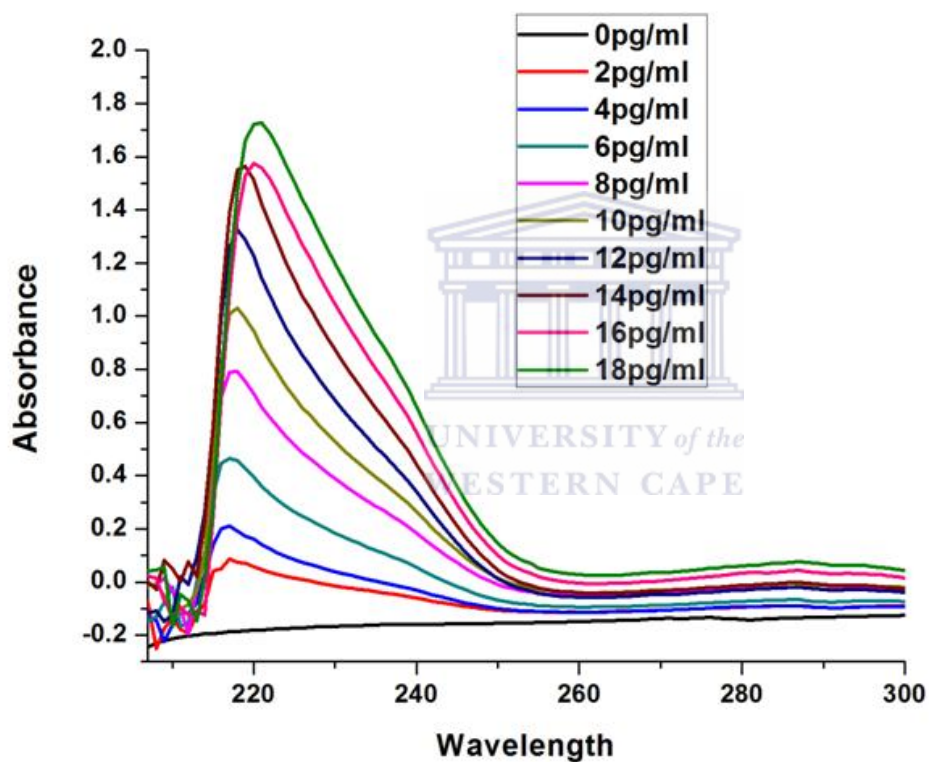


Figure 68: UV/Vis antibody/antigen binding confirmation.

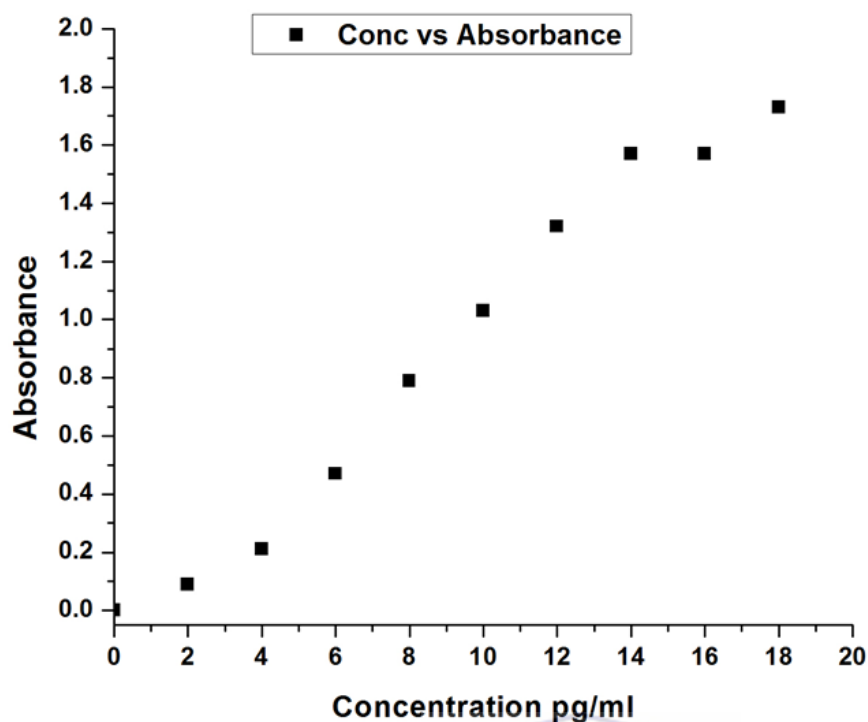


Figure 69: UV/Vis antibody/antigen binding confirmation calibration curve.

For both fluorene derivative immunosensor and xanthene derivative immunosensor the affinity binding between Ab/Ag was established as an increase in  $\Delta R_{ct}$ . It is evident from the complex plot of the immunosensor response to analyte that there is a marked difference in the interfacial electrokinetics after each addition of analyte solution as the charge transfer decreased showing binding. Due to a decrease in charge transfer resistance ( $R_{ct}$ ) of the system as a function of increasing concentration the typical semi-circle nature which tells us about the electron transfer kinetics of the system, changed towards a more capacitive representation. These results indicate that the binding between immobilized Ab and Ag in solution was taking place efficiently with the time scale of the experiment. The Ab/Ag binding complex has higher electroactivity indicating that efficient electronic wiring was established between Ab sites and substrate. This is evidenced by decreased charge transfer from  $1.23 \times 10^6 \Omega$  to  $7.28 \times 10^5 \Omega$  for fluorene derivative immunosensor and  $4.40 \times 10^6 \Omega$  to  $4.29 \times 10^6 \Omega$  for xanthene derivative immunosensor. Limit of detection have been found to be 1.50 pg/ml for GCE/F/Ab and 2.42 pg/ml for GCE/X/Ab respectively.

In comparison from the UV/Vis data sensitivity was calculated ( $1 \times 10^{11}$ ) and it was found to be more than that of clathrates immunosensors. The antibody molecules are free in solution hence the high sensitivity in UV. For the clathrates immunosensors the antibody molecules are immobilized onto the platforms and that restricts its affinity binding capacity because binding sites are restricted. The extent of binding is governed by the availability of antibody and the size of the analyte molecule. However these clathrates immunosensors were applied in real sample analysis and the calibration obtained was used to determine the parvalbumin content in these real samples.



## Chapter 7

*Immunosensor application to real samples of fish and fish products will be discussed. The samples are made from fish extracts for example oil. They were tested to find out if they contain parvalbumin and how much was the parvalbumin content.*

### 7.1 Applications

Seven samples were analysed namely: Snoek also known as thyrsites atun is a commercial food fish that belongs to the Gempylidae family. Snoek is oily, extremely bony and has very fine scales which are almost undetectable, making it unnecessary to scale the fish while cleaning. It has a very distinctive taste. Snoek can be baked, poached, fried or smoked, but the traditional way to serve it is grilled over the coals with boiled sweet potatoes. It was purchased from the local fisherman.

Peck's anchovette fish paste savoury spread made from cape herring, mackerel, anchovies, salt, corn flour, sugar, soya protein, spices, colourants, flavour and ascorbic acid. Fish belonging to the Clupeiformers (sardine and anchovy) with cross-reactivity to the herring has been reported to be the cause of occupational cell-mediated contact allergic dermatitis [85]. It was purchased from the local supermarket.

Tuna is a saltwater finfish that belongs to the tribe Thunnini. Tuna is a good source of omega-3 fatty acid. The level of omega-3 oil found in canned tuna is highly variable, since some common manufacturing methods destroy much of the omega-3 oil in the fish. It is also a good source of protein, vitamin B6, phosphorus, vitamin B12 and selenium. The bad thing about tuna it is high in sodium. Canned tuna in salt water was used. It was bought from the local supermarket.

Eye shadow is a cosmetic that is applied on the eyelids and under the eyebrows. People use eye shadow simply to improve their appearance, but it is also commonly used in theatre and other plays to create a memorable look with bright bold colours. Lipstick is a cosmetic product containing pigments, oils, waxes and emollients that applies colour, texture and protection to the lips. Lipstick is typically but not exclusively worn by women. Shimmery lipstick may contain mica, silica, fish scale and synthetic pearl particles to give them a

glittery or shimmery shine. Both eye shadow and lipstick were bought from the local cosmetic store, essence products with no ingredients information.

Scott's emulsion is an additional source of vitamins and minerals in children. It is a well trusted vitamin and mineral supplement that contains vitamin A and D, cod liver oil and calcium hypophosphite. An adequate intake of vitamin A is essential for the proper development of a healthy body and its normal functioning at every stage of life. Scott's emulsion also helps build a healthy body with a natural resistance to infections such as coughs and colds. Scott's emulsion was purchased from the local pharmacy store.

Omega 3&6 is a combination of omega 3 essential fatty acids from cold water salmon oil and cold pressed flaxseed oil from plant origin as well as omega 6 fatty acids from cold pressed borage oil. Essential fatty acids play an important role in maintaining heart and brain health, good blood circulation and healthy functioning of the eyes, skin, joints, hair, immune and nervous system. The body cannot manufacture these essential fatty acids, so we have to ingest it through proper diet and supplementation. Omega 3&6 was bought from the local pharmacy store.

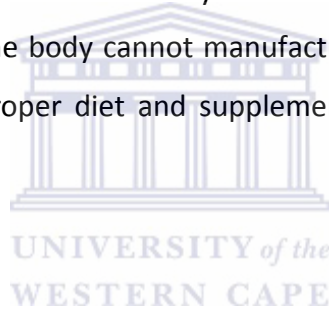




Figure 70: Fish and fish products used as sample for immunosensor application.

## 7.2 Sample preparation

Approximately 5g of each sample was weighed into a beaker and 20 ml of phosphate buffer was added. They were then heated to boil for 20 minutes and cooled to room temperature. The mother liquor was decanted into a vessel and it was analysed using EIS.

## 7.3 Results and discussion

In order to compare the selectivity of flourene derivative immunosensor and xanthene derivative immunosensor for parvalbumin in real samples EIS was performed by using these two immunosensors with fish and fish products extracts. The samples were analysed in duplicate. Two fish species and five fish products were examined. For each sample measurement new immunosensor was developed. Snoek fish mostly contain a white muscle and the white muscle is known to have a high content of parvalbumin. Lopata et al and co-

workers have reported IgE cross-reactivity among fish species consumed predominantly snoek fish was one of them. They have established that there are two allergenic isoforms of snoek parvalbumin and that indicated that the commercial antibody used was not effective in detecting all isoforms present in fish species [86]. A parvalbumin content of 1.34 pg/ml was observed using flourene derivative immunosensor and 1.41 pg/ml using xanthenes derivative immunosensor. Scott's emulsion consists of cod liver oil and cod fish is known to have high parvalbumin content. The concentration of parvalbumin in scott's emulsion was estimated to be 9.10 pg/ml using flourene derivative and 2.30 pg/ml using xanthenes derivative. Omega 3&6 contains salmon oil and the salmon is famous for its salmon pink colour. It showed no reaction for both immunosensors indicating that it does not contain traces of parvalbumin or the amount of parvalbumin is too small to be detected.

Lipstick contains fish scales predominantly from herring fish. It has shown to have parvalbumin content of 6.53 pg/ml from flourene derivative immunosensor and 5.15 pg/ml from xanthenes derivative immunosensor. Eye shadow was analysed and the parvalbumin content was estimated to be 1.40 pg/ml using flourene derivative immunosensor and 1.31 pg/ml using xanthene derivative immunosensor. Tuna fish consists of pink to dark red muscle tissue. Dark muscles are known to contain small traces of parvalbumin. Tuna fish showed no reaction for both immunosensors indicating that the parvalbumin content is too low to be detected. Fish paste contains a combination of herring and anchovies, the parvalbumin content have been estimated to be 8.23 pg/ml using flourene derivative and 7.40 pg/ml using xanthene derivative. The results are summarized in table 9. Both immunosensors are in agreement of the quantity of parvalbumin present in the sample, the results are slightly different except for the Scott's whereby xanthene derivative immunosensor detected a very low quantity than flourene derivative.

| <b>Sample</b>        | <b>Flourene derivative<br/>immunosensor<br/>pg/ml. Ave, n=2</b> | <b>Xanthene derivative<br/>immunosensor<br/>pg/ml. Ave, n = 2</b> |
|----------------------|---|---|
| <b>Snoek</b>         | 1.34  | 1.41  |
| <b>Scott's</b>       | 9.10  | 2.30  |
| <b>Omega 3&amp;6</b> | No traces of parvalbumin  | No traces of parvalbumin  |
| <b>Lipstick</b>      | 6.53  | 5.15  |
| <b>Eye shadow</b>    | 1.4   | 1.31  |
| <b>Tuna</b>          | No traces of parvalbumin  | No traces of parvalbumin  |
| <b>Fish paste</b>    | 8.23  | 7.40  |

Table 9: Summary of results obtained from EIS for samples.

Skin prick test was performed by Hilger and co-workers [87] on patients with fish allergy. One of the patients showed allergic symptom with a concentration of 0.07  $\mu\text{g/ml}$  parvalbumin. Even at low concentration people who are allergic to fish can react (show symptoms). The lowest detection limit was found to be 0.05 ng/ml parvalbumin [66]. Both xanthene derivative immunosensor and flourene derivative immunosensor were able to measure significantly lower concentrations (2.42 pg/ml and 1.50 pg/ml) than in the previous studies [66; 87]. Immunosensors prepared were reproducible, repeatable and stable and retained the bioactivity of the biomolecule. All samples were in the linear range of both immunosensors. Flourene derivative and xanthene derivative, their porosity facilitated antibody immobilization through non site region allowing the binding site to be available for antigen binding.

## Chapter 8

### *Conclusion and thesis summary*

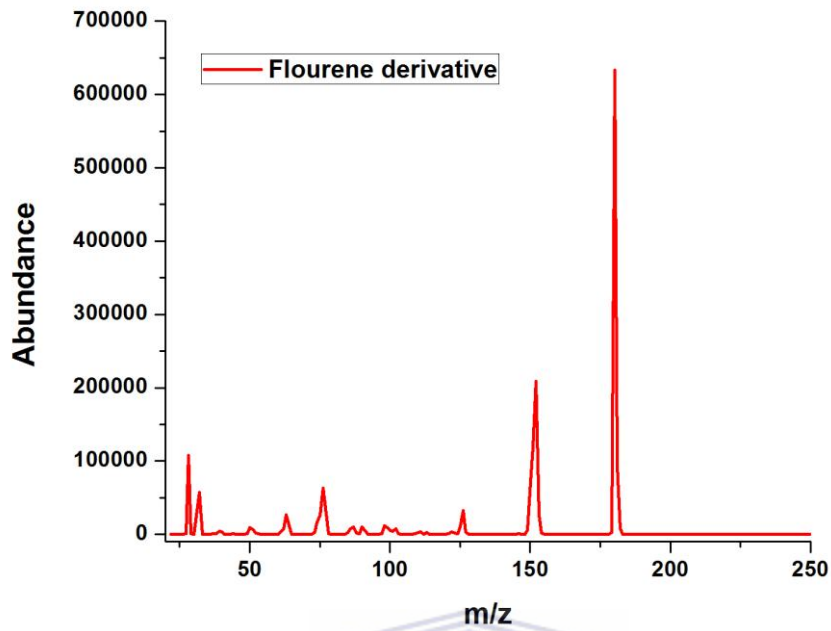
Two noncyclic organic compounds namely 9,9'-(Ethyne-1,2-diyl)bis(Flouren-9-ol) and 9-(4-methoxyphenyl)-9H-xanthen-9-ol were synthesized successfully and immunosensor developed on these two compound platforms by immobilization of an antibody, was prepared in a simple and quick manner. Both flourene derivative and xanthene derivative prepared as thin films at GC electrode were characterized successfully using DSC, FTIR, UV/Vis, Flourescence, CV, SWV and PXR. FTIR confirmed their structures. CV and SWV confirmed the presence of reversible redox couple and SWV was used to determine the formal potential which was found to be -134 mV for flourene derivative and -73 mV for xanthene derivative vs Ag/AgCl. The formal potential was used for monitoring the binding between the analytes and the immunosensors using EIS. For both compounds a yellow solution was observed with flourene derivative more intense in colour. From flourescence results a small stokes shifts was observed for both compounds. These two compounds behaved in a similar manner due to their  $\pi$ - $\pi^*$  transitions, structural rigidity and bulkiness. Flourene derivative has a rigid planar biphenyl unit and xanthene derivative has an hydroxyl moiety as well as a pyranly oxygen.

Capacitance, as measured by EIS was quantitatively related to the concentration dependent binding of analyte to the immunosensor. Flourene derivative immunosensor showed a high sensitivity for the analyte with a detection limit of 1.50 pg/ml. Xanthene derivative immunosensor also showed a high sensitivity of the analyte with detection limit of 2.42 pg/ml. The sensitivity and the detection limit were determined sing EIS. Flourene derivative immunosensor was found to be more sensitive than xanthene derivative immunosensor, with good repeatability and reproducibility. The detection limit of these immunosensors for the selected analyte was much lower than the detection limit of other analytical methods [65; 66]. UV/Vis absorption spectroscopy was used to confirm the binding of the analyte to the native antibody in solution, by measuring the response as a function of concentration. Both immunosensors were successfully applied in fish species and fish products analysis. Tuna and omega 3&6 showed no traces of parvalbumin. Low concentrations of parvalbumin in snoek, lipstick, eyeshadow, scott's and fish paste were determined successfully. In

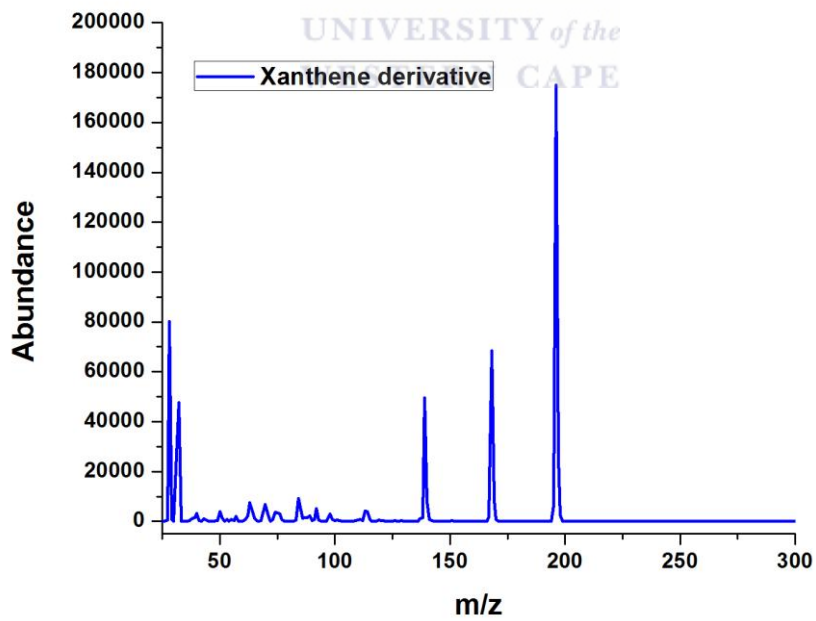
comparison, the EIS was found to be more sensitive than ELISA method. ELISA is time consuming compared to the EIS.

Supramolecular structures are constructed by non-covalent interactions and self-assembly and their stoichiometry and topology depend on the phenomenon of molecular recognition which occurs between the host and guest molecules and the resultant structure can in principle explain its reactivity and stability. Hydrogen bonding is the most important intermolecular interaction that influences molecular recognition. Morphological and physical properties of flourene derivative immunosensor and xanthene derivative immunosensor make them very versatile sensing platforms with high sensitivity to the presence of biochemical species which penetrate inside the pores. New novel platform immunosensor has been successfully developed. The synthesis was quick, easy and done inhouse (UWC sensorlab). Both immunosensors were developed using a non-labelled antibody which was directly attached to the platform. Unlike in ELISA there was no blocking or washing step while developing the immunosensors. The higher sensitivity shows that there was a better antibody orientation. This indicates enhanced molecular recognition. The antibody was attached via nonsite directed approach allowing binding sites to be available for analyte binding. These platforms are effective for biomolecule immobilization and retain bioactivity. They are capable of directly detecting antibody/antigen interactions. It was established that the mechanism of adsorption is controlled by physical forces. Real sample analysis was performed efficiently in real time with minimum sample preparation.

## Appendix 1



Appendix 1a: Mass spectrum of flourene derivative.



Appendix 1b: Mass spectrum of xanthene derivative.

## References

- [1] T.H. Brehmer, P.P. Korkas, E. Weber, Fluoroclathrands—a new type of chemical sensor materials for optical vapour detection. *Sensors and Actuators B: Chemical* 44 (1997) 595-600.
- [2] F. Tsagkogeorgas, M. Ochsenkühn-Petropoulou, R. Niessner, D. Knopp, Encapsulation of biomolecules for bioanalytical purposes: Preparation of diclofenac antibody-doped nanometer-sized silica particles by reverse micelle and sol-gel processing. *Analytica Chimica Acta* 573 (2006) 133-137.
- [3] J.C. Zhou, M.H. Chuang, E.H. Lan, B. Dunn, P.L. Gillman, S.M. Smith, Immunoassays for cortisol using antibody-doped sol-gel silica. *Journal of Materials Chemistry* 14 (2004) 2311-2316.
- [4] K. Bowman-James, Macrocyclic Ligands, in, *Encyclopedia of Inorganic Chemistry*, John Wiley & Sons, Ltd, 2006.
- [5] M.-C. Hennion, V. Pichon, Immuno-based sample preparation for trace analysis. *Journal of Chromatography A* 1000 (2003) 29-52.
- [6] B.C. Dave, B. Dunn, J.S. Valentine, J.I. Zink, Sol-gel encapsulation methods for biosensors. *Analytical Chemistry* 66 (1994) 1120A-1127A.
- [7] D. Tang, R. Yuan, Y. Chai, Y. Liu, J. Dai, X. Zhong, Novel potentiometric immunosensor for determination of diphtheria antigen based on compound nanoparticles and bilayer two-dimensional sol-gel as matrices. *Analytical and Bioanalytical Chemistry* 381 (2005) 674-680.
- [8] E. Gizeli, C.R. Lowe, Immunosensors. *Current Opinion in Biotechnology* 7 (1996) 66-71.
- [9] S.S. Pathak, H.F.J. Savelkoul, Biosensors in immunology: the story so far. *Immunology Today* 18 (1997) 464-467.
- [10] O. Tokarsky, D.L. Marshall, Immunosensors for rapid detection of *Escherichia coli* O157:H7 — Perspectives for use in the meat processing industry. *Food Microbiology* 25 (2008) 1-12.
- [11] X. Jiang, D. Li, X. Xu, Y. Ying, Y. Li, Z. Ye, J. Wang, Immunosensors for detection of pesticide residues. *Biosensors and Bioelectronics* 23 (2008) 1577-1587.
- [12] J. Lin, H. Ju, Electrochemical and chemiluminescent immunosensors for tumor markers. *Biosensors and Bioelectronics* 20 (2005) 1461-1470.

- [13]D.R. Shankaran, K.V. Gobi, N. Miura, Recent advancements in surface plasmon resonance immunosensors for detection of small molecules of biomedical, food and environmental interest. *Sensors and Actuators B: Chemical* 121 (2007) 158-177.
- [14]H. van Vunakis, Practice and theory of enzyme immunoassays: By P. Tijssen, Laboratory Techniques in Biochemistry and Molecular Biology. Edited by R. H. Burdon and P. H. van Knippenberg, Elsevier, Amsterdam/ New York, 1985. xxvi + 549 pp. *Analytical Biochemistry* 162 (1987) 309-310.
- [15]P.B. Lippa, L.J. Sokoll, D.W. Chan, Immunosensors—principles and applications to clinical chemistry. *Clinica Chimica Acta* 314 (2001) 1-26.
- [16]K. Maehashi, K. Matsumoto, Y. Takamura, E. Tamiya, Aptamer-Based Label-Free Immunosensors Using Carbon Nanotube Field-Effect Transistors. *Electroanalysis* 21 (2009) 1285-1290.
- [17]R. Jenison, S. Gill, A. Pardi, B. Polisky, High-resolution molecular discrimination by RNA. *Science* 263 (1994) 1425-1429.
- [18]A.A. Haller, P. Sarnow, In vitro selection of a 7-methyl-guanosine binding RNA that inhibits translation of capped mRNA molecules. *Proceedings of the National Academy of Sciences* 94 (1997) 8521-8526.
- [19]M. Sassanfar, J.W. Szostak, An RNA motif that binds ATP. *Nature* 364 (1993) 550-553.
- [20]C. Mannironi, A. Di Nardo, P. Fruscoloni, G.P. Tocchini-Valentini, In Vitro Selection of Dopamine RNA Ligands†. *Biochemistry* 36 (1997) 9726-9734.
- [21]H.C. Goicoechea, A.C. Olivieri, A. Muñoz de la Peña, Determination of theophylline in blood serum by UV spectrophotometry and partial least-squares (PLS-1) calibration. *Analytica Chimica Acta* 384 (1999) 95-103.
- [22]H. Ulrich, C.A. Trujillo, A.A. Nery, J.M. Alves, P. Majumder, R.R. Resende, A.H. Martins, DNA and RNA Aptamers: From Tools for Basic Research Towards Therapeutic Applications. *Combinatorial Chemistry & High Throughput Screening* 9 (2006) 619-632.
- [23]E.N. Brody, L. Gold, Aptamers as therapeutic and diagnostic agents. *Reviews in Molecular Biotechnology* 74 (2000) 5-13.
- [24]S. Tombelli, M. Minunni, M. Mascini, Analytical applications of aptamers. *Biosensors and Bioelectronics* 20 (2005) 2424-2434.

- [25]S.-E. Kim, K.-Y. Ahn, J.-S. Park, K.R. Kim, K.E. Lee, S.-S. Han, J. Lee, Fluorescent Ferritin Nanoparticles and Application to the Aptamer Sensor. *Analytical Chemistry* 83 (2011) 5834-5843.
- [26]K. Sefah, J.A. Phillips, X. Xiong, L. Meng, D. Van Simaey, H. Chen, J. Martin, W. Tan, Nucleic acid aptamers for biosensors and bio-analytical applications. *Analyst* 134 (2009) 1765-1775.
- [27]H. Yang, J. Ji, Y. Liu, J. Kong, B. Liu, An aptamer-based biosensor for sensitive thrombin detection. *Electrochemistry Communications* 11 (2009) 38-40.
- [28]T.P. Janeway CA Jr, Walport M, , *Immunobiology: The Immune System in Health and Disease.* , in, Garland Science, 2001.
- [29]G.W. Litman, J.P. Rast, M.J. Shablott, R.N. Haire, M. Hulst, W. Roess, R.T. Litman, K.R. Hinds-Frey, A. Zilch, C.T. Amemiya, Phylogenetic diversification of immunoglobulin genes and the antibody repertoire. *Molecular Biology and Evolution* 10 (1993) 60-72.
- [30]Y.K. Sykulev, R.S. Nezlin, The dynamics of glycan-protein interactions in immunoglobulins. Results of spin label studies. *Glycoconjugate Journal* 7 (1990) 163-182.
- [31]V. Shmanai, T. Nikolayeva, L. Vinokurova, A. Litoshka, Oriented antibody immobilization to polystyrene macrocarriers for immunoassay modified with hydrazide derivatives of poly(meth)acrylic acid. *BMC Biotechnology* 1 (2001) 4.
- [32]D. Beale, A. Feinstein, Structure and function of the constant regions of immunoglobulins. *Quarterly Reviews of Biophysics* 9 (1976) 135-180.
- [33]J. Penalva, Puchades, R. & Maquieira, A. , Analytical Properties of Immunosensors Working in. *Acs Symposium Series* 71 (1999) 3862-3872.
- [34]L.M. Nadler, P. Stashenko, R. Hardy, W.D. Kaplan, L.N. Button, D.W. Kufe, K.H. Antman, S.F. Schlossman, Serotherapy of a Patient with a Monoclonal Antibody Directed against a Human Lymphoma-associated Antigen. *Cancer Research* 40 (1980) 3147-3154.
- [35]G. Kohler, C. Milstein, Continuous cultures of fused cells secreting antibody of predefined specificity. *Nature* 256 (1975) 495-497.
- [36]K.J. Berger, D.A. Guss, Mycotoxins revisited: Part I. *The Journal of emergency medicine* 28 (2005) 53-62.

- [37]N.W. Turner, S. Subrahmanyam, S.A. Piletsky, Analytical methods for determination of mycotoxins: A review. *Analytica Chimica Acta* 632 (2009) 168-180.
- [38]J.L. Richard, Some major mycotoxins and their mycotoxicoses—An overview. *International Journal of Food Microbiology* 119 (2007) 3-10.
- [39]M.L. Martins, H.M. Martins, F. Bernardo, Aflatoxins in spices marketed in Portugal. *Food Additives and Contaminants* 18 (2001) 315-319.
- [40]Y.-n. Yin, L.-y. Yan, J.-h. Jiang, Z.-h. Ma, Biological control of aflatoxin contamination of crops. *Journal of Zhejiang University - Science B* 9 (2008) 787-792.
- [41]P. Bayman, J. Baker, Ochratoxins: A global perspective. *Mycopathologia* 162 (2006) 215-223.
- [42]R. Mateo, Á. Medina, E.M. Mateo, F. Mateo, M. Jiménez, An overview of ochratoxin A in beer and wine. *International Journal of Food Microbiology* 119 (2007) 79-83.
- [43]O. Cornely, &lt;i>Aspergillus&/i> to Zygomycetes: Causes, Risk Factors, Prevention, and Treatment of Invasive Fungal Infections. *Infection* 36 (2008) 296-313.
- [44]A.W. Schaafsma, D.C. Hooker, Climatic models to predict occurrence of Fusarium toxins in wheat and maize. *International Journal of Food Microbiology* 119 (2007) 116-125.
- [45]M.O. Moss, Fungi, quality and safety issues in fresh fruits and vegetables. *Journal of Applied Microbiology* 104 (2008) 1239-1243.
- [46]M.W. Trucksess, P.M. Scott, Mycotoxins in botanicals and dried fruits: A review. *Food Additives & Contaminants: Part A* 25 (2008) 181-192.
- [47]A.A.P. Ferreira, C.S. Fugivara, H. Yamanaka, A.V. Benedetti, Preparation and Characterization of Immunosenors for Disease Diagnosis. (2011).
- [48]P.T. Kissinger, W.R. Heineman, Cyclic voltammetry. *Journal of Chemical Education* 60 (1983) 702.
- [49]H. Angerstein-Kozłowska, B. Conway, W. Sharp, The real condition of electrochemically oxidized platinum surfaces: Part I. Resolution of component processes. *Journal of Electroanalytical Chemistry and Interfacial Electrochemistry* 43 (1973) 9-36.
- [50]P. Cabot, F. Centellas, J. Garrido, P. Sumodjo, A. Benedetti, R. Nakazato, The influence of the electrochemical treatment on Cu-Al-Ag alloys in deaerated 0.5 M NaOH. *Journal of applied electrochemistry* 21 (1991) 446-451.

- [51]D.G. Horta, D. Bevilaqua, H.A. Acciari, O.G. Júnior, A.V. Benedetti, Optimization of the use of carbon paste electrodes (CPE) for electrochemical study of the chalcopyrite. *Química Nova* 32 (2009) 1734-1738.
- [52]E. Calvo, C. Danilowicz, C. Lagier, J. Manrique, M. Otero, Characterization of self-assembled redox polymer and antibody molecules on thiolated gold electrodes. *Biosensors and Bioelectronics* 19 (2004) 1219-1228.
- [53]D. Tang, R. Yuan, Y. Chai, Electrochemical immuno-bioanalysis for carcinoma antigen 125 based on thionine and gold nanoparticles-modified carbon paste interface. *Analytica chimica acta* 564 (2006) 158-165.
- [54]T. Biegler, D. Rand, R. Woods, Limiting oxygen coverage on platinized platinum; relevance to determination of real platinum area by hydrogen adsorption. *Journal of Electroanalytical Chemistry and Interfacial Electrochemistry* 29 (1971) 269-277.
- [55]B. Dogan-Topal, S.A. Ozkan, B. Uslu, The analytical applications of square wave voltammetry on pharmaceutical analysis. *The Open Chemical and Biomedical Methods Journal* 3 (2010) 56-73.
- [56]A.J. Bard, L.R. Faulkner, Fundamentals and applications. *Electrochemical Methods* 2 (1980).
- [57]B.-Y. Chang, S.-M. Park, Electrochemical impedance spectroscopy. *Annual Review of Analytical Chemistry* 3 (2010) 207-229.
- [58]R. Jenkins, R. Snyder, Introduction to X-ray powder diffractometry, Wiley-Interscience, 2012.
- [59]H.P. Klug, L.E. Alexander, X-ray diffraction procedures: for polycrystalline and amorphous materials. *X-Ray Diffraction Procedures: For Polycrystalline and Amorphous Materials*, 2nd Edition, by Harold P. Klug, Leroy E. Alexander, pp. 992. ISBN 0-471-49369-4. Wiley-VCH, May 1974. 1 (1974).
- [60]E. Curtis, L.R. Nassimbeni, H. Su, J.H. Taljaard, Xanthenol clathrates: Structures and solid-solid reactions. *Crystal growth & design* 6 (2006) 2716-2719.
- [61]N. Faleni, Inclusion behaviour of related organic host compounds, in, 2012.
- [62]A. Jacobs, L.R. Nassimbeni, K.L. Nohako, G. Ramon, J.H. Taljaard, Enclathration by a xanthenol host via solid–solid reactions: structures and kinetics. *New Journal of Chemistry* 33 (2009) 1960-1964.

- [63]E. Weber, S. Nitsche, A. Wierig, I. Csöreg, Inclusion Compounds of Diol Hosts Featuring Two 9-Hydroxy-9-fluorenyl or Analogous Groups Attached to Linear Spacer Units. *European Journal of Organic Chemistry* 2002 (2002) 856-872.
- [64]W.S. Matthews, J.E. Bares, J.E. Bartmess, F. Bordwell, F.J. Cornforth, G.E. Drucker, Z. Margolin, R.J. McCallum, G.J. McCollum, N.R. Vanier, Equilibrium acidities of carbon acids. VI. Establishment of an absolute scale of acidities in dimethyl sulfoxide solution. *Journal of the American Chemical Society* 97 (1975) 7006-7014.
- [65]Y. Lu, T. Ohshima, H. Ushio, Rapid detection of fish major allergen parvalbumin by surface plasmon resonance biosensor. *Journal of food science* 69 (2004) C652-C658.
- [66]A. Dahlman-Höglund, A. Renström, P.H. Larsson, S. Elsayed, E. Andersson, Salmon allergen exposure, occupational asthma, and respiratory symptoms among salmon processing workers. *American journal of industrial medicine* 55 (2012) 624-630.
- [67]H.R. Larsen, Omega 3 Oils: The Essential Nutrients. Retrieved November 22 (2002) 2010.
- [68]T. Arumanayagam, P. Murugakoothan, Optical Conductivity and Dielectric Response of an Organic Aminopyridine NLO Single Crystal. *J. of Minerals & Materials Characterization & Engineering* 10 (2011) 1225-1231.
- [69]K.-T. Wong, Y.-M. Chen, Y.-T. Lin, H.-C. Su, C.-c. Wu, Nonconjugated hybrid of carbazole and fluorene: A novel host material for highly efficient green and red phosphorescent OLEDs. *Organic letters* 7 (2005) 5361-5364.
- [70]M. Ranger, D. Rondeau, M. Leclerc, New well-defined poly (2, 7-fluorene) derivatives: photoluminescence and base doping. *Macromolecules* 30 (1997) 7686-7691.
- [71]K.D. Belfield, M.V. Bondar, O.V. Przhonska, K.J. Schafer, W. Mourad, Spectral properties of several fluorene derivatives with potential as two-photon fluorescent dyes. *Journal of Luminescence* 97 (2002) 141-146.
- [72]K.M. Omer, S.Y. Ku, K.T. Wong, A.J. Bard, Efficient and Stable Blue Electrogenerated Chemiluminescence of Fluorene-Substituted Aromatic Hydrocarbons. *Angewandte Chemie International Edition* 48 (2009) 9300-9303.
- [73]K. Fujii, K. Fukui, Crystal polymorph of fluorene derivative and production method thereof, in, Google Patents, 2012.

- [74]G. Pohlers, J. Scaiano, R. Sinta, A novel photometric method for the determination of photoacid generation efficiencies using benzothiazole and xanthene dyes as acid sensors. *Chemistry of materials* 9 (1997) 3222-3230.
- [75]V. Martínez Martínez, F. López Arbeloa, J. Bañuelos Prieto, T. Arbeloa López, I. López Arbeloa, Characterization of rhodamine 6G aggregates intercalated in solid thin films of laponite clay. 1. Absorption spectroscopy. *The Journal of Physical Chemistry B* 108 (2004) 20030-20037.
- [76]T. Shimo, M. Matsushita, H.I. Omar, K. Somekawa, Solid-state and solution photocycloadditions of 4-acyloxy-2-pyrones with maleimide. *Tetrahedron* 61 (2005) 8059-8064.
- [77]C. Retna Raj, R. Ramaraj, Electrochemical study of the cyclodextrin encapsulation of a macrocyclic nickel complex. *Electrochimica acta* 44 (1999) 2685-2691.
- [78]G.G. Surpateanu, M. Becuwe, N.C. Lungu, P.I. Dron, S. Fourmentin, D. Landy, G. Surpateanu, Photochemical behaviour upon the inclusion for some volatile organic compounds in new fluorescent indolizine  $\beta$ -cyclodextrin sensors. *Journal of Photochemistry and Photobiology A: Chemistry* 185 (2007) 312-320.
- [79]P. He, J. Ye, Y. Fang, I. Suzuki, T. Osa, Voltammetric responsive sensors for organic compounds based on organized self-assembled lipoyl- $\beta$ -cyclodextrin derivative monolayer on a gold electrode. *Analytica Chimica Acta* 337 (1997) 217-223.
- [80]K. Kato, T. Saito, S. Seelan, M. Tomita, Y. Yokogawa, Reaction properties of catalytic antibodies encapsulated in organo substituted  $\text{SiO}_2$  sol-gel materials. *Journal of bioscience and bioengineering* 100 (2005) 478-480.
- [81]J. Wang, P.V.A. Pamidi, K.R. Rogers, Sol-gel-derived thick-film amperometric immunosensors. *Analytical Chemistry* 70 (1998) 1171-1175.
- [82]K.C. Grabar, R.G. Freeman, M.B. Hommer, M.J. Natan, Preparation and characterization of Au colloid monolayers. *Analytical Chemistry* 67 (1995) 735-743.
- [83]R. Liang, J. Qiu, P. Cai, A novel amperometric immunosensor based on three-dimensional sol-gel network and nanoparticle self-assemble technique. *Analytica chimica acta* 534 (2005) 223-229.

- [84]J. Chen, J. Tang, F. Yan, H. Ju, A gold nanoparticles/sol-gel composite architecture for encapsulation of immunoconjugate for reagentless electrochemical immunoassay. *Biomaterials* 27 (2006) 2313-2321.
- [85]T. Van Do, S. Elsayed, E. Florvaag, I. Hordvik, C. Endresen, Allergy to fish parvalbumins: studies on the cross-reactivity of allergens from 9 commonly consumed fish. *Journal of Allergy and Clinical Immunology* 116 (2005) 1314-1320.
- [86]J.E. Beale, M.F. Jeebhay, A.L. Lopata, Characterisation of purified parvalbumin from five fish species and nucleotide sequencing of this major allergen from Pacific pilchard, *Sardinops sagax*. *Molecular immunology* 46 (2009) 2985-2993.
- [87]C. Hilger, L. Thill, F. Grigioni, C. Lehnert, P. Falagiani, A. Ferrara, C. Romano, W. Stevens, F. Hentges, IgE antibodies of fish allergic patients cross-react with frog parvalbumin. *Allergy* 59 (2004) 653-660.

